Russian Chemical Reviews **81** (7) 606 – 637 (2012) © 2012 Russian Academy of Sciences and Turpion Ltd

DOI 10.1070/RC2012v081n07ABEH004243

Complex phosphates formed by metal cations in oxidation states I and IV

V I Pet'kov

Contents

I. Introduction 606
II. Acid and neutral phosphates of tetravalent transition metals and alkali metals with the ratio phosphorus : d metal = 2 607
III. Complex and mixed phosphates of d and f transition (E^{IV}) and alkaline metals with the P : E^{IV} ratios of 1.5 and 3 615
IV. Conclusion 631

Abstract. Data on the synthesis, structure and physicochemical characteristics of phosphates formed by M^{I} and E^{IV} cations, in particular, double and more complex phosphates in which M^{I} has been partially replaced by H^{+} or $(M')^{I}$ and PO_4^{3-} has been partially replaced by TO_4^{n-} (T = Si, As, B, Mo) are generalized and described systematically. The key factors responsible for the formation of a particular type of structure are analyzed. The possibilities are considered for preparing structures of a desired type and symmetry and for fine tuning of properties of obtained crystals by varying the cationic and anionic components of the phosphate with retention of stable structural fragments of the crystal ensemble and by selecting an appropriate method of synthesis. The ways of practical application of complex phosphates taking into account their structural features are demonstrated. The bibliography includes 395 references.

I. Introduction

The progress in the solid state chemistry — the science concerned with the structure, properties and methods of synthesis of solids and directed to the elaboration of basically new materials — is largely related to the preparation of multicomponent chemical compounds and the development of new processes (including the synthesis) and conditions of subsequent treatment of products and materials.[1] A key approach to the chemical design of materials is the use of crystal chemical data, which provide deeper understanding of the relationship between the composition, the structure and the properties of compounds.

As regards modelling of novel compounds with a specified structure and properties, of considerable interest is the structural type NZP or NASICON (Na Superionic Conductor), which has drawn keen attention of a broad circle of researchers during the last 20 years.[2–9] The natural mineral kosnarite $KZr_2(PO_4)_3$, first described by Brownfield *et al.*,[10] also belongs to this structural type.

The NZP family with the basic structure of the phosphate $NaZr_2(PO_4)_3$ (space group $R\bar{3}c$, $a = 8.8045$ Å, $c = 22.7585$ Å)[11] comprises compounds and solid solutions described by the crystal chemical formula $(M1)_{0\to1}(M2)_{0\to3}.\{[L_2(TO_4)_3]^{p-}\}_{3\infty}$, where $\{[L_2(TO_4)_3]^{p-}\}_{3\infty}$ is the structure framework (p is the charge), and $(M1)_{0\to1}$, $(M2)_{0\to3}$ are different types of extraframework cation sites with designated site occupancy in each type.[12] The structure framework is formed by the LO_6 octahedra and TO_4 tetrahedra connected by sharing corners (Fig. 1); the M1 and M2 voids of different size are convenient for accommodation of a broad range of cations compensating the framework charge (compensation cations).

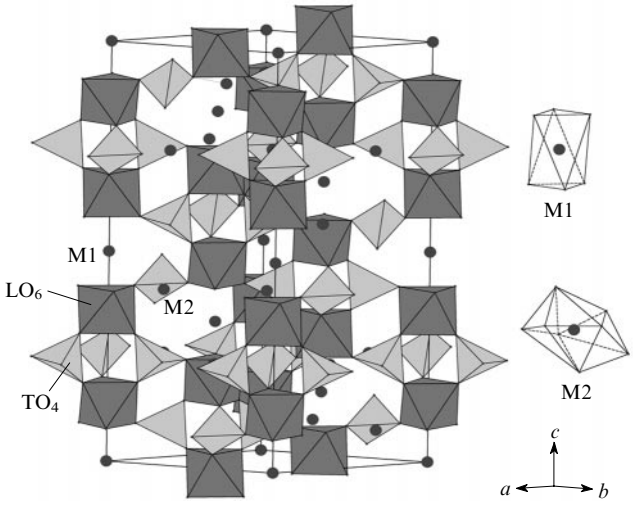


Figure 1. Crystal structure of NZP.[4]
The framework of L octahedra and T tetrahedra and the extraframework M1 and M2 sites and their coordination polyhedra are shown. A unit cell is outlined.

V I Pet'kov Department of Chemistry, N I Lobachevsky Nizhnii Novgorod State University, prosp. Gagarina 23, 603950 Nizhnii Novgorod, Russian Federation. Fax (7-831) 462 30 85, tel. (7-831) 462 32 34, e-mail: petkov@uic.nnov.ru

Received 15 May 2011
Uspekhi Khimii **81** (7) 606 – 637 (2012); translated by Z P Svitanko

Most of representatives of the NZP family have phosphorus as the anion-forming element T with tetrahedrally arranged chemical bonds. There exist NZP phases in which phosphorus is completely or partially replaced by silicon, germanium, arsenic, vanadium, sulfur, molybdenum, tungsten or aluminium. The structure-forming octahedral cations L with predominantly covalent character of metal–oxygen bond have oxidation states from +5 to +1. For example, these are Nb^{5+}, Sb^{5+}, Ta^{5+}, Ti^{4+}, Zr^{4+}, Hf^{4+}, Ge^{4+}, Sn^{4+}, Mo^{4+}, U^{4+}, Np^{4+}, Pu^{4+}, Sc^{3+}, Y^{3+}, Ln^{3+}, V^{3+}, Cr^{3+}, Fe^{3+}, Al^{3+}, Ga^{3+}, In^{3+}, Ti^{3+}, Mg^{2+}, Mn^{2+}, Cu^{2+}, Co^{2+}, Ni^{2+}, Zn^{2+}, Na^{+}, *etc*. The framework L sites are often occupied by combinations of these cations. The extraframework M1 and M2 sites can be occupied by identical or different cations in oxidation states from +1 to +4 or remain vacant depending on the oxidation states of ions located in the L and T sites because the whole compound must be electrically neutral. The factors determining the most probable arrangement of atoms in M and L sites are the oxidation state and the size of cations. The M sites are usually occupied by cations with lower oxidation state and greater radius.

The enhanced stability of the NZP structure against the change in the chemical composition, temperature and pressure is provided by relatively rigid structural fragments $L_2(TO_4)_3$ having strong bonds within the group and evenly distributed voids of different size, which serve as buffers upon framework distortions caused by interaction with extraframework cations. Owing to the broad isomorphism of cations in all crystallographic sites (M1, M2, L and T), diverse options for framework charge compensation and the possibility of occupation of framework sites by ions in different oxidation states and of different size, the set of compounds and solid solutions both known and predicted based on crystal chemical data becomes fairly extensive.[3,4,13]

Detailed knowledge of the structures of NZP-related materials was used to prepare, by means of iso- and heterovalent substitutions in the framework and in the cavities, superionic NASICON materials with low superionic transition temperatures and cationic conduction.[7,14–16] The enhanced interest in NZP-related structures is also due to the growing prospects of using them as high-tech materials with unique ability almost not to expand upon heating.[4,17] The manufacture of NZP ceramics with ultra-low (at low anisotropy) thermal expansion based on inorganic phosphates was started by the company Low Thermal Expansion Ceramics (LoTEC, now SMAHT Ceramics Inc.).[18] The multifunctional character of these materials having high melting and decomposition points (1173–1973 K) and physicomechanical parameters [flexural strength, 70 MPa; Young's modulus, 70 GPa; Rockwell's hardness (HRA), 89; density, 3200–3650 $kg\,m^{-3}$],[18,19] chemical and radiation stability,[3,20] low thermal conductivity,[19,21,22] allows them to be used in articles requiring high thermal shock resistance (furnace baffles and their parts, fixtures for a high-tolerance brazing, semiconductor wafer fixtures, catalyst supports, optical benches), in electronics (ceramic electrolytes, substrates), in mechanical engineering and transport systems (engine parts), in power engineering (radiation-resistant heat-insulating material; immobilizing matrix for safe disposal of radioactive wastes) and in chemical engineering (selective catalysts).

This review gives an analysis of published data including authors' results dealing with double and triple phosphates of d and some f transition elements in the oxidation state +4 and alkali metals, the crystal structure of which depends on the cation nature and ratio and the synthesis temperature. The attention is focused on the crystal chemical research of compounds with the NZP (NASICON) structural motif. Specific features of the phosphates with large E^{IV} cations of f elements for which the structural type changes to give $KTh_2(PO_4)_3$-type structures are discussed. The data on acid and mixed orthophosphates containing H^+ ions (and water molecules involved in structure formation) apart from M^I and E^{IV} cations and also various anions are integrated. The crystal chemical features of layered phases related to the change in the interlayer distances and the degree of hydration are considered. The possibility of targeted change in the composition of cationic and anionic components of phosphates allows varying the size and symmetry of the unit cells of framework and layered structures and ensures smooth modification and control of their properties, in particular, thermal expansion, ionic mobility, as well as ion exchange processes and catalytic characteristics.

Each group of complex phosphates of M^I and E^{IV} cations comprises various compositions. These groups have much in common in the structures and physicochemical characteristics, and it is expedient to consider them from a common standpoint. As the system-forming feature, we will use the ratio of the numbers of phosphorus and E^{IV} metal atoms within the compound because particularly these atoms having the highest oxidation states, according to the crystal chemical behaviours, largely determine what structure is formed. The information about these groups of phosphates is covered only partially in new reviews.[5,13,23,24] The publications considering strategies of materials design based on these compounds starting with the unit cell structure and ending in the polycrystalline (ceramic) structure with inherent defects are fragmentary. Therefore, this review surveys the currently available data on the progress in the synthesis of complex M^I and E^{IV} phosphates at different structural levels, the consideration being focused on the results that were not covered by earlier reviews.

II. Acid and neutral phosphates of tetravalent transition metals and alkali metals with the ratio phosphorus : d metal = 2

Most of anhydrous phosphates $M^I_2E^{IV}(PO_4)_2$ are prepared from hydrated compounds $M^I_2E^{IV}(PO_4)_2\cdot n\,H_2O$ at temperatures from 423 to 673 K. The preparation of the hydrated products is based on the ability of compounds $E^{IV}(HPO_4)_2\cdot n\,H_2O$ to exchange proton for a metal ion when made to react with solutions of salts and hydroxides.[25] The studies of the phosphates $M^I_2E^{IV}(PO_4)_2$, $M^I_2E^{IV}(PO_4)_2\cdot n\,H_2O$, $M^IHE^{IV}(PO_4)_2\cdot n\,H_2O$ and $E^{IV}(HPO_4)_2\cdot n\,H_2O$ were concentrated on their synthesis, phase formation, polymorphic transformations, ion exchange properties and proton conduction.[25–35] Fairly intensive research concerns the products of intercalation of amines, alcohols and other organic derivatives that contain functional groups able to bind to protons in the structures of Group 4 d-metal hydrogen phosphates. Studies into the synthesis and properties of ion-conductive hybrid materials based on polymer membranes containing inorganic nano-

particles of Group 4 metal hydrogen phosphates are being in progress.[36–45]

1. Synthesis and structure of acid phosphates of tetravalent metals

Among hydrated almost insoluble acid phosphates of metals in the oxidation state +4, best studied is zirconium hydrogen phosphate monohydrate $Zr^{IV}(HPO_4)_2 \cdot H_2O$ (α-ZrP).[27,46–57] The interest in this compound is caused by its highest stability, among the phosphates $E^{IV}(HPO_4)_2 \cdot H_2O$, against water at elevated temperature and pressure,[58,59] against ionizing radiation[59,60] and strong oxidants.[61] These features in combination with the presence of protons in α-ZrP determine its ion exchange properties and suitability for use in nuclear engineering for the isolation of radioactive elements (Cs, Sr, actinides) from aqueous solutions and for removal of corrosion products from the circuit water of nuclear reactors.[23,27,59,62,63]

Zirconium hydrogen phosphate can be prepared by long-term refluxing of a mixture of zirconium oxide dichloride with excess phosphoric acid[46] or by concentrating the corresponding solution with addition of hydrofluoric acid.[64] In this case, slow decomposition of zirconium fluoride complexes affords well-formed α-ZrP crystals.[65] By using oxalic acid instead of HF, it is possible to avoid the difficulties caused by evaporation of the acid and obtain the microcrystals of α-ZrP in a higher yield over a shorter period of time.[57] The reaction of zirconium alkoxide [for example, a solution of $Zr(OPr^n)_4$ in n-propanol] with phosphoric acid provides a shorter route to α-ZrP and decreases the temperature of its crystallization.[50] Acid phosphates of other metals in the oxidation state +4, $E^{IV}(HPO_4)_2 \cdot n\,H_2O$ (E = Ti, Ge, Sn, Hf, Pb, Th, U, Pu), are formed upon mixing of a solution of orthophosphoric acid taken most often in a large excess with a solution of E^{IV} salt or oxide. Depending on the preparation conditions, the products contain different numbers of water molecules of crystallization.[23,25,47,66]

The crystallographic studies of α-$E^{IV}(HPO_4)_2 \cdot H_2O$ have shown that they all belong to the monoclinic system, have layered structures and the same crystal morphology (Table 1). The unit cell parameters and volumes increase linearly with increase in the E^{IV} cation radius in two series: phosphates of Group 4 metals (Ti, Hf, Zr) have greater unit cell parameters *a*, *b* and volume but smaller parameter *c* as compared with phosphates of Group 14 elements (Ge, Sn, Pb). The differences between the two series of α-$E^{IV}(HPO_4)_2 \cdot H_2O$ compounds are due to the type of $E^{IV}-O$ chemical bond, which is nearly ionic for Group 4 metals and is polar covalent for Group 14 elements. The structures of these compounds[66–69,71,72,77] are formed by $[E^{IV}(HPO_4)_2]_{2\infty}$ layers composed of slightly distorted $E^{IV}O_6$ octahedra and HPO_4 polyhedra (Fig. 2).† The formation of $P-O-E^{IV}$ bonds involves three oxygen atoms of the anion, while the fourth atom points to the interlayer space and is bonded to hydrogen. Between the layers, there are octahe-

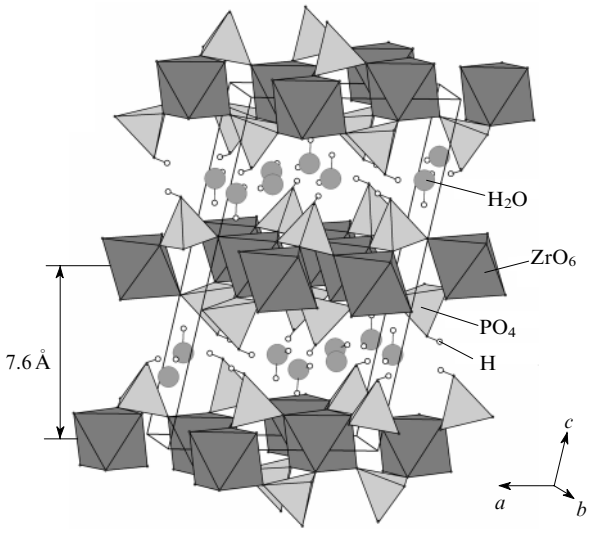


Figure 2. Fragment of the structure of α-$Zr(HPO_4)_2 \cdot H_2O$.[69]

† The structures shown in Figs 2–4, 6 and 7 were constructed by the author using atom coordinates from the original publications referred to in the figure captions.

Table 1. Crystallographic characteristics of the compounds $E^{IV}(HPO_4)_2 \cdot n\,H_2O$ with known structures.

Compound	Space group	*Z*[a]	Unit cell parameters				Ref.
			a/Å	*b*/Å	*c*/Å	*β*/deg	
α-$Ti(HPO_4)_2 \cdot H_2O$	$P2_1/c$	4	8.630	5.006	16.189	110.20	67
	$P2_1/n$	4	8.6403	5.0093	15.5097	101.324	66
α-$Ge(HPO_4)_2 \cdot H_2O$	$P2_1/c$	4	8.2920	4.7880	16.4058	108.985	68
α-$Zr(HPO_4)_2 \cdot H_2O$	$P2_1/n$	4	9.060	5.297	15.414	101.71	69
α-$Sn(HPO_4)_2 \cdot H_2O$	$C2/c$	4	8.6115	4.9643	15.861	100.03	66
	$P2_1/n$	4	8.618	4.971	15.983	100.22	70
α-$Pb(HPO_4)_2 \cdot H_2O$	$P2_1/n$	4	8.6238	4.9870	16.1250	100.615	66
α-$Hf(HPO_4)_2 \cdot H_2O$	$P2_1/c$	4	8.995	5.243	16.22	111.23	71
	$P2_1/n$	4	9.0142	5.25665	15.4768	101.636	72
α-$Zr(HPO_4)_2 \cdot 0.5\,H_2O$	$C2/c$	4	9.1478	5.3242	15.288	103.848	73
γ-$Ti(H_2PO_4)(PO_4) \cdot 2\,H_2O$	$P2_1$	2	5.186	6.3505	11.865	102.52	74
γ-$Zr(H_2PO_4)(PO_4) \cdot 2\,H_2O$	$P2_1$	2	5.3825	6.6337	12.4102	98.687	75
γ-$Hf(H_2PO_4)(PO_4) \cdot 2\,H_2O$	$P2_1$	2	5.3499	6.5949	12.3939	98.594	76

[a] *Z* is the number of formula units per unit cell.

dral cavities. The water molecules are held at the centres of cavities by hydrogen bonds where the oxygen atom functions as the donor for two rather strong hydrogen bonds with the protons of neighbouring acid groups; one of the water protons forms a weak hydrogen bond with oxygen of the third acid group, while the second one is not involved in hydrogen bonding. Neutron diffraction studies showed a slight difference in the orientation of water molecules in the interlayer space of α-$E^{IV}(HPO_4)_2 \cdot H_2O$.[71] The hydrogen phosphate α-$Zr(HPO_4)_2 \cdot 0.5\,H_2O$ differs from the monohydrate by the hydrogen bond system.[73]

The proton-withdrawing ability of the HPO_4^{2-} groups in hydrogen phosphate is reduced by their coordination by cation in the oxidation state $+4$ having considerable polarizing properties. These groups tend to dissociate by the reaction

$$XO_3P-O-H + H_2O \rightleftharpoons XO_3P-O^- + H_3O^+$$

where XO_3P-O^- is a phosphate lattice fragment with the total oxidation state -1, incorporating the metal E^{IV}. As a result, compounds exhibit only cation exchange properties.[78]

Table 2 summarizes the interlayer distances and ion-exchange capacities of metal hydrogen phosphate hydrates with the oxidation state $+4$ of the metal. The interlayer distances in the γ-modifications of hydrogen phosphates [γ-$E^{IV}(HPO_4)_2 \cdot 2\,H_2O$] are much greater (Fig. 3) [30, 33, 75, 87] than in the α-modifications, which facilitates ion exchange processes. The structure has two types of PO_4 polyhedra. In the first type, all four oxygen atoms are shared with the $E^{IV}O_6$ octahedra and in the second type, only two O atoms are shared and the other are bonded to protons.[75, 88] Consequently, the $H_2PO_4^-$ anions become displaced into the interlayer space, resulting in moving apart of the layers (see Table 2). The bonding between the layers and, correspondingly, additional stability of the structure are provided by the hydrogen bonds between the phosphate oxygen atoms and water molecules. Note that anhydrous τ-$Zr(HPO_4)_2$ has a framework structure (composed of ZrO_6 octahedra linked by the HPO_4 tetrahedra) and a very narrow crystallization field close to the field of ZrP_2O_7; therefore, it is difficult to produce τ-$Zr(HPO_4)_2$ samples without ZrP_2O_7 impurity.[89]

Table 2. Interlayer distance and calculated ion exchange capacity of metal hydrogen phosphate hydrates in the oxidation state $+4$.

Compound	Interlayer distance / Å	Ion exchange capacity / mg equiv. g^{-1}	Ref.
α-$Ti(HPO_4)_2 \cdot H_2O$	7.56	7.75	67, 79
α-$Ge(HPO_4)_2 \cdot H_2O$	7.76	7.08	70, 80
α-$Zr(HPO_4)_2 \cdot H_2O$	7.60	6.64	81–83
α-$Sn(HPO_4)_2 \cdot H_2O$	7.81	6.08	66
α-$Hf(HPO_4)_2 \cdot H_2O$	7.58	5.15	72
α-$Pb(HPO_4)_2 \cdot H_2O$	7.92	4.79	66
α-$Zr(HPO_4)_2 \cdot 0.5\,H_2O$	7.42	–	73
γ-$Ti(HPO_4)_2 \cdot 2\,H_2O$	11.6	7.24	30, 67, 84, 85
γ-$Zr(HPO_4)_2 \cdot 2\,H_2O$	12.2	6.26	75, 86
γ-$Hf(HPO_4)_2 \cdot 2\,H_2O$	12.1	–	76

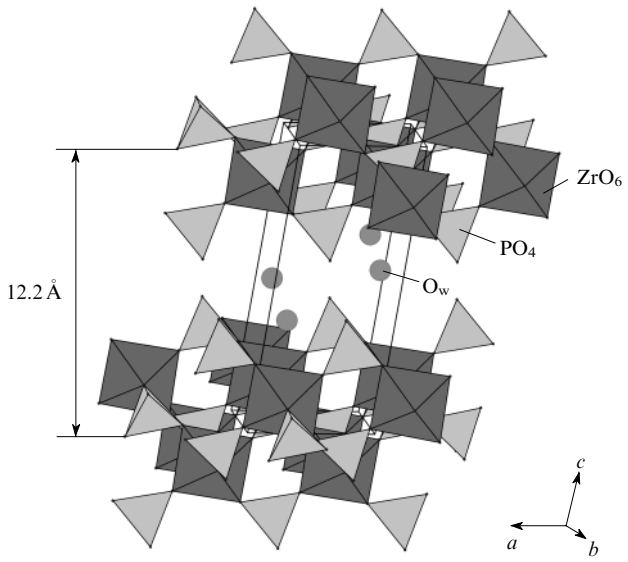


Figure 3. Fragment of the structure of γ-$Zr(HPO_4)_2 \cdot 2\,H_2O$.[75] Here and below O_w are the oxygen atoms of the water molecule.

Under ion exchange conditions, the M^+ cations can be inserted into the interlayer space and replace the protons of the acid groups

$$XO_3P-O-H + H_2O + M^+ = XO_3P-O-M^I + H_3O^+$$

The mechanism and energy characteristics of ion exchange for α- and γ-phosphates are determined by the structure of the initial hydrogen phosphate and the structural changes that occur during the exchange, while the possibility of the exchange is determined by the ratio of interlayer distances in the α- and γ-phosphates and the ratio of the exchanging ion radii and susceptibilities for hydration.

2. Synthesis and structure of the hydrated phosphates $M^IHE^{IV}(PO_4)_2$ and $M^I_2E^{IV}(PO_4)_2$

The replacement of protons in $E^{IV}(HPO_4)_2 \cdot H_2O$ by alkali metal cations occurs most often in two steps and affords new hydrated layered compounds of two types, $M^IHE^{IV}(PO_4)_2$ and $M^I_2E^{IV}(PO_4)_2$. The reactions that occur in the first and second steps of the exchange are described by the following equations:

$$E^{IV}(HPO_4)_2 \cdot H_2O + M^+ + HO^- + (m-2)\,H_2O = M^IHE^{IV}(PO_4)_2 \cdot m\,H_2O$$

$$M^IHE^{IV}(PO_4)_2 \cdot m\,H_2O + M^+ + HO^- + (n-m-1)\,H_2O = M^I_2E^{IV}(PO_4)_2 \cdot n\,H_2O$$

The formation of two substitution products may be due to the structural non-equivalence of the hydrogen atoms in hydrogen phosphates and steric hindrance to the accommodation of the second cation.

The diffusion of the M^I cations in α-$E^{IV}(HPO_4)_2 \cdot H_2O$ requires that they pass through a coordination polyhedron face formed by oxygen atoms with the entrance radius of 1.3 Å.[69] The Li^+ and Na^+ cations penetrate rather easily. Larger cations, K^+, Rb^+, Cs^+ in titanium phosphate and Rb^+, Cs^+ in zirconium phosphate, have to overcome a

substantial energy barrier. In this case, for the ion exchange to occur, a high pH of the solution should be maintained. The low activity of hydrogen ions in solution allows some more protons to come out from the ion exchange matrix. The matrix thus acquires a negative charge to give a potential difference between the ion exchanger and the solution, which predetermines the diffusion of the bulky cations inside the cation exchanger. Therefore, the exchange in α-$E^{IV}(HPO_4)_2 \cdot H_2O$ with lithium and sodium ions occurs in acidic solutions, while the exchange with caesium ions occurs only in alkalis.[30,81,90] Alberti *et al.*[81] performed sorption of caesium ions on zirconium hydrogen phosphate in the presence of traces of sodium ions. Sodium cations replace some of the protons on the crystal surface; as a result, the interplanar distances increase from 7.6 to 11.8 Å; the gap between the $[Zr(HPO_4)_2]_{2\infty}$ planes expands, and the caesium cations enter the lattice when pH is about 4. In the case of γ-$E^{IV}(HPO_4)_2 \cdot 2\,H_2O$ with much greater interplanar distance as compared with α-$E^{IV}(HPO_4)_2 \cdot H_2O$, the energy barrier is almost missing and the exchange of any cations easily occurs in acidic solutions.[30]

The kinetics of ion exchange in α-phosphates is controlled by the mutual diffusion of alkali metal and hydrogen cations through the layer of the emerging exchange product.[91] For coarsely crystalline samples, the exchange is rather slow and the equilibrium can be reached in several days.[92] In the exchange of protons for alkali metal ions in zirconium hydrogen phosphate, the H^+/Na^+ exchange occurs most rapidly; however, even in this case, the metastable phase $Na_2Zr(PO_4)_2 \cdot 3\,H_2O$ is formed and its disappearance may extend to several weeks.[92,93] The kinetic data for the H^+/Li^+ exchange in titanium hydrogen phosphate maintain the same trends that have been noted for the exchange in zirconium hydrogen phosphate; in the case of H^+/Na^+ exchange, the solid solutions Na_xH_{2-x}. .$Ti(PO_4)_2 \cdot n\,H_2O$ are formed.[94] The H^+/M^+ exchange (M = Li, Na) in tin hydrogen phosphate also involves the formation of the solid solutions $H_{2-x}M_xSn(PO_4)_2 \cdot n\,H_2O$.[95] The most likely reason for transition from the exchange mechanism occurring as drift of the interface between the two coexisting phases to the mechanism involving the formation of solid solutions is the decrease in the ion-exchange resin particle size.[91]

During the ion exchange in α-phosphates, the M^I cations reside in the interlayer space in the vicinity of the centre of an octahedron composed of oxygen atoms of the anions (Fig. 4) not coordinated by the cation in the oxidation state +4.[96–99] The size of any M^I cation is much smaller than the octahedral cavity in the interlayer space, which results in compression of these octahedra along the threefold axis. However, the decrease in the free volume is minor due to weak interaction of neighbouring layers and small charge of the phosphate oxygens caused by polarization by the atom in the oxidation state +4. This gives rise to the possibility of filling the interlayer space by water molecules. The large size of cavities between the $[E^{IV}(HPO_4)_2]_{2\infty}$ layers and the water molecules present in the coordination sphere of the singly charged cations account for their displacement from highly symmetrical positions. The M^I cation forms stronger bonds with some oxygen atoms of the anionic lattice and the interlayer distance is most often increased with respect to that in the initial acid phosphate. Depending on the formation conditions, one and the same compound may be hydrated to different extents. The number of water molecules changes in steps rather than smoothly on going from one degree of hydration to another. The replacement of the proton in $E^{IV}(HPO_4)_2 \cdot n\,H_2O$ by an alkali metal ion modifies the type of interaction of the water of crystallization in the hydrate lattice. Whereas in the monohydrates of hydrogen phosphates of d transition metals E^{IV}, the water molecule is hydrogen-bonded to the oxygen and hydrogen atoms of the hydrogen phosphate group, in the orthophosphates $M^I_2E^{IV}(PO_4)_2 \cdot n\,H_2O$, there is ion – dipole interaction between the alkali metal ion M^I and the water molecules of crystallization.

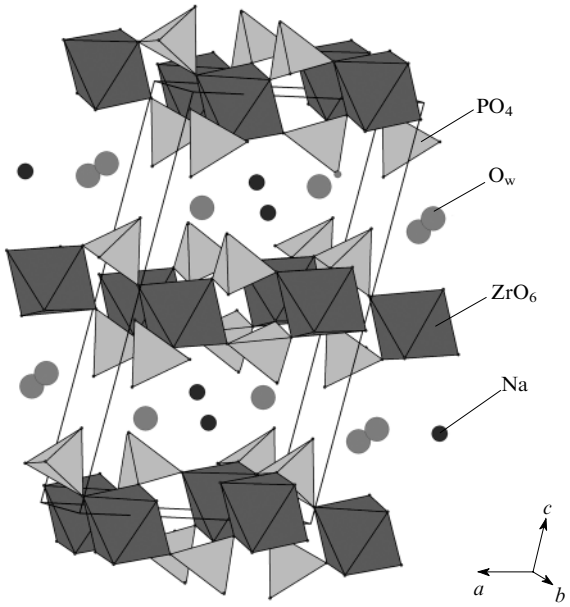


Figure 4. Fragment of the structure of $NaHZr(PO_4)_2 \cdot H_2O$.[98]

The synthesis of $M^I_2E^{IV}(PO_4)_2 \cdot n\,H_2O$ and $M^IHE^{IV}(PO_4)_2 \cdot n\,H_2O$ by the well-developed potentiometric titration procedure has been described for lithium,[30,100,101] sodium,[30,102,103] potassium,[30,104,105] rubidium and caesium[30,106–108] derivatives. The crystallographic characteristics of mixed-metal neutral and hydrogen phosphates generally described as $M^I_xE^{IV}_y(HPO_4)_z(PO_4)_u \cdot n\,H_2O$ are summarized in Table 3.

In the structure of products obtained upon complete replacement of protons by alkali metal ions, the M^I coordination sphere is formed in a specific way with the participation of the oxygen atoms of the anions and water molecules. The reason is that the number of highly symmetrical positions in the octahedron centre is half the number of M^I cations. Indeed, in $Na_2Zr(PO_4)_2 \cdot 3\,H_2O$ (Fig. 5),[99] four crystallographically different sodium atoms, Na(1)–Na(4), have different environments and coordination numbers (C.N.) of 7, 7, 6 and 4, respectively. The local environment of the Na^+ ion contains one to four water molecules and two to five oxygen atoms of the anions. Among these oxygen atoms, there are also atoms participating in the formation of the P–O–Zr bond. Unlike the low-symmetry $Na_2Zr(PO_4)_2 \cdot 3\,H_2O$ structure belonging to the triclinic system,[99] in the structure of monoclinic $(NH_4)_2$. .$Zr(PO_4)_2 \cdot H_2O$,[119] the two crystallographically nonequivalent ammonium ions are surrounded by five oxygen atoms, four of these belonging to the anions and the fifth one belonging to the H_2O molecule. This water molecule is

Table 3. Crystallographic characteristics of $M^{I}_{x}E^{IV}_{y}(HPO_4)_z(PO_4)_u \cdot n\,H_2O$.

Compound	Space group [a]	Z	Unit cell parameters				Ref.
			a Å	b Å	c /Å	β (or α, β, γ) /deg	
$NaZr(HPO_4)(PO_4) \cdot 5\,H_2O$	monoclinic	–	9.02	5.36	24.1	100	102
$NaZr(HPO_4)(PO_4) \cdot H_2O$ [b]	$P2_1/c$	4	8.8264	5.3494	16.0275	101.857	98
	monoclinic	–	8.88	5.35	16.67	109.3	102
$NaZr(HPO_4)(PO_4)$ [b]	$P2/c$	4	8.8666	5.3583	16.1284	115.96	109
	monoclinic	–	8.83	5.33	18.1	126.3	102
$KZr(HPO_4)(PO_4)$ [b]	$P2/c$	4	9.2208	5.3280	16.6336	114.351	96
$NH_4Zr(HPO_4)(PO_4)$ [b]	$P2_1/m$	2	5.3284	6.6217	11.326	96.63	110
$NaHf(HPO_4)(PO_4) \cdot 5\,H_2O$	monoclinic	4	9.079	5.354	24.01	100.05	103
$NaHf(HPO_4)(PO_4) \cdot H_2O$	"	4	8.870	5.340	16.83	109.65	103
β-$NaHf(HPO_4)(PO_4)$	"	4	8.730	5.160	18.12	123.75	103
$Li_3Zr_{1.5}(PO_4)_3$	$P2_1/n$	4	12.327	8.884	8.817	90.35	111
$Na_2Zr(PO_4)_2 \cdot 3\,H_2O$ [b]	$P1$	1	8.9192	10.5824	5.4045	α = 94.238, β = 90.164, γ = 111.013	99
	monoclinic	–	8.97	5.37	22.0	116.8	102
$Na_2Zr(PO_4)_2 \cdot H_2O$	"	–	9.18	5.26	23.9	134.6	102
α-$Na_2Zr(PO_4)_2$	"	–	8.74	5.38	20.9	124.5	102
	"	–	8.76	5.29	19.12	127.2	102
$Na_2Zr(PO_4)_2$	$R\bar{3}c$	6	8.792		22.723		112
$Na_3Zr_{1.5}(PO_4)_3$	trigonal	–	8.79		22.72		113
$K_2Zr(PO_4)_2$ (see [b])	$P\bar{3}$	1	5.176		9.011		114
	trigonal	–	5.2		9		115
	"	–	5.716		9.012		116
	cubic	–	9.0				117
$K_3Zr_{1.5}(PO_4)_3$	$R\bar{3}c$	–	8.708		23.964		118
$(NH_4)_2Zr(PO_4)_2 \cdot H_2O$ [b]	$P2_1/c$	4	9.131	5.417	19.19	102.7	119
$Na_2Hf(PO_4)_2 \cdot 3\,H_2O$	monoclinic	4	8.961	5.336	22.24	117.35	103
$Na_2Hf(PO_4)_2 \cdot H_2O$	"	4	8.743	5.371	20.95	124.36	103
α-$Na_2Hf(PO_4)_2$	"	4	8.747	5.380	20.936	124.42	103
β-$Na_2Hf(PO_4)_2$	"	4	8.779	5.308	19.025	126.52	103
γ-$Na_2Hf(PO_4)_2$	trigonal	–	8.794		22.698		103
$Li_2Sn(PO_4)_2 \cdot 2\,H_2O$	monoclinic	–	9.042	4.900	16.51	111.6	120
$Li_2Sn(PO_4)_2 \cdot H_2O$	"	–	9.02	4.916	16.67	111.7	120
$Li_2Sn(PO_4)_2$	"	–	8.67	4.95	16.63	110.4	120
$K_2Sn(PO_4)_2$	$P\bar{3}$	1	4.980		9.124		114

[a] When the space group has not been reliably determined, the system is given; [b] for these compounds, the crystal structure has been determined.

located between the NH_4^+ ions and forms a bridging hydrogen bond $NH_4^+ - HOH - NH_4^+$. Both phosphates have similar layered structures. The lowering of the crystal symmetry from monoclinic in $(NH_4)_2Zr(PO_4)_2 \cdot H_2O$ to triclinic in $Na_2Zr(PO_4)_2 \cdot 3\,H_2O$ is due to different formation mechanisms of phosphates: single-step intercalation of NH_3 into α-ZrP for the former compound and two-step ion exchange of the α-ZrP protons for the Na^+ ions in the latter.

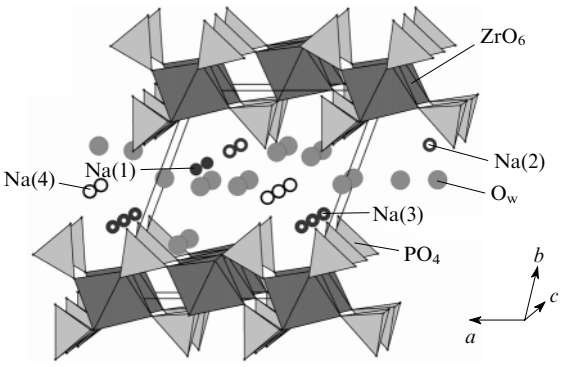


Figure 5. Fragment of the structure of $Na_2Zr(PO_4)_2 \cdot 3\,H_2O$.[99]

The removal of the same amounts of water from compounds of different cations M^{I} is accompanied by different energy effects. This is related to the pattern of ordering of water molecules in the compound structure and their bonding both with the interlayer cation and the E^{IV} – phosphate layer and with one another. The enthalpies of the dehydration involving the salt forms

$$M^{I}_2E^{IV}(PO_4)_2 \cdot n\,H_2O(s) \longrightarrow M^{I}_2E^{IV}(PO_4)_2(s) + n\,H_2O(liq)$$

decrease with an increase in the alkali metal ionic radius (Table 4). This effect is similar to a decrease in the dehydration enthalpies of alkali metal ions following the increase in the ion size and attests to inclusion of water molecules into the coordination environment of the M^{I} cation. The

Table 4. Enthalpies (kJ mol^{-1}) of the dehydration of $M^I_2E^{IV}(PO_4)_2 \cdot n\,H_2O$ at 298.15 K.

Initial crystal hydrate (E = Zr)	$\Delta_r H^\circ$	$\Delta_r h^\circ$ (see [a])	Initial crystal hydrate (E = Hf)	$\Delta_r H^\circ$	$\Delta_r h^\circ$ (see [a])	Ref.
$Li_2Zr(PO_4)_2 \cdot 4\,H_2O$	64.03	16.0	$Li_2Hf(PO_4)_2 \cdot 4\,H_2O$	69.26	17.5	121
$Na_2Zr(PO_4)_2 \cdot 3\,H_2O$	38.37	13.0	$Na_2Hf(PO_4)_2 \cdot 3\,H_2O$	39.87	13.5	122
$K_2Zr(PO_4)_2 \cdot 4\,H_2O$	32.62	11.0	$K_2Hf(PO_4)_2 \cdot 3\,H_2O$	34.84	11.5	123

[a] Average enthalpy of the dehydration per mole of liberated liquid water.

cation – water dipole interaction inside the lattice has a slight energy. The water molecules of crystallization remain molecularly individual in all compounds, although in the case of lithium and sodium derivatives, the ion – dipole interaction is expressed to a larger extent.

3. Synthesis and structure of the anhydrous phosphates $M^I_2E^{IV}(PO_4)_2$ and $M^IHE^{IV}(PO_4)_2$

The dehydration and thermolysis of $M^I_2E^{IV}(PO_4)_2 \cdot n\,H_2O$ and $M^IHE^{IV}(PO_4)_2 \cdot m\,H_2O$ with layered structure proceeds in the vast majority of cases along the same route:[29, 94, 103, 107, 124 – 128]

$$M^I_2E^{IV}(PO_4)_2 \cdot n\ H_2O \xrightarrow[-n\,H_2O]{348-373\ K} M^I_2E^{IV}(PO_4)_2 \xrightarrow[-0.5\,M^I_3PO_4]{673-1073\ K} 0.5\,M^IE^{IV}_2(PO_4)_3$$

$$2\,M^IHE^{IV}(PO_4)_2 \cdot m\,H_2O \xrightarrow[-2m\,H_2O]{293-673\ K} 2\,M^IHE^{IV}(PO_4)_2 \xrightarrow[-0.5\,M^IPO_3]{523-973\ K,\ -H_2O} M^IE^{IV}_2(PO_4)_3$$

The removal of the water of crystallization from the interlayer space with simultaneous moving of the layers towards one another results in a considerable decrease in the unit cell parameter c for the compounds $M^I_2E^{IV}(PO_4)_2 \cdot n\,H_2O$ and $M^IHE^{IV}(PO_4)_2 \cdot m\,H_2O$ (see Table 3). The crystal structure of anhydrous hydrogen phosphates $M^IHE^{IV}(PO_4)_2$ is formed by mixed-type layers composed of E^{IV} octahedra and PO_4 tetrahedra, the interlayer space being occupied by the M^I cations (Fig. 6).[96, 97, 109] The subsequent thermal decomposition of both acid and neutral phosphates induces structure rearrangement to give framework products $M^IE^{IV}_2(PO_4)_3$ related to the NZP type.[29, 129] According to the publications,[107, 130] on heating to 573 and 373 K, respectively, the compounds $K_2Zr(PO_4)_2 \cdot 3\,H_2O$ and $Rb_2Zr(PO_4)_2 \cdot H_2O$ lose only the water of crystallization, while anhydrous salts retain the layered structure up to 1273 K. The temperature ranges of water removal cited in various publications and the decomposition temperatures of hydrates of acid and neutral orthophosphates of the same metals M^I and E^{IV} often do not coincide. This is obviously due to different sample heating rates in thermal investigations, ambiguity in determination of the numbers of water molecules per formula unit of the same compounds and perhaps to different structures of the compounds being studied that have the same composition.

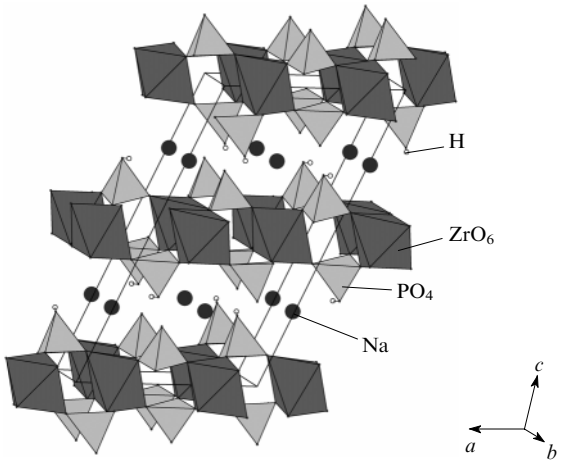


Figure 6. Fragment of the structure of $NaHZr(PO_4)_2$.[109]

The formation of anhydrous phosphates $M^I_2E^{IV}(PO_4)_2$ and $M^IHE^{IV}(PO_4)_2$ from hydrated compounds obtained by the proton/alkali metal cation ion exchange in aqueous solutions is faced with certain difficulties due to different degrees of crystallinity of the used metal phosphates with the metal oxidation state +4, their thermal instability at temperatures of 523 – 1073 K and sensitivity to minor changes in the conditions of synthesis (the order and velocity of mixing of the initial solutions, the chemical form, the reactant concentration and ratio, the acidity of the medium, the solution temperature, the duration of heating, keeping of the precipitates in the mother liquors and other characteristics). These factors hamper the control over the products of synthesis, and the synthesis of anhydrous salts by dehydration of hydrated salts is costly and requires much time.

It is obvious that for the formation of the phosphates $M^I_2E^{IV}(PO_4)_2$ and $M^IHE^{IV}(PO_4)_2$ with reproducible structure and properties, it is necessary to eliminate, whenever possible, the intermediate products, especially representing well-crystallizable phases with low diffusion mobility. The synthetic methods where the mixture of components is used as the precursor and the components react to give directly the desired product over a reasonable time intervals are only being developed and their potential has not been fully uncovered. Presumably, the solid-phase reactions

$$E^{IV}(HPO_4)_2 + 2\,M^ICl \longrightarrow M^I_2E^{IV}(PO_4)_2 + 2\,HCl$$

give $M^I_2E^{IV}(PO_4)_2$ at the molar ratio phosphate : chloride = 1 : 2, whereas at 1 : 1 ratio, NZP-like phases $M^IE^{IV}_2(PO_4)_3$ are formed. It was found [131] that solid-phase ion exchange reactions occur in mixtures of tin hydrogen phosphate with Na and K chlorides at 673 – 1023 K to give mono- and disubstituted phosphates $M^IHSn(PO_4)_2$ and $M^I_2Sn(PO_4)_2$. On further heating of the tin hydrogen phosphate – alkali metal chloride system at a phosphate : chloride molar ratio of 1 : 1, the compounds $M^ISn_2(PO_4)_3$ are formed, whereas at a 1 : 2 ratio, the major product is

$M^I_2Sn(PO_4)_2$. The possibility of this type of reaction in zirconium and hafnium double phosphates was reported in a number of papers.[78,132,133] Ultrasonic treatment can initiate the solid-phase H^+/Cs^+ ion exchange in the $Zr(HPO_4)_2 \cdot H_2O \cdot CsCl$ system at low temperature (343 ± 5 K). The ion exchange in an acoustic field increases the temperature of dehydration of the hydrogen phosphate and solid-phase exchange.[134]

Direct solid-phase reaction of M^IPO_3 with $E^{IV}O_2$ in a 2 : 1 molar ratio is presumably a convenient method for the synthesis of $M^I_2E^{IV}(PO_4)_2$. One more approach is the preparation of these phosphates by crystallization from a flux. The phosphate $K_2Zr(PO_4)_2$ was obtained by fusing together a mixture of K_2CO_3, ZrO_2 and KPO_3 (taken in excess) at 1273 K for several hours followed by fast cooling of the melt to 1193 K and slow cooling at 0.4 K h^{-1} to 1063 K.[114] The excess of K_2O prevented the formation of $KZr_2(PO_4)_3$. The hexagonal crystals of $K_2Zr(PO_4)_2$ were isolated from the solidified melt in boiling water.

The compounds $M^I_2E^{IV}(PO_4)_2$ have several peculiar structural features. In this group of phosphates, zirconium compounds were studied in most detail. A comparison of data reported in various papers has shown[102,104,111–114,117,118,125,128,130,135–139] that the structures of $M^I_2Zr(PO_4)_2$ samples are affected by the method and conditions of their synthesis. The anhydrous compounds, which were obtained by dehydration of the crystal hydrates prepared by the ion exchange between α-ZrP and the appropriate alkali metal salts in aqueous solutions, are layered structures inheriting the structure of the starting zirconium hydrogen phosphate. X-Ray diffraction studies of $M^I_2E^{IV}(PO_4)_2$ formed upon decomposition of hydrated forms consisted only in recording the X-ray diffraction patterns, the interplanar distance determined from the first small-angle reflection being usually the only value derived from the diffraction patterns. The results were not identical to one another. In some cases, several crystal modifications may exist for the phosphates $M^I_2Zr(PO_4)_2$ (M = Li, Na),[29,100,113,125,135] and $Na_2Hf(PO_4)_2$.[103] Indeed, in the case of $Na_2Zr(PO_4)_2 \cdot H_2O$, as the temperature increases from 413 to 1073 K, monohydrate is converted consecutively to three modifications of anhydrous $Na_2Zr(PO_4)_2$.[29,135] The unit cell parameters for various modifications of $Na_2Zr(PO_4)_2$ and $Na_2Hf(PO_4)_2$ (see Table 3) were calculated with the assumption that structure rearrangement during the H^+/Na^+ exchange and dehydration occurs within the monoclinic system with retention of the layered type. However, no direct structural studies were performed for these crystal phases.

The solid-phase synthesis or sol–gel process (in the presence of Cl^-) and heat treatment between 773 and 1173 K may yield phases of the framework structure[113,139] the composition of which is given by $M^I_3Zr_{1.5}(PO_4)_3$ (M = Li, Na, K). The introduction of 2.5 compensation M^I cations, for example Na^+, into the framework voids of $\{[Na_{0.5}Zr_{1.5}(PO_4)_3]^{2.5-}\}_{3\infty}$ is possible for the case of their random distribution among extraframework M1 and M2 sites (see Fig. 1) together with vacancies; this suggests the existence of polymorphism for $M^I_3Zr_{1.5}(PO_4)_3$ similar to that inherent in most sodium-containing phosphates $Na_3E^{III}_2(PO_4)_3$ (E = Fe, Sc, In, Cr) and $Na_3E^{III}(PO_4)_2$ (E = Y, Ln, In).[8,140] The powder X-ray diffraction data for $Na_2Zr(PO_4)_2$ obtained by the solid-phase method showed that it resembles $NaZr_2(PO_4)_3$,[112,113,118] while the sol–gel process afforded the monoclinic structure of the same compound.[118,139] The data on the thermal stability of $Na_2Zr(PO_4)_2$ are also ambiguous: according to one publication,[141] it decomposes at 1208 K before melting; other researchers[142] observed congruent melting at 1573 K for this phosphate.

The presence of several crystal modifications was noted for the double lithium zirconium phosphate.[100,125,136] For the solid-phase synthesis of $Li_2Zr(PO_4)_2$, binary or ternary mixtures: $2NH_4H_2PO_4 + Li_2CO_3 + ZrO_2$, $2NH_4H_2PO_4 + Li_2ZrO_3$ or $LiZr_2(PO_4)_3 + Li_3PO_4$ were used.[136] The synthesis was performed at 473–1173 K. The powder X-ray diffraction pattern of the resulting compound (the set of interplanar distances) differs from the X-ray diffraction data measured for the phosphate obtained by ion exchange.[100,125,137] The differential thermal analysis (DTA) curve for the phosphate $Li_2Zr(PO_4)_2$ obtained by the solid-phase method shows three endothermic peaks: at 1123, 1323 and 1473–1543 K. Presumably,[136] the reversibility of the first two effects is related to polymorphic transformations. The third effect is irreversible being due to the sample melting. The $4Li^+ \rightarrow Zr^{4+}$ replacement accompanied by a decrease in the lithium content in the unit cell of $Li_2Zr(PO_4)_2$ affords the solid solutions $Li_{2-4x}Zr_{1+x}(PO_4)_2$ with $0 \leqslant x < 0.25$.[136]

The phosphate $K_2Zr(PO_4)_2$ obtained by crystallization from a flux is the only phosphate $M^I_2E^{IV}(PO_4)_2$ that has been investigated by single-crystal X-ray diffraction to determine the crystal structure (Fig. 7).[114] In the structure of the phosphate, the close-packed ZrO_6 layers are perpendicular to the *c* axis. Every ZrO_6 octahedron is connected through oxygen atoms with six slightly distorted PO_4 tetrahedra. The potassium atoms (C.N. 7) reside between the layers. The P–O interatomic distances are 1.508–1.548, Zr–O 2.072, K–O 2.606–2.990 Å. Under definite conditions of synthesis, $K_2Zr(PO_4)_2$ crystallizes in the hexagonal[114,118] or cubic[117] modifications. The compound melts with decomposition at 1723 K.[142]

Thus, the results of powder X-ray diffraction suggest that, depending on the method of synthesis, the phosphates $M^I_2E^{IV}(PO_4)_2 (\equiv M^I_3E^{IV}_{1.5}(PO_4)_3)$ may have either layered or framework structure. The atomic structures of these phosphates [except for $K_2Zr(PO_4)_2$] have not been studied to date; therefore, the refinement of the crystal chemical properties of anhydrous $M^I_2E^{IV}(PO_4)_2$ is of interest by itself.

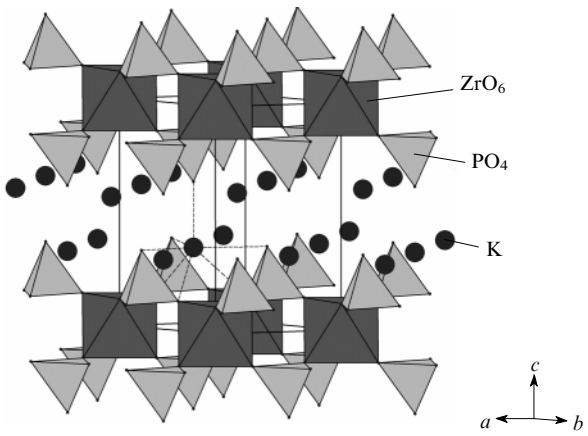


Figure 7. Fragment of the structure of $K_2Zr(PO_4)_2$.[114]

4. Properties of layered phosphates

Using acidic calorimetry, the standard enthalpies of formation ($\Delta_f H^\circ$) of $M^I_2E^{IV}(PO_4)_2$ (M = Li, Na, K; E = Zr, Hf) and their crystal hydrates were determined at 298.15 K.[121–123] The phosphates $M^I_2E^{IV}(PO_4)_2 \cdot n\,H_2O$ were synthesized by pH-metric titration of $E^{IV}(HPO_4)_2 \cdot H_2O$ with aqueous solutions of alkali metal hydroxides. Anhydrous compounds were prepared by dehydrating the corresponding crystal hydrates. The difference between the standard enthalpies of formation of anhydrous products and the crystal hydrates is virtually the same for zirconium and hafnium compounds at any M^I, being equal to

$$\Delta(\Delta_f H^\circ) = \\ = [\Delta_f H^\circ(M^I_2E^{IV}(PO_4)_2) - \Delta_f H^\circ(M^I_2E^{IV}(PO_4)_2 \cdot n\,H_2O)] = \\ = 299.0 \pm 3.0 \text{ kJ}$$

per mole of water of crystallization (Table 5). The effect of water of crystallization results in $\Delta_f H^\circ(298)$ of crystal hydrates being higher than that of anhydrous compounds. In addition, the difference between the standard enthalpies of formation of zirconium compounds and related hafnium compounds is

$$\Delta(\Delta_f H^\circ) = \\ = \Delta_f H^\circ[M^I_2Zr(PO_4)_2 \text{ or } M^I_2Zr(PO_4)_2 \cdot n\,H_2O] - \\ - \Delta_f H^\circ[M^I_2Hf(PO_4)_2 \text{ or } M^I_2Hf(PO_4)_2 \cdot n\,H_2O] = \\ = 18.5 \pm 2.5 \text{ kJ mol}^{-1}.$$

The standard enthalpies of hydrogen exchange in the structure of α-$E^{IV}(HPO_4)_2$ for lithium, sodium and potassium ions

$$2\,M^+(aq.) + \alpha\text{-}M^{IV}(HPO_4)_2(s) \longrightarrow \\ \longrightarrow M^I_2E^{IV}(PO_4)_2(s) + 2\,H^+(aq.)$$

linearly decrease following the decrease in the enthalpy of dehydration of alkali metal ions in aqueous solutions ($\Delta_h H^\circ$). Using these $\Delta_h H^\circ(M^+, aq.)$ correlations for rubidium and caesium ions, the enthalpies of the above reactions involving these ions were determined; the standard enthalpies of formation of $M^I_2E^{IV}(PO_4)_2$ are 3636, 3655, 3664 and 3683 kJ mol^{-1} for $Rb_2Zr(PO_4)_2$, $Rb_2Hf(PO_4)_2$, $Cs_2Zr(PO_4)_2$ and $Cs_2Hf(PO_4)_2$, respectively.

The accumulation of thermodynamic data for chemical reactions involving these compounds would show which of the possible reactions can proceed spontaneously under specified conditions (temperature, pressure, concentration) and also how the conditions must be changed to induce the reaction of interest to proceed in the desired direction to give products in reasonable yields.

Table 5. Standard enthalpies of formation (kJ mol^{-1}) of $M^I_2E^{IV}(PO_4)_2$ and their crystal hydrates at 298.15 K.

Anhydrous phosphate	$-\Delta_f H^\circ$	Crystal hydrate	$-\Delta_f H^\circ$	Ref.
$Li_2Zr(PO_4)_2$	3651.5	$Li_2Zr(PO_4)_2 \cdot 4\,H_2O$	4769.0	121
$Li_2Hf(PO_4)_2$	3578.5	$Li_2Hf(PO_4)_2 \cdot 4\,H_2O$	4791.0	121
$Na_2Zr(PO_4)_2$	3554.5	$Na_2Zr(PO_4)_2 \cdot 3\,H_2O$	4450.5	122
$Na_2Hf(PO_4)_2$	3573.0	$Na_2Hf(PO_4)_2 \cdot 3\,H_2O$	4470.5	122
$K_2Zr(PO_4)_2$	3623.5	$K_2Zr(PO_4)_2 \cdot 3\,H_2O$	4513.5	123
$K_2Hf(PO_4)_2$	3640.5	$K_2Hf(PO_4)_2 \cdot 3\,H_2O$	4533.0	123

Layered phosphates have not yet found industrial use, which is largely due to the lack of convenient methods for their preparation; nevertheless, they are studied in detail as model objects for investigations of the exchange sorption and for generalization of thermodynamic and kinetic views on ion exchange in inorganic matrices.[32, 51, 93, 133, 143] An advantage of layered compounds is high concentration of the accessible sorption sites or ion exchange groups. The possibility of selecting compounds with different interlayer distances can be used to trace in detail the effect of this parameter on the process dynamics.

The studies devoted to ion transport processes and chemical modification of the layered phosphate surface leading to enhancement of transport properties appear promising.[29, 34, 39, 54, 95, 137, 144–150] By the example of α-ZrP, which is one of the best known solid proton-conducting electrolytes, it was shown that the conductivity of a system consisting of coarse particles does not depend on their size, while as the particle size decreases below 100 nm, the conductivity rapidly grows.[151] This behaviour can be attributed to the increase in the specific surface area of the compound following the decrease in the particle size. The H^+ ions (and water molecules), which are located on the surface of the compound and have enhanced mobility due to the uncompensated valence (hydrogen) bonds and lower steric hindrance to the transfer in the near-surface layer, also carry along the ions from deeply lying layers. For the crystal of α-ZrP, the fraction of mobile (surface) ions increases with temperature.[151]

The properties of proton-conducting single-phase samples can be enhanced by using composites containing nanoparticles of inorganic substances (or polymers). The conductivity increases due to phase interfaces. In this case, the particle size is comparable with the thickness of the surface Debye layer, and the smaller the particle size of the initial components, the greater the specific area of the interface and the higher the conductivity. For some composite materials of this type, the ionic conductivity reaches 10^{-3}–3×10^{-1} S cm^{-1} (Refs 42, 152–155). The data on the composition, structure and properties of ion-conducting nanocomposites, including inorganic composites and hybrid membrane materials based on polymers, can be found, for example, in reviews.[45, 156]

Considerable effort is made to study the products of intercalation of amines, alcohols and other organic compounds with functional groups capable of binding to protons in Group 4 d transition metal hydrogen phosphates.[31, 33, 35, 36, 38, 41, 44, 53, 157–165] Original quasi-two-dimensional nanoreactors as rigid graphite-like planes connected by flexible polymethylene bridges were produced based on the decane-1,10-diphosphonate derivative of zirconium γ-phosphate $ZrPO_4[O_2P(OH)_2]_{1-x}[O_2P(OH)-(CH_2)_{10}-(HO)PO_2]_{x/2} \cdot m\,H_2O$.[166] The distances between the graphite-like planes in these reactors can be varied by changing either the number of $(CH_2)_n$ bridge atoms (for example, n = 4, 6, 8, 10, 12, 16) or the number (density) of bridges. The reversible compression–expansion of the interplanar space is achieved by stimulating the conformational transitions in the polymethylene chains from a coil (the planes are close to one another) to an extended chain (the planes are furthest separated). These transitions can be smoothly adjusted by tuning the nanoreactor to a specified

volume by filling with a solvent. This system resembles a 'squeeze-box' and its reversible compression–expansion simulates the muscle contraction. Catalysts can be placed on this molecule and catalytic reactions can be performed. It can also serve as a multifunctional and reversibly operating molecular container capable of capturing specified molecules and releasing these molecules upon change in the conditions.

III. Complex and mixed phosphates of d and f transition (E^{IV}) and alkaline metals with the P : E^{IV} ratios of 1.5 and 3

There is vast literature on the preparation procedures for the phosphates $M^{I}E_2^{IV}(PO_4)_3$ and $M_5^{I}E^{IV}(PO_4)_3$ that belong to the NZP and related families. The key approaches to the synthesis of poly and single crystals of compounds are based on reactions that occur in solid phases, aqueous solutions (sol–gel process and hydrothermal synthesis) and melts (alkali metal chlorides and nitrates, boron oxide).

1. Synthesis

In the preparation of the phosphates $M^{I}E_2^{IV}(PO_4)_3$ and $M_5^{I}E^{IV}(PO_4)_3$ by solid-phase sintering ('ceramic method') (Fig. 8), the salts (chlorides, nitrates, carbonates, oxalates) or oxides of metals M and E and ammonium hydrogen and dihydrogen phosphate are used as the starting compounds. A thin mixture of stoichiometric amounts of the starting compounds (batch) is subjected to heat treatment at definite temperatures with intermediate dispersion.[112, 167, 168] In some cases, the powders are pressed to discs and sintered at high ($\geqslant$1273 K) temperatures to ensure more complete conversion and to produce ceramic samples. The phase composition of the initial batch, the method of initiation (including mechanochemical activation and repetition of the grinding–pressing–annealing cycle) and the reaction conditions (temperature, time and annealing atmosphere) can be varied depending on the particular procedure. The temperature of the synthesis can be derived using empirical Tamman's rule: $T_{react} \geqslant (2/3-3/4)T_m$ (of the product or the most high-melting reactant); the synthesis time (τ) can be estimated from the size of the reactant particles (l) and the diffusion coefficient (D) of the slowest ion:

$$\tau \sim \frac{l^2}{D}.$$

The drawbacks of the solid-phase method is that the formation of the final product requires long time, higher annealing temperatures compared to those in other processes and thorough dispersion of the powders in each step.[169] It is possible to increase the reactivity of the batch, which mainly depends on the nature and the decomposition temperature of the starting reactants, and the solid-phase

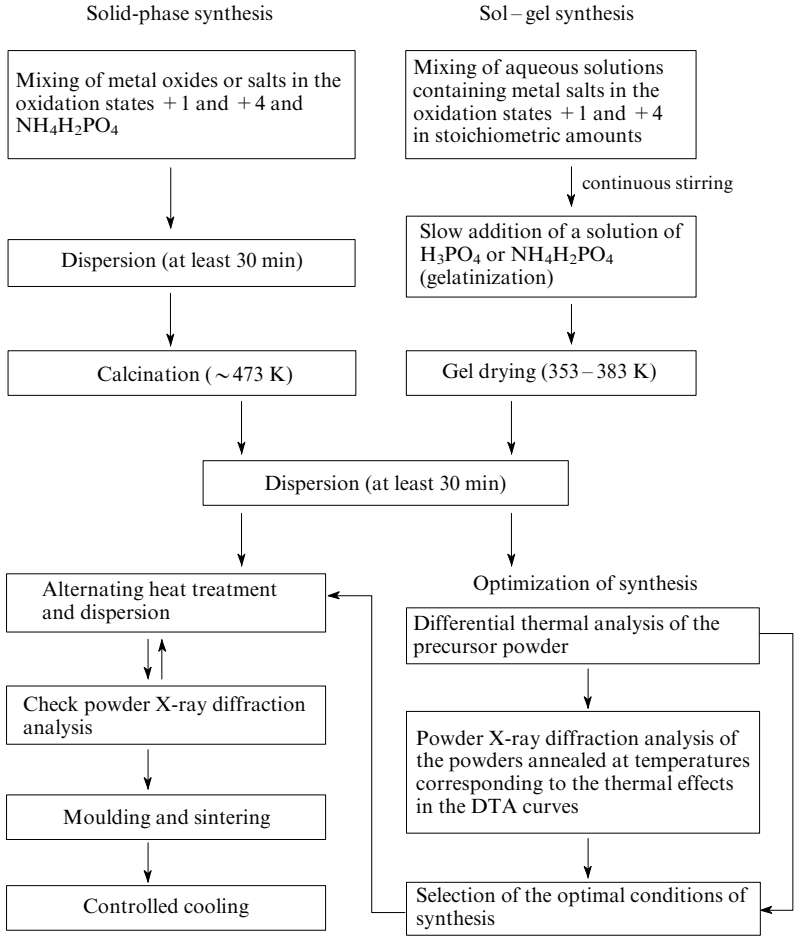


Figure 8. Chart of the production of the phosphates $M^{I}E_2^{IV}(PO_4)_3$ and $M_5^{I}E^{IV}(PO_4)_3$.[9]

reaction rate (by several orders of magnitude) by mechanochemical activation,[170,171] in particular, treatment of solids and solid mixtures in a mill (vibration or planetary mill, disintegrating mill). The superfine milling gives rise to new active sites on the fresh solid surface and accelerates diffusion processes.

Yet another version of solid-phase synthesis in which the reaction product $M^{I}E_2^{IV}(PO_4)_3$ is formed at much lower temperature (323–423 K) is based on the reaction of d transition metal hydrogen phosphate and the corresponding neutral alkali metal phosphate:

$$6\,E^{IV}(HPO_4)_2 + M^{I}_3PO_4 \xrightarrow{323-423\ K} 3\,M^{I}E_2^{IV}(PO_4)_3 + 6\,H_2O + 2\,P_2O_5$$

The duration of the synthesis varies from 1 to 4 h depending on the chosen temperature. At the end of the process, cooling to room temperature affords a cake consisting of the reaction product, the remaining reactants (present in excess) and other compounds formed in the reactions. The phosphates $M^{I}E_2^{IV}(PO_4)_3$ are almost insoluble in water and in aqueous solutions of mineral acids, and they can be washed with water or acidified aqueous solutions to remove other components (alkali metal phosphates). The reaction of α-ZrP with lithium carbonate and zirconium oxide may produce the NASICON phase $LiZr_2(PO_4)_3$ at a relatively low temperature (873 K), preventing the partial loss of lithium caused by high volatility of its compounds.[172] Highly crystalline phosphate is formed at 1473 K: to this end, the powder obtained in the first stage of the synthesis is pressed into pellets and covered by the same powder in which the lithium content is increased by 10%.

The solid-phase synthesis may be the preferred method for preparing phosphates for structural studies if a mixture of components that react to give directly the final products is used as the precursor or if the pure target product cannot be obtained from solutions or melts.

The efforts of many research groups in recent years have been directed to improvement of the sol–gel process based on the sol–gel transition in aqueous sols or on the hydrolytic polymerization of metal alkoxides or other organic compounds of metals.[173–179] According to the first version of this method (see Fig. 8), aqueous solutions of inorganic M^{I} and E^{IV} salts are poured together under stirring, then a solution of the phosphorus reactant is added, and the resulting gel is dried at 353–383 K and subjected to consecutive heat treatment under free access of air at definite temperatures. The stepwise heating is alternated with dispersion in each stage. The second version of sol–gel synthesis is based on the use of co-hydrolysis of alkoxides and other organic compounds of metals. If ethanol serves as the liquid phase of the gel, the reaction is carried out using the ambient moisture or directly an aqueous solution of the inorganic component added to the organic solution. The polycondensation stage results in compression of the homogeneous gel until the gel is dry. The transformation of the gel into the final product is accomplished by alternating sintering, dispersing and pressing. The key problem is in the different rates of hydrolysis of different metal alkoxides.

Yet another version of the sol–gel process is the citrate method proposed by Pechini.[180] This method is based on the ability of α-hydroxycarboxylic acid to chelate metal cations and undergo polycondensation (esterification) with polyhydric alcohols. Most often, citric acid and ethylene glycol are used. Esterification is performed at 393–423 K. The subsequent thermolysis of the gel affords a finely dispersed (nanostructured) form of the final product.[181]

The advantages of the solution processes include the easy preparation of solutions and easy control of the solution composition and powder particle size and morphology, and the resulting high degree of product homogeneity and purity. The process time is reduced and the temperature of product formation decreases as compared with the solid-phase reaction conditions. The least studied stage of the synthesis is the variation of the solid particle size with time, particle aggregation and, hence, the possible formation of 'rigid' (with ionic-covalent chemical bonds) agglomerates of ultradispersed particles. The 'rigid' agglomerates in the ceramic structure formed upon sintering have an effect similar to the effect of foreign inclusions, leading to deterioration of mechanical properties.[182,183]

Crystallization from solutions becomes more versatile when high pressures are used. The hydrothermal method considerably extends the existence region of the liquid phase and allows the synthesis of crystalline phosphates at moderate temperatures (473–623 K). Often it provides well-formed crystals suitable for X-ray diffraction. Two modifications of this method are known.[128,184–189] According to the first one, the starting reactants (metal hydroxides, oxides and salts, phosphoric acid, α-ZrP) are mixed in water in specified molar ratios and kept at 473–623 K in an autoclave for a specified period of time. The most important factors for the formation of phases of a desired composition include the initial pH of the solution ($1 < pH < 2$) and the temperature conditions. According to the second modification, stoichiometric amounts of aqueous solutions of M^{I} and E^{IV} salts are poured together under continuous stirring at room temperature and then a solution of phosphoric acid is added. The gel thus formed is dried at ~353 K, mixed again with water and kept under hydrothermal conditions at 473–623 K. Baranchikov and co-workers[190,191] ascertained that ultrasonic treatment during the hydrothermal synthesis can substantially increase the crystallization rate of X-ray amorphous gels giving highly dispersed powders.

The use of the hydrothermal method requires considerable time and cost to elucidate the features of the formation of solid products, *i.e.*, to choose the optimal reactant ratios, temperature and pressure. It is difficult to prepare phosphates of complex composition by this method.

In other solvents (or in melts), the selection of the synthesis conditions is related to the solvent nature. For the preparation of the orthophosphates $M^{I}E_2^{IV}(PO_4)_3$, the reactions are performed in metal chlorides at temperatures 10–20° higher than the melting point of the corresponding alkali metal halide: at 893, 1093, 1063, 1013 and 943 K for LiCl, NaCl, KCl, RbCl and CsCl, respectively. A stoichiometric mixture of zirconium (titanium, hafnium) hydrogen phosphate and alkali metal chloride is heated to the specified temperature and maintained at this temperature for 0.5–2 h.[192] The melt is cooled and the soluble fraction is extracted with acidified water, while the insoluble fraction is dried. More rarely, crystallization from a flux of alkali metal nitrate is used.[116,193,194]

The phosphates $M^{I}E_2^{IV}(PO_4)_3$ and $M^{I}_5E^{IV}(PO_4)_3$ can also be obtained using reactions in multicomponent systems $E^{IV}O_2-M^{I}PO_3-M^{I}_4P_2O_7-M^{I}_2P_4O_{11}$ (Refs 142, 195, 196) in which molten phosphates function simultaneously as

reactants and solvents or the reaction of zirconium (hafnium) chloride dissolved in a melt of alkali metal chloride with a neutral alkali metal orthophosphate.[192] In the latter case, the reaction

$$E^{IV}Cl_4 + M^I_3PO_4 \xrightarrow{M^ICl} M^IE^{IV}_2(PO_4)_3$$

M = Li, Na, K, Rb, Cs; E = Zr, Hf

takes place in the liquid phase at 893–1093 K depending on the flux agent chosen.

One more method is based on the ability of NZP phosphates to undergo ion exchange, which allows preparing new compounds by replacing one alkali metal by another in a boron oxide melt. The reactants comprise freshly prepared oxide $E^{IV}O_2$ and phosphate M^IHPO_4.[11, 197] The reaction is carried out at 1473 K for 18–20 h. Then the temperature is slowly decreased and the resulting cake is washed by boiling in acidified water.

Drawbacks of the solution and melt processes are long-term drying and washing of samples and often high temperature.

Single crystals can be synthesized by all known methods, namely, growing in the solid phase, from solutions and from melts.[16, 139, 198–203] Experiments on NZP phosphate crystallization demonstrate great difficulties associated with the preparation of large single crystals of these compounds. The difficulties are caused by specific structural features and thermal behaviour of the NZP compounds: incongruent melting of many phosphates, their partial dissociation to give other phases, inclusion of the second phase and high reactivity of the melts. Altogether, this causes a substantial deterioration of the quality of grown crystals. To our knowledge, no universal procedures or even eutectics that can serve as high-temperature solutions for growing phosphate single crystals are available: each procedure is individual to a certain extent. Thus, the crystals of $NaZr_2(PO_4)_3$ with a size of up to several millimetres were grown from a solution in the melt.[199] As the starting reactants, Na_2CO_3, ZrO_2 and $NH_4H_2PO_4$ were used; a melt of a NaF and V_2O_5 mixture was used as the solvent. The crystal nucleation from a flux agent (volume 100–150 cm^3) was performed on a rotating platinum rod. In the $Na_2O-ZrO_2-P_2O_5-NaF-V_2O_5$ system, depending on the temperature and concentration of the components, the phases ZrO_2, $Na_5Zr(PO_4)_3$ and $NaZr_2(PO_4)_3$ may crystallize. The hexagonal plates of $Na_5Zr(PO_4)_3$ grow in the region depleted in ZrO_2. The crystals of $NaZr_2(PO_4)_3$ are formed from the flux with $0.07\,Na_2O \cdot 0.07\,ZrO_2 \cdot 0.32\,P_2O_5 \cdot 0.47\,NaF \cdot 0.07\,V_2O_5$ composition in the temperature range from 1023 to 1223 K on cooling the system at a rate of 0.5–2 K h^{-1}.

Apart from the classical methods described above, there are methods of synthesis based on chemical or electrochemical intercalation of cations into NZP matrices.[204–206] A necessary condition of intercalation (insertion) is the presence of metal atoms having variable oxidation state (*e.g.*, titanium) in the host structure and cations in the structure channels. Some lithium and sodium derivatives were prepared by redox reactions with reducing agents such as butyllithium or sodium in naphthalene. In this case (unlike high-temperature synthesis methods), the cavities in the NZP structure are filled with cations. By using electrochemical methods, it is possible to control the synthesis of materials with different occupancies of structural channels by cations and to carry out ion exchange by rather simple charge–discharge operation. The resulting phases are usually structural analogues of the starting compound and are metastable.

The controlled combustion synthesis of NZP compounds is based on exothermic self-sustained reaction between the components using an internal heat evolution source.[207] For this synthesis, an aqueous solution of metal and ammonium salts in the specified ratio is prepared, the combustible organic compound is added, and the resulting gel is dried. After decomposition of the gel, the product spontaneously ignites during heating. Further heat treatment produces the desired complex phosphate. For example, the initial batch for the preparation of sodium dizirconium phosphate is prepared from sodium nitrate, zirconium oxide dinitrate, ammonium hydrogen phosphate, ammonium perchlorate and carbonyldihydrazine [$H_2NNHC(O)NHNH_2$]. At 673 K, the products of decomposition of carbonyldihydrazine (HNCO, CO, NH_3) and metal M and E nitrates (nitrogen oxides) give rise to a large amount of gases, ignite and induce a short-term heating of the mixture to 1373 K. The formation of $NaZr_2(PO_4)_3$ can be represented by the equation

$$NaNO_3 + 2\,ZrO(NO_3)_2 + 3\,(NH_4)_2HPO_4 + 5\,NH_4ClO_4 + 3\,CH_6N_4O \longrightarrow NaZr_2(PO_4)_3 + 3\,CO_2 + 30\,H_2O + 14\,N_2 + 5\,HCl + 2\,O_2$$

[54 moles of gases per mole of $NaZr_2(PO_4)_3$ are formed]. The active stage of the process takes several tens of seconds. This time is sufficient for the phase formation reactions to take place but too short for removal of the components upon vaporization. As the advantages of the method, one should note its cost effectiveness (the expenses for initiating the reaction are much lower than the energy needed to perform long-term high-temperature annealing in the 'ceramic' synthesis), the equipment simplicity and high speed of the combustion process. However, the last-mentioned point is also responsible for obvious drawbacks: the fast combustion process is difficult to control; in addition, during the active stage of the process, the desired reaction often has no enough time to proceed to completion.

A number of sodium-containing crystalline and glass-like double NZP phosphates were successfully prepared[208–211] by microwave heating of mixtures of the hydrated phosphate $NaH_2PO_4 \cdot 2\,H_2O$ or the anhydrous phosphate $NH_4H_2PO_4$ with various oxides and salts [TiO_2, ZrO_2, Na_2CO_3, $ZrO(NO_3)_2 \cdot 5\,H_2O$, *etc.*]. The absorption of microwave electromagnetic radiation resulting in the sample heating is due to orientational transitions of the dipole water molecules of crystallization. By microwave irradiation (2.45 GHz), sodium hydrogen phosphate can be rapidly heated to 1000 K and above. The activation of the reaction mixture by microwave treatment appreciably reduces both the reaction time and the energy consumption as the heating source is located inside the reaction zone. The time of synthesis of phosphates is 6–15 min, and powder sintering to form a compact material with a density close to the theoretical density (at temperatures much lower than the usual sintering temperature) is completed in 30 min.

Analysis of the vast literature devoted to the preparation of $M^IE^{IV}_2(PO_4)_3$ and $M^I_5E^{IV}(PO_4)_3$ shows that the choice of the synthesis method relies on the chemical characteristics of the starting compounds and the required oxidation states

of cations in the final structure. In the synthesis of chemically homogeneous phosphates, for the optimal organization of the reaction zone, on the route from the starting reactants to the target crystalline product, it is expedient to use precursors with definite reproducible chemical and phase composition and activity (the latter is determined by their chemical and thermal prehistory) and synergism of various types of treatment (heating, pressure, intensive grinding, ultrasonic and microwave fields), which removes the intermediate decomposition products as readily crystallizing phases with low diffusion mobility and ensures the formation of X-ray amorphous intermediate states and final crystalline products at temperatures as low as possible.[212]

2. Structure

The key common structural feature of the phosphates $M^{I}E_2^{IV}(PO_4)_3$ and $M_5^{I}E^{IV}(PO_4)_3$ is that they belong to the NZP (NASICON)[112] and scandium tungstate (SW)[213] structural types, which are widely encountered among inorganic salts with tetrahedral PO_4^{3-} anions.[2–5,8,214] They refer to three-dimensional structures based on the $\{[L_2(PO_4)_3]^{p-}\}_{3\infty}$ framework.

The crystal chemical analysis of phosphate structures with $\{[L_2(PO_4)_3]^{p-}\}_{3\infty}$ frameworks carried out by Pet'kov *et al.*[12] demonstrated that the main structure-forming units are stable separate groups, lanterns (Fig. 9), consisting of two L octahedra connected by three bridging P tetrahedra; inside the lantern, there is a small cavity with a trigonal prismatic geometry. The chemical bonds within this group are much stronger than the bonds of these groups with one another or with cations that occupy the framework cavities and participate in the formation of the compound. Different mutual orientations of the lanterns under the influence of iso- and heterovalent replacements of the cations, both those located in the proper framework sites and those located in the cavities between the L and P polyhedra, and under the influence of external treatment (temperature, pressure) give rise to the structural diversity of this type of objects.[4]

The chart of symmetry relationships between the structures of compounds having the $\{[L_2(PO_4)_3]^{p-}\}_{3\infty}$ frameworks reported by Pet'kov *et al.*[4,12] is shown in Fig. 10. The central point shows the most highly symmetrical structure with space group $R\bar{3}c$. The parent NZP structures, $NaZr_2(PO_4)_3$ and $KZr_2(PO_4)_3$, crystallize particularly in this space group. The groups shown above are subgroups

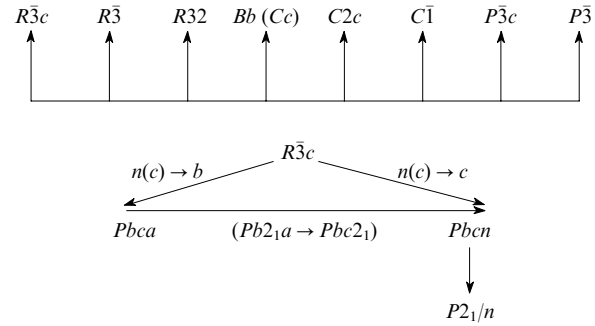


Figure 10. Symmetry relationships of phosphate structures with the $\{[L_2(PO_4)_3]^{p-}\}_{3\infty}$ frameworks (see text).[12]

of $R\bar{3}c$. The change in the symmetry of these structures is caused by minor distortions of the frameworks upon inclusion of various atoms into the framework and diverse types of filling of the cavities. The space groups located below correspond to the phosphates whose frameworks are composed of fragments of the initial framework. Furthermore, due to structural transformations caused by redistribution of chemical interactions in the crystal and accompanied by decrease in the symmetry, $P2_1/n$ symmetry is inherited only from space group *Pbcn* and does not contain symmetry elements of space group $R\bar{3}c$. The rhombohedral symmetry of the framework arises in the case of stacking packing of tetranuclear complexes that consist of two P tetrahedra combined into a closed structure with two L octahedra, while the monoclinic structure is formed in the case of herringbone packing of the same groups (Fig. 11).[215] Different spatial arrangements of these L and P polyhedra in these frameworks gives rise to diverse numbers and shapes of the arising cavities with retention of stable structural fragments (lanterns).

Among the double phosphates of M^{I} and E^{IV} cations, the compounds $M^{I}E_2^{IV}(PO_4)_3$ are most abundant (Table 6). X-Ray diffraction data are available for many of them. The greatest number of $M^{I}E_2^{IV}(PO_4)_3$ have the NZP structure and trigonal symmetry. Their crystal structures represent frameworks of $E^{IV}O_6$ octahedra and PO_4 tetrahedra, which are connected through common oxygen atoms and form infinite columns parallel to a $\bar{3}$ axis (the *c* axis of the unit cell); the numbers of extraframework sites of two types (M1 and M2) are related as 1 : 3 (see Fig. 1). The M1 site is

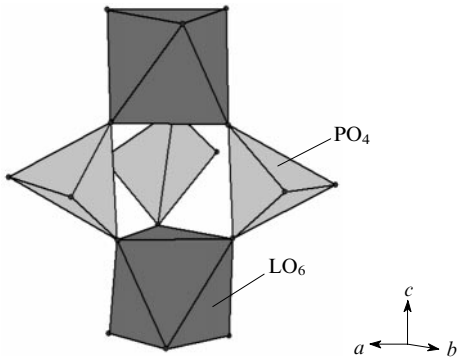


Figure 9. Schematic view of the structure-forming unit of the $\{[L_2(PO_4)_3]^{p-}\}_{3\infty}$ framework ('lantern').[12]

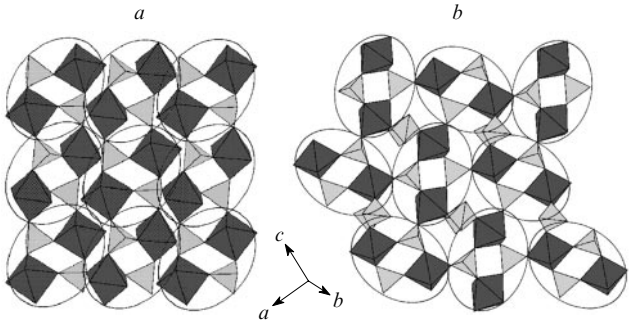


Figure 11. Stacking (*a*) and herringbone (*b*) packing of the tetranuclear complexes $2LO_6-2PO_4$ in the structures of compounds with the $\{[L_2(PO_4)_3]^{p-}\}_{3\infty}$ frameworks (author's data).

Table 6. Crystallographic characteristics of $M^{I}E_2^{IV}(PO_4)_3$.

Compound	Space group [a]	Unit cell parameters				Ref.
		a /Å	*b* /Å	*c* /Å	*β* (or α, *β*, *γ*) /deg	
$LiTi_2(PO_4)_3$ (see [b])	$R\bar{3}c$	8.51173		20.8524		167
$NaTi_2(PO_4)_3$ (see [b])	$R\bar{3}c$	8.4854		21.7994		216, 217
$KTi_2(PO_4)_3$ (see [b])	$R\bar{3}c$	8.367		23.074		218
	$P2_13$	9.77				219
$RbTi_2(PO_4)_3$ (see [b])	$R\bar{3}c$	8.290		23.530		220
$CsTi_2(PO_4)_3$ (see [b])	$Ia\bar{3}d$	19.909				221
$NH_4Ti_2(PO_4)_3$	$R\bar{3}c$	8.318		23.44		222
	$P2_13$	9.928				222
$CuTi_2(PO_4)_3$ (see [b])	$R\bar{3}c$	8.5271		21.32		223
$AgTi_2(PO_4)_3$	$R\bar{3}c$	8.4734		22.114		224
$TlTi_2(PO_4)_3$	$R\bar{3}c$	8.313		23.56		225
$LiZr_2(PO_4)_3$ (see [b])	$R\bar{3}c$ (423 K)	8.85493		22.1440		226
	$C\bar{1}$	15.0718	8.8556	9.1234	α = 89.660, *β* = 123.912, *γ* = 90.429	227
	$P2_1/n$	8.81277	8.94520	12.37540	90.801	228
	Pbna (623 K)	8.84303	8.9420	12.41301		228
$NaZr_2(PO_4)_3$ (see [b])	$R\bar{3}c$	8.8045		22.7585		11
$KZr_2(PO_4)_3$ (see [b])	$R\bar{3}c$	8.71		23.89		229
$RbZr_2(PO_4)_3$	$R\bar{3}c$	8.66		24.38		197
$CsZr_2(PO_4)_3$ (see [b])	$R\bar{3}c$	8.5758		24.9061		230
$HZr_2(PO_4)_3$	$R\bar{3}c$	8.803		23.23		231
	cubic	10.165				232
$(H_3O)Zr_2(PO_4)_3$ (see [b])	$R\bar{3}c$	8.7528		23.6833		233
$NH_4Zr_2(PO_4)_3$ (see [b])	$R\bar{3}c$	8.7088		24.2197		233
	cubic	10.186				234
$CuZr_2(PO_4)_3$ (see [b])	$R\bar{3}c$	8.892		22.19		235
$AgZr_2(PO_4)_3$	$R\bar{3}c$	8.818		22.881		236
$GaZr_2(PO_4)_3$ (see [b])	$R\bar{3}c$	8.72198		23.8820		237
$LiHf_2(PO_4)_3$ (see [b])	$R\bar{3}c$ (320 K)	8.83070		22.0272		238
	$P\bar{1}$ (175 K)	8.69447	8.74104	9.07206	α = 118.6297, β = 90.6805, γ = 119.1605	238
$NaHf_2(PO_4)_3$	$R\bar{3}c$	8.7707		22.66		239
$KHf_2(PO_4)_3$ (see [b])	$R\bar{3}c$	8.6819		23.862		240
$RbHf_2(PO_4)_3$	$R\bar{3}c$	8.63		24.34		201
$CsHf_2(PO_4)_3$	$R\bar{3}c$	8.54		24.81		201
$CuHf_2(PO_4)_3$	$R\bar{3}c$	8.840		22.128		241
$AgHf_2(PO_4)_3$	$R\bar{3}c$	8.873		22.82		242
$LiGe_2(PO_4)_3$ (see [b])	$R\bar{3}c$	8.2722		20.4825		243
$NaGe_2(PO_4)_3$ (see [b])	$R\bar{3}$	8.109		21.536		244
$KGe_2(PO_4)_3$ (see [b])	$R\bar{3}$	8.0066		22.566		245
$AgGe_2(PO_4)_3$	$R\bar{3}c$	8.066		21.819		241
$NaGeTi(PO_4)_3$ (see [b])	$R\bar{3}$	8.305		21.69		246
$LiSn_2(PO_4)_3$ (see [b])	$R\bar{3}c$ (450 K)	8.63328		21.5326		238
	$P\bar{1}$ (250 K)	8.40296	8.44080	8.88969	α = 118.1153, β = 90.1804, γ = 119.6825	238
$NaSn_2(PO_4)_3$ (see [b])	$R\bar{3}c$ (1073 K)	8.5659		22.6902		247
	$R\bar{3}$ (673 K)	8.5481		22.5772		247
$CuSn_2(PO_4)_3$ (see [b])	$R\bar{3}c$	8.588		21.96		248
$AgSn_2(PO_4)_3$	$R\bar{3}c$	8.459		22.683		241
$NaTh_2(PO_4)_3$ (see [b])	*Cc*	17.37	6.81	8.13	101.03	249
$KTh_2(PO_4)_3$ (see [b])	*C2/c*	17.57	6.863	8.138	101.77	250
$NH_4Th_2(PO_4)_3$ (see [b])	*C2/c*	17.880	6.906	8.152	104.39	251
$KU_2(PO_4)_3$ (see [b])	$R\bar{3}c$	9.113		24.997		252
	C2/c	17.479	6.758	8.019	102.01	253, 254
$RbU_2(PO_4)_3$	$R\bar{3}c$	9.059		25.60		255
$KUTh(PO_4)_3$	*C2/c*	17.560	6.8202	8.0951	101.908	253
$NaNp_2(PO_4)_3$	trigonal	9.137		24.24		255
	Cc	17.15	6.693	7.971	101.4	24, 255
$KNp_2(PO_4)_3$	trigonal	9.081		25.14		255
	monoclinic	17.49	6.853	8.00	101.9	255
$RbNp_2(PO_4)_3$	$R\bar{3}c$	9.113		25.68		255

Table 6 (continued).

Compound	Space group [a]	Unit cell parameters				Ref.
		a /Å	b /Å	c /Å	β (or α, β, γ) /deg	
$NaPu_2(PO_4)_3$	trigonal	9.109		23.84		255
	Cc	17.18	6.759	7.97	101.3	24, 255
$KPu_2(PO_4)_3$	$R\bar{3}c$	9.050		24.81		255
	monoclinic	17.29	6.77	7.95	102.8	255
$RbPu_2(PO_4)_3$	trigonal	9.030		25.40		255

[a] The temperature at which the data were obtained is given in parentheses; when the space group has not been reliably determined, the system is given; [b] for these compounds, the crystal structure has been determined.

located inside the columns between the lanterns formed by octahedra and tetrahedra, while the M2 site is between the neighbouring columns. At room temperature, the M^I cations fully occupy the M1 sites, while M2 remain vacant.[256]

A comparison of the results of X-ray diffraction studies [4, 7, 167, 255, 257] demonstrates a certain correlation between the size of the metal cations and crystallographic parameters a and c of the hexagonal cell of the NZP-type phosphates $M^IE_2^{IV}(PO_4)_3$ (Fig. 12): the flexible framework changes its size to be adjusted to cations of different size that occupy the M1 sites. For the $\{[L_2(PO_4)_3]^{p-}\}_{3\infty}$ frameworks (L = Ge, Ti, Sn, Hf, Zr, Pu), an increase in the cation size in the M1 site leads to structure extension along the c axis and compression along the a axis. It is obvious that the occupation of the M1 sites by large cations increases the parameter c (see Fig. 1). This is accompanied by deformation of the PO_4 tetrahedra. The internal O–P–O angle increases along the c axis, which shortens the distance between the parallel columns and decreases the parameter a.

The atomic structures of some $M^IZr_2(PO_4)_3$ have not been studied but were predicted using the semiempirical

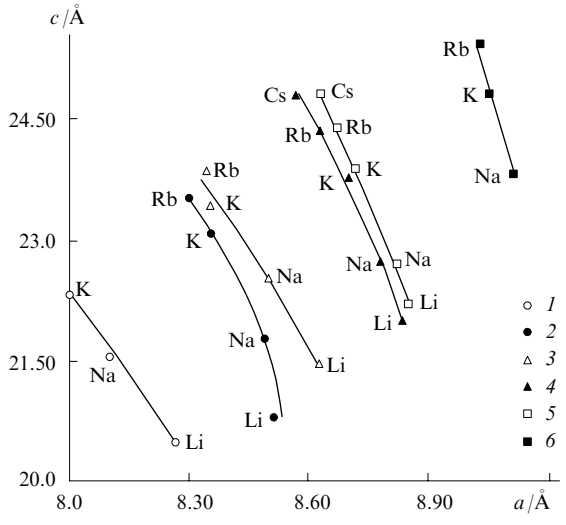


Figure 12. Unit cell parameters a and c of the phosphates $M^IE_2^{IV}(PO_4)_3$.[4]
E^{IV} = Ge (*1*), Ti (*2*), Sn (*3*), Hf (*4*), Zr (*5*), Pu (*6*). The lines that connect the points corresponding to identical framework cations E^{IV} show the tendency for increasing c and decreasing a with increase in the size of M^I cations that occupy the M1 sites in the NZP structure.

atomistic modelling method involving the search for the energy minimum of the interatomic interaction of the crystalline assembly and based on the crystal chemical approach.[258] The interatomic distances responsible for the final spatial arrangement of atoms in the crystal structure are determined by the Coulomb interaction forces between the atoms bearing some effective charges and short-range attraction–repulsion interactions. Among the possible atom arrangements in the structure of a compound, the arrangement that corresponds to the free energy minimum at the given pressure and temperature is implemented. Hence, the key principle for finding this stable crystal structure is to minimize the structural energy with respect to all variable parameters (lattice parameters, atomic coordinates and charges, *etc.*). For crystals with purely ionic chemical bonds, the structural energy can be expressed through the lattice energy, while for covalent and metallic crystals it can be expressed through the atomization energy. The search for the energy minimum of the interatomic interaction in the crystal can be performed by the General Utility Lattice Programme (GULP) developed by J D Gale,[259] the top software for this purpose.

Eremin *et al.*[260] developed a set of pair potentials capable of correctly reproducing the crystal structures of lithium, sodium and potassium zirconium phosphates (the deviation between the calculated and experimental unit cell parameters was not more than 1.5%, that for interatomic distances was not more than 0.13 Å) and accomplished structural modelling of rubidium and caesium zirconium phosphates. The results of modelling of the crystal structure of $RbZr_2(PO_4)_3$ are illustrated in Fig. 13. The structure of $CsZr_2(PO_4)_3$ was later refined by the Rietveld method.[230] The difference between the calculated and experimental unit cell parameters was 1.4%. Using the set of potentials obtained for the phosphates $M^IZr_2(PO_4)_3$, the maximal cation size that can fit into the M1 site is r_{max} = 1.73 Å.[260] This value is greater than the effective radius of Cs^+ (C.N. 6) by 0.06 Å and smaller than this radius of Fr^+; it can be expected that the hypothetical compound $FrZr_2(PO_4)_3$ would be unstable in the NZP structure. In view of the fact that the interatomic interaction potential for a pair of atoms determined for a particular compound can be transferred to related structures where the same pair of atoms is also in contact, it is easy to realize that the transferability of pair potentials from one system to another is a great advantage in modelling the crystal structure and properties.

The structure of lithium-containing phosphates $LiE_2^{IV}(PO_4)_3$ (see Table 6) largely depends on the method

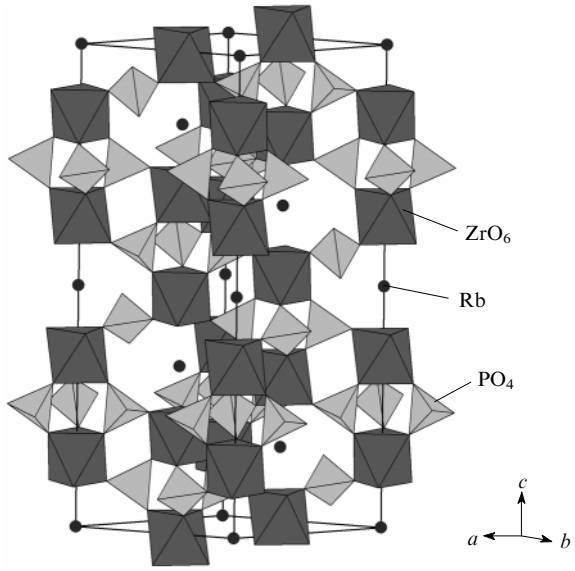


Figure 13. Fragment of the structure of $RbZr_2(PO_4)_3$.[260]

of synthesis, heat treatment and storage conditions.[5, 113, 226–228, 238, 261–265] The phosphates $LiTi_2(PO_4)_3$ and $LiGe_2(PO_4)_3$ have NZP structures;[167, 243] for lithium-containing zirconium, hafnium and tin phosphates, the presence of other polymorphs, in addition to the rhombohedral NZP modification, was established.

The phosphate $LiZr_2(PO_4)_3$ synthesized by the solid-phase method at 1473 K exists as the α-modification (according to designations given by Catti and Stramare[226]) with the rhombohedral symmetry (space group $R\bar{3}c$), which is stable down to 323 K, and on further cooling it undergoes phase transition to the triclinic α′-modification (space group $C\bar{1}$).[227] If the synthesis is carried out below 1173 K, this compound crystallizes in the orthorhombic β-modification (structural type SW, space group *Pbna*), which is transformed into more distorted monoclinic β′-phase (space group $P2_1/n$) on cooling below 573 K.[228] Both these transitions are reversible. Modifications that correspond to different structural types with different packing of framework fragments, α(α′) and β(β′), are not interconverted, according to the data of Catti *et al.*[228]

According to Morin *et al.*,[238] the compounds $LiHf_2(PO_4)_3$ and $LiSn_2(PO_4)_3$ synthesized by the solid-phase reaction at 1273–1373 K are formed in the rhombohedral modification; they undergo transition to the triclinic phase (space group $P\bar{1}$) at 256 and 373 K, respectively.

In both the triclinic and rhombohedral modifications of the crystal structure of $LiZr_2(PO_4)_3$, the tetranuclear complexes $2\,ZrO_6-2\,PO_4$ are packed according to the stacking pattern (see Fig. 11 *a*). The key structural changes that accompany the $\alpha \rightarrow \alpha'$ transition are due to redistribution of the extraframework lithium cations in the unit cell.[226] In the α-phase, the lithium ions are disordered over six tetrahedral sites located in the octahedral M1 cavity. The site occupancy is ~0.12. The neutron diffraction measurements of lithium cation redistribution in the α-phase in the range of 423–873 K showed[266] that as the temperature increases, the occupancy of the M2 sites by lithium increases from 0.1 to 0.22. In the α′-phase, the Li^+ cations randomly occupy the independent Li1 and Li2 sites, which are displaced from the centres of the interconnected M1 and M2 cavities of the rhombohedral NZP structure, and thus occur in a distorted tetrahedral environment.[227] The site occupancy by lithium cations is incomplete (0.71 and 0.29, respectively). Due to the displacement of Li^+ ions from ideal rhombohedral positions in the α′-phase, some of the lithium atoms are ordered in the pairs of relatively closely spaced centrosymmetric positions distributed in a half of octahedral cavities (Fig. 14). The dynamic disorder of lithium ions over various positions gives rise to the hysteresis loop: the $\alpha' \rightleftharpoons \alpha$ transition occurs over a fairly broad temperature range (~40°) rather than in one point, and the phase transition during cooling occurs at considerably lower temperature.[5, 267]

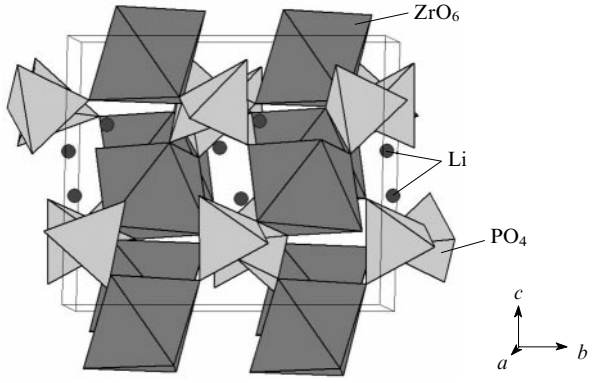


Figure 14. Fragment of the structure of triclinic α′-$LiZr_2(PO_4)_3$.[227]

Thus, the temperature-induced phase transition, $\alpha' \rightarrow \alpha$, in the lithium zirconium phosphate, as in the structural analogues $LiHf_2(PO_4)_3$ and $LiSn_2(PO_4)_3$, consists in a change in the spatial arrangement of lithium cations in the framework cavities. This is an order–disorder-type transition; a characteristic feature of this transition is that the symmetry group of the low-temperature phase is a subgroup of the symmetry group of the high-temperature phase. The framework type of the structure, the distorted octahedral coordination of lithium ions, the great average Li–O bond length (2.27 Å) and a fairly large number of vacant positions in the high-temperature modification produce favourable conditions for ion transport.[268]

The compounds β-$LiZr_2(PO_4)_3$ (space group *Pbna*) and β′-$LiZr_2(PO_4)_3$ (space group $P2_1/n$) crystallize in an SW structural type with herringbone packing of the $2\,ZrO_6-2\,PO_4$ complexes (see Fig. 11 *b*). The structure cavities in known phosphates of this structural type are not completely occupied: the number of sites in the cavities exceeds the number of cations that occupy them. The structure framework is penetrated by channels of three types. The channel cross-section in the narrowest parts is <0.9 Å; therefore, the SW structural type is preferred for the phosphates in which the cavities are occupied by rather small cations whose size does no differ much from the size of the framework-forming cation.

In the structure of orthorhombic β-$LiZr_2(PO_4)_3$, the lithium cations are disordered over four sites two of which are symmetrically independent and have occupancies of 0.34 and 0.16.[228] In the monoclinic β′-phase, the lithium ions are ordered (Fig. 15). The structural mechanism of the $\beta' \rightarrow \beta$

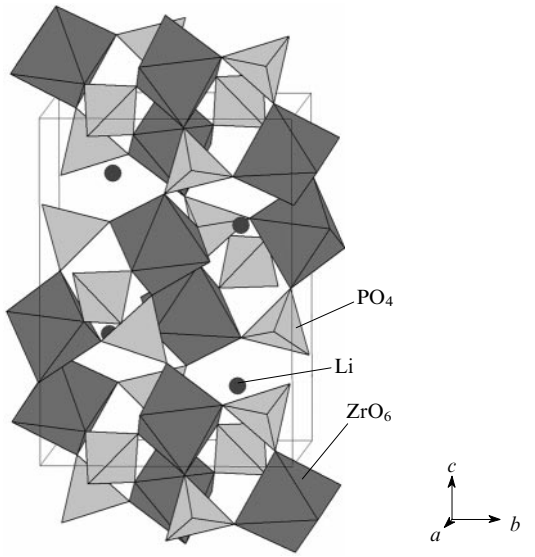


Figure 15. Fragment of the structure of monoclinic β'-$LiZr_2(PO_4)_3$.[228]

transition is degeneration of four-fold crystallographic sites of lithium to eight-fold sites and disordering of lithium cations in the unit cell over these sites. No new spatial positions appear but the non-equivalence between the pairs of existing four-fold sites is eliminated. Thus, the $\beta' \rightleftharpoons \beta$ phase transition in $LiZr_2(PO_4)_3$, like the $\alpha' \rightleftharpoons \alpha$ transition, is of the order–disorder type. The most pronounced difference between the cells of structurally related but topologically not identical α'- and β'-modifications is related to their volumes: the α'-cell is larger than the β'-cell by 3.6%. One may expect a reconstructive $\alpha' \rightleftharpoons \beta'$ phase transition upon a pressure and temperature change.

Depending on the external conditions, phosphate structures with splitting of cationic positions may possess either superionic conductivity (the ion mobility is so high that the ion leaves its coordination polyhedron and moves along the bulky conduction channels) or ferro(antiferro) activity (the ion displacement is within one coordination polyhedron).[6,91] The superionic conductivity is clear-cut in the phosphates $LiE_2^{IV}(PO_4)_3$ and solid solutions based on them.[14,268–275] The replacement of lithium ions in $LiZr_2(PO_4)_3$ by hydrogen ions gives rise to proton conductors $(H_3O)Zr_2(PO_4)_3$ and $HZr_2(PO_4)_3$ (Refs 276 and 277, Table 6). Both compounds exhibit phase transitions.[278–280]

The phosphates of d-transition metals $M^IE_2^{IV}(PO_4)_3$ (M = Na, K, Rb, NH_4, Cu, Ag) (see Table 6) crystallize in the NZP structure (space group $R\bar{3}c$, $R\bar{3}$). For $KTi_2(PO_4)_3$ and $NH_4E_2^{IV}(PO_4)_3$ (E = Ti, Zr), modifications with the langbeinite structure (cubic system, space group $P2_13$) are also known.[219,222,234] The ion exchange synthesis of langbeinite-like modifications of $LiZr_2(PO_4)_3 \cdot 0.7\,H_2O$ and $NaZr_2(PO_4)_3 \cdot 0.3\,H_2O$ from $(H_3O)Zr_2(PO_4)_3$ in solutions of the corresponding metal chlorides was reported.[232]

The compounds $CsE_2^{IV}(PO_4)_3$ (E = Ti, Zr, Hf) crystallize in various structural types (see Table 6). The geometric hindrance related to the ratio of the sizes of the large extraframework cation, caesium, and the rather small framework-forming cation, titanium, gives rise to $CsTi_2(PO_4)_3$ with a framework differing from NZP or langbeinite and with a cubic symmetry unit cell.[221]

The framework of $CsTi_2(PO_4)_3$ composed of TiO_6 octahedra and PO_4 tetrahedra sharing corners can be represented as close-packed columns connected to one another (Fig. 16). The caesium cations in the Cs(1) and Cs(2) sites are surrounded by 12 and 8 oxygen atoms, respectively. The core of each column consists of alternating $Ti(2)O_6$ octahedra and 12-coordinate Cs(1) cations luing on the $\bar{3}$ axis (space group $Ia\bar{3}d$). This core is surrounded successively by rings of PO_4 tetrahedra, $Ti(1)O_6$ octahedra and PO_4 tetrahedra. The octahedrally coordinated framework sites between these columns are occupied by the Ti(1) and Ti(2) cations. In the framework, one can distinguish groups of two octahedra and two tetrahedra oriented along different directions. Each cavity of the structure of $CsTi_2(PO_4)_3$ is surrounded by eight TiO_6 octahedra and eight PO_4 tetrahedra connected to one another. The structure cavities form a three-dimensional system of channels running through the framework. The Cs(1) sites are located at the channel intersection points, while Cs(2) are inside the cavity. The Cs(1) cationic site is a hexacapped trigonal prism. The eight-coordinate Cs^+ cations are disordered between two closely spaced randomly occupied Cs(2) sites.

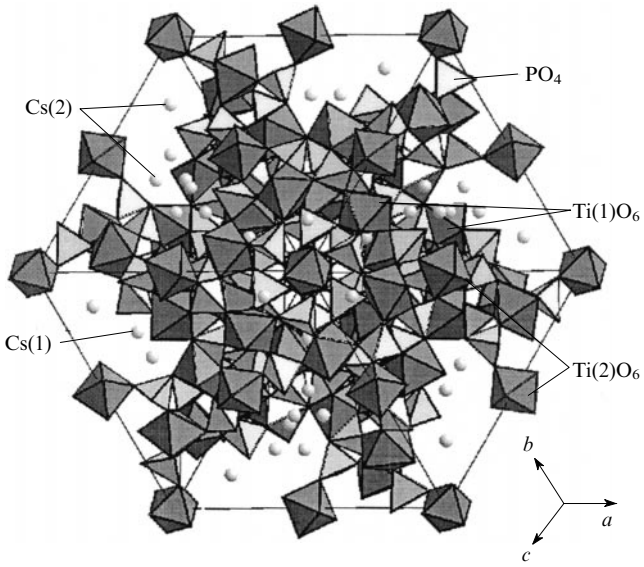


Figure 16. Fragment of the structure of $CsTi_2(PO_4)_3$.[221]

The compounds $M^IE_2^{IV}(PO_4)_3$ are distinguished by high thermal stability as compared with $M\,{}_2^IE^{IV}(PO_4)_2$. Melting (decomposition) points of the phosphates $M^IZr_2(PO_4)_3$ (M = Li, Na, K) are 1963, 1923 and 1883 K, respectively.[195] The phosphate $CsZr_2(PO_4)_3$ is stable up to at least 1500 K.[281] It is a promising material with ultra-low thermal expansion,[4] which is able to effectively capture caesium (^{137}Cs, ^{134}Cs) radioisotopes present in nuclear wastes.[3,282]

For compounds with the NZP structural type, the number of extraframework cations may vary from 0 [compounds with empty frameworks, for example, $L^I_{1/4}L^V_{7/4}(PO_4)_3$, where L^I = Li, L^V = Nb, Ta][283] to 4 (phosphates with completely filled cationic positions) per formula unit. As a rule, when the number of ions compensating the framework charge is close to 1, they first of all occupy the M1 sites of the cavities and only after they have been occupied, the M2 sites start to be occupied. Depending on

the distribution pattern of cations in the cavities and slight displacements of ions that form the framework, minor distortions of the trigonal cell and a symmetry lowering may occur. Indeed, the phosphates $Na_5E^{IV}(PO_4)_3$ (E = Ti, Zr, Hf) with completely filled cationic sites crystallize at room temperature in the NZP structureal type, space group $R32$.[202, 203, 284] The sodium cations together with titanium, zirconium or hafnium ions form the $\{[NaE^{IV}(PO_4)_3]^{4-}\}_{3\infty}$ framework by occupying half of its octahedral sites and function as compensation cations by occupying the extraframework sites (Fig. 17). At room

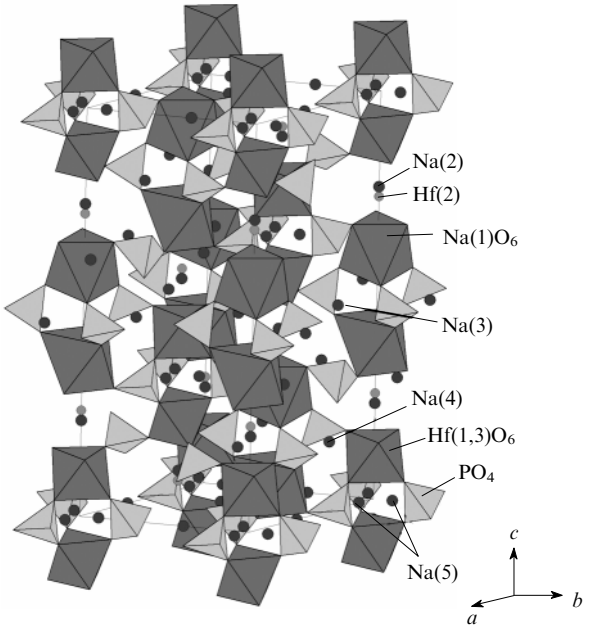


Figure 17. Fragment of the structure of $Na_5Hf(PO_4)_3$.[284]

temperature, the E^{IV} cations occupy one type of sites in the $Na_5Ti(PO_4)_3$ structure being disordered between two closely spaced sites in $Na_5Zr(PO_4)_3$ and $Na_5Hf(PO_4)_3$ so that in the columns composed of octahedra and tetrahedra, the octahedra alternate: $NaO_6-NaO_6-E^{IV}O_6-E^{IV}O_6-$. An increase in the size of the structure-forming E^{IV} cation with the maximum possible content of sodium for the composition $Na_5E^{IV}(PO_4)_3$ results in simultaneous increase in the unit cell parameters a and c (Fig. 18).[284] The distributions of the Na^+ cations in the cavities of these structures have minor differences. In $Na_5Ti(PO_4)_3$, unlike compounds with space group $R\bar{3}c$, the Na^+ sites in the cavities between the columns split into three types: two nine-fold sites (one fully occupied and one partly occupied) and one general 18-fold site (partly occupied). In $Na_5Zr(PO_4)_3$ and $Na_5Hf(PO_4)_3$, the cavities situated inside the columns composed of octahedra and tetrahedra are mainly occupied by the Na^+ cations and a minor part of Zr^{4+} or Hf^{4+} cations. The positions between the polyhedral columns are occupied by only sodium cations (eight-coordinate).

The enantiotropic phase transition of $Na_5Zr(PO_4)_3$ and $Na_5Hf(PO_4)_3$ from one solid modification to another at 407 and 517 K, respectively, is accompanied by a change in the coordinates and occupancies of sodium and E^{IV} sites with retention of symmetry of the crystal structure.[285, 286] The

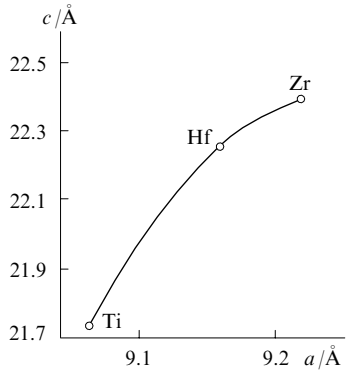


Figure 18. Unit cell parameters of the phosphates $Na_5E^{IV}(PO_4)_3$ (E = Ti, Zr, Hf).[202, 203, 284]
The line shows the regular increase in the parameters a and c with increase in the size of the E^{IV} cations in the L sites of the $\{[NaE^{IV}(PO_4)_3]^{4-}\}_{3\infty}$ framework.

phosphates $Na_5E^{IV}(PO_4)_3$ (E = Ti and Zr) melt with decomposition at 1083 and 1433 K, respectively.[141, 286]

The phosphate $Na_5Zr(PO_4)_3$ was also obtained in the metastable modification (space group $R\bar{3}c$) by the sol–gel synthesis using metal chlorides.[139] Chemical analysis showed that this compound contains some chloride ions, which stabilize this modification. This compound decomposes in the temperature range of 1123–1373 K within several tens of hours to give $Na_2Zr(PO_4)_2$.

Samples of the presumable composition $M_5Zr(PO_4)_3$ (M = Li, K, Rb, Cs) are not formed, being mixtures of different phases: $M_2Zr(PO_4)_2$ and condensed alkali metal phosphates.[111, 287]

The rhombohedral symmetry of the solid solution $Na_{5-4x}Zr_{1+x}(PO_4)_3$ $(0.04 < x < 0.15)$ based on $Na_5Zr(PO_4)_3$ remains unchanged upon the substitution $4\,Na^+ \rightarrow Zr^{4+}$.[141, 288] The partial ordering of the additional zirconium cations in the solid solution gives rise to a superstructure, a jumpwise increase in the parameter c and, hence, the unit cell volume.

Phases of variable composition $Na_{5-x}M^I_xE^{IV}(PO_4)_3$ (M = Li, K, Rb, Cs; E = Ti, Zr), structural analogues of NZP, are known.[287, 289] However, no direct structural studies of these phases were performed.

Thus, despite the structural distortions in various compounds of the NZP family, their common structural pattern (the arrangement of the main framework elements) remains unchanged. This gives room for a wide variety of possible substitutions in all cationic positions without destruction or crucial rearrangement of the initial motif and for the formation of series of solid solutions by means of iso- and heterovalent substitution of the M^I and E^{IV} cations.

Considering the crystal chemical views, Pet'kov and coworkers[289–295] predicted, synthesized and investigated the variable composition phases $M_{1-x}M'_xE^{IV}(PO_4)_3$ (M, M′ = Li, Na, K, Rb, Cs) — ternary phosphates of Group 4 metals and alkali metals belonging to the NZP structural type (Table 7). The possibility of formation of these solid solutions is due to the crystallization of the end members of the series in one structural type at relatively small difference between the radii of the cations being replaced. The crystallographic parameters of solid solutions smoothly change in the single-phase composition ranges (Fig. 19). Note that

Table 7. Concentration limits of existence of solid solutions (NZP structural type, space group $R\bar{3}c$) in the systems $M_{1-x}M'_xE^{IV}(PO_4)_3$ (E = Ti, Zr, Hf).[295]

M	M′	Ti		Zr		Hf
		x	$\Delta d/d_1$ (%) (see [a])	x	$\Delta d/d_1$ (%) (see [a])	x
Li	Na	0–1	9	0–1	11	0–1
	K	mixture of phases	21	mixture of phases	24	0–1
Na	K	0–1	11	0–1	10	0–1
	Rb	0–0.3, 0.7–1	15	0–1	11	0–1
	Cs	0–0.2	–	0–0.3, 0.7–1	13	0–0.3, 0.7–1
K	Rb	0–1	4	0–1	1	0–1
	Cs	0–0.3	–	0–1	3	0–1
Rb	Cs	mixture of phases	–	0–1	2	0–1

[a] $\Delta d/d_1$ is the difference between the alkali metal – oxygen bond lengths in triple phosphates divided by the smaller bond length

$$\Delta d/d_1 = \frac{d_{M'-O} - d_{M-O}}{d_{M-O}}.$$

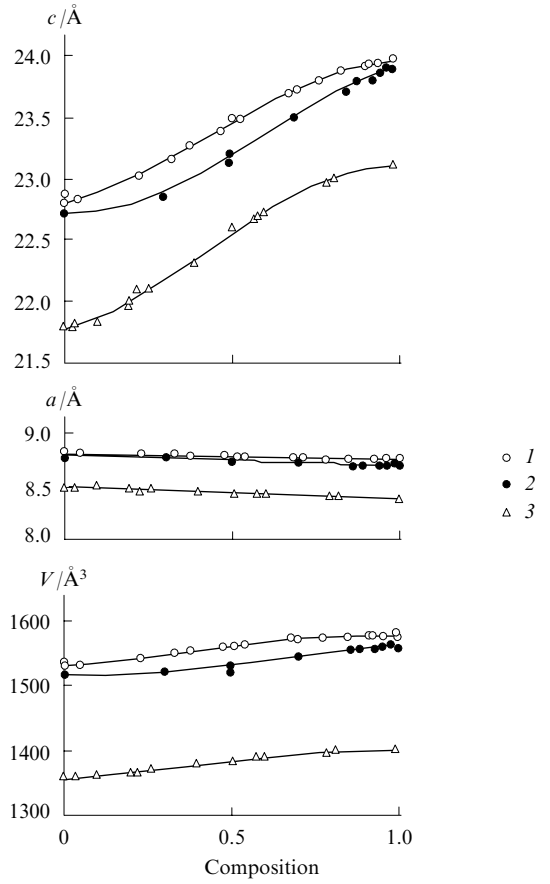


Figure 19. Crystallographic parameters a, c and cell volume (V) of the phosphates $Na_{1-x}K_xE_2^{IV}(PO_4)_3$ *vs.* composition (x).[289–291] E^{IV} = Zr (*1*), Hf (*2*), Ti (*3*).

the change in the spectral pattern following the smooth variation of the phase composition is gradual.[287, 290, 295, 296] The effect of the alkali metal cation on the geometry of the anionic group is most pronounced for the bending vibrational bands of the PO_4 tetrahedra, which are narrower and sharper than the stretching bands.

The alkali metal cations in the phosphates $Na_{0.5}K_{0.5}E_2^{IV}(PO_4)_3$ (E = Ti, Hf), $K_{0.5}Rb_{0.5}Ti_2(PO_4)_3$ and $Li_{0.5}K_{0.5}Hf_2(PO_4)_3$ are statistically disordered in the fully occupied octahedral M1 sites located in the framework cavities inside the columns parallel to the c axis (Fig. 20).[282, 291, 294, 295] The M(M′)–O bond lengths in the double phosphates $MTi_2(PO_4)_3$ and triple phosphates $M_{0.5}M'_{0.5}Ti_2(PO_4)_3$ depend linearly on the size of the alkali metal cation (Fig. 21), and for the triple phosphates, they obey the additivity property relative to the bond lengths in double phosphates. For these compounds, one can consider the average 'formal' alkali cation radius in the framework cavities

$$r(M_{0.5}M'_{0.5}) = 0.5[r(M) + r(M')]$$

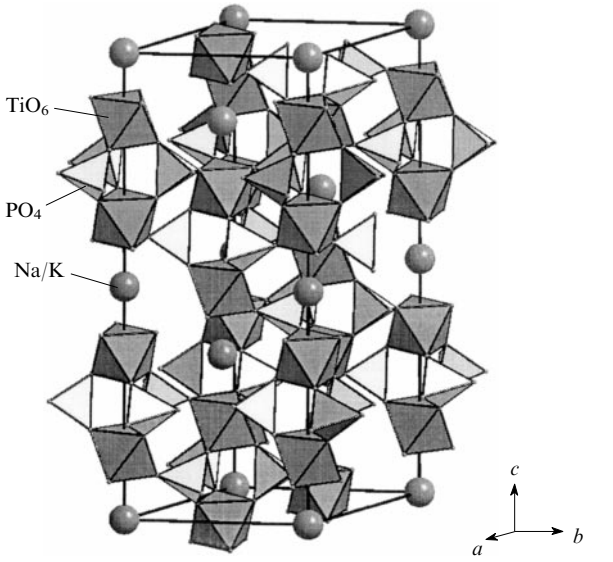


Figure 20. Fragment of the structure $Na_{0.5}K_{0.5}Ti_2(PO_4)_3$.[294]

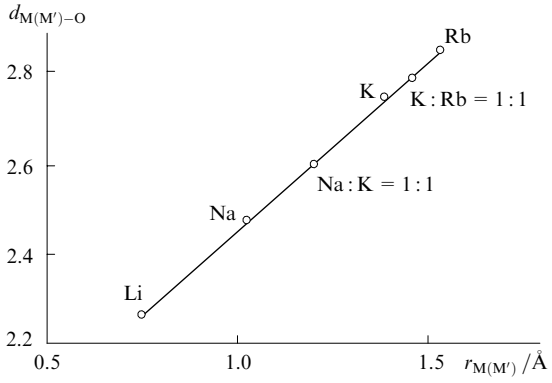


Figure 21. Variation of the alkali metal (or 'formal' alkali metal)–oxygen bond length [$d_{M(M')-O}$] in double [$M^ITi_2(PO_4)_3$] and triple [$M_{0.5}M'_{0.5}Ti_2(PO_4)_3$] phosphates *vs.* the radius of the alkali metal cation.[294]

The framework-forming cation–oxygen bond lengths (Ti–O, P–O) in titanium and alkali metal phosphates depend little on the radius of the extraframework cation. This can be attributed to the fact that the covalent chemical bonds of the framework are much stronger than the bonds with the ions that occupy the structure cavities. When larger cations enter the M1 sites located between two surfaces of the adjacent $E^{IV}O_6$ octahedra, the substantial increase in the alkali metal–oxygen bond length entails an increase in the parameter *c* (Fig. 22). The increase in the bond lengths in the octahedra and the change in the $O-E^{IV}-O$ bond angles entail the deformation of the PO_4 tetrahedra sharing the corners with them. The tetrahedra rotate around the twofold symmetry axes (directed perpendicular to the cell *c* axis), which reduces the distance between the parallel columns and decreases the parameter *a*. It is the correlated rotation of the framework fragments that is responsible for the monotonic increase in the parameters *c* and *V* and decrease in the lattice parameter *a* of the solid solutions $M_{1-x}M'_xE_2^{IV}(PO_4)_3$ following an increase in the content of the larger alkali metal cation in the phosphate (see Fig. 19).

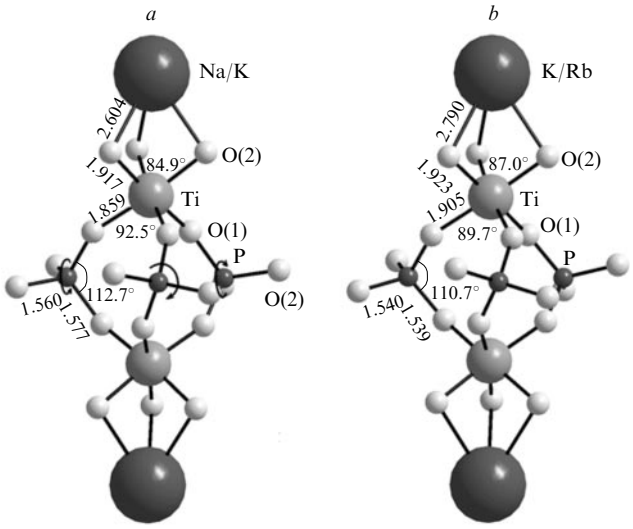


Figure 22. Deformation of the structural fragments of the framework depending on the radius of the 'formal' alkali metal cation in the extraframework M1 sites for $Na_{0.5}K_{0.5}Ti_2(PO_4)_3$ (*a*) and $K_{0.5}Rb_{0.5}Ti_2(PO_4)_3$ (*b*).[294]

The concentration limits of existence of the solid solutions in the titanium-, zirconium- and hafnium-containing phosphates depend on the relative difference in the interatomic alkali metal–oxygen distances ($\Delta d/d_1$) in the double phosphates $ME_2^{IV}(PO_4)_3$ and $M'E_2^{IV}(PO_4)_3$ (see Table 7). The continuous series of solid solutions can exist at room temperature if the relative difference in the M–O and M′–O interatomic distances does not exceed 11% [an exception is $Li_{1-x}K_xHf_2(PO_4)_3$]. When $\Delta d/d_1 \geqslant 21\%$, no significant isomorphous substitutions can be found in the phosphate systems. Since the ion radii of Hf^{4+} (0.71 Å) and Zr^{4+} (0.72 Å) are similar, the phase formation patterns in the zirconium and hafnium phosphate systems resemble one another. The formation of a continuous series of the solid solutions $Li_{1-x}K_xHf_2(PO_4)_3$ despite the great difference between the radii of Li^+ and K^+ ions is caused by the effect of the hafnium electronic structure, which is manifested as the stability of the rhombohedral modification of $LiHf_2(PO_4)_3$ [compared to $LiZr_2(PO_4)_3$] over a broad temperature range.[238] In the series of titanium phosphates, the introduction of Cs^+ cations [which are large as compared with the size of the NZP framework cavities and, hence, $CsTi_2(PO_4)_3$ has a framework type of structure but other than NZP] results in lowering of the miscibility boundary; however, together with alkali metal cations having smaller size, caesium is able to be accommodated in the framework cavities (see Table 7). The existence of the solid solutions $M^IE_{2-x}^{IV}E'^{IV}_x(PO_4)_3$ with isovalent substitution of the structure-forming cations in the oxidation state +4 [274, 297–300] suggests that the concentration fields of solid solutions of NZP structures in titanium-containing systems can be extended by partial replacement of Ti^{4+} by larger cations: Sn^{4+}, Hf^{4+} or Zr^{4+} at a controlled average radius of the extraframework cation.

After annealing of the solid solutions $M_{1-x}M'_xTi_2(PO_4)_3$ at 1473 K for 6 h, they partly decomposed.[290] Titanium dioxide was present as the impurity phase. Other decomposition products were apparently alkali metal polyphosphates. The phases of variable composition $M_{1-x}M'_xZr_2(PO_4)_3$ and $M_{1-x}M'_xHf_2(PO_4)_3$ did not undergo any changes on annealing up to 1273–1573 K.[295, 301]

The thermodynamic calculations based on the results of studies of cation-exchange equilibria in the $NaE_2^{IV}(PO_4)_3-KE_2^{IV}(PO_4)_3-NaCl-KCl-H_2O$ systems at 723–973 K and a pressure of 1–2 MPa showed that the solid solutions $Na_{1-x}K_xE_2^{IV}(PO_4)_3$ are characterized by a considerable deviation from the ideality.[292, 293] The Gibbs function of mixing of solid solutions under the studied conditions is negative over the whole range of compositions. Titanium phosphates are characterized by a greater deviation from ideality than zirconium and hafnium phosphates; this may result in earlier decomposition of the solid solutions $Na_{1-x}K_xTi_2(PO_4)_3$ under more drastic pressure and temperature conditions. Under the studied conditions, the solid solutions are stable with respect to decomposition into double phosphates, and the framework structures of these compounds are stable at high pressure and temperature, in particular, in the presence of an aqueous salt solution.

The solid solutions of NZP structures containing cations of two or more alkali metals at high concentration can be formed upon the phosphate curing of spent radionuclide-contaminated alkaline chloride melts in pyroelectrochemical nuclear-fuel processing and upon waste immobilization from other processes.[289, 302–304] The existence of NZP modifications of the phosphates of f elements (uranium, neptunium and plutonium), $M^IE_2^{IV}(PO_4)_3$ (see Table 6), and the solid solutions $KZr_{2-x}U_x(PO_4)_3$ ($x \leqslant 0.2$)[254] can be employed to incorporate actinides into orthophosphate matrices. The plutonium phosphate $NaPu_2(PO_4)_3$ (60 mass % ^{239}Pu) showed no changes in the chemical or phase composition over a two-year observation period.[255] γ-Irradiation of samples of NZP phosphates (absorbed dose of up to 5×10^8 Gy) does not induce their chemical or phase destruction.[305]

The phosphates $M^IE_2^{IV}(PO_4)_3$ with large E^{IV} cations represented by f elements (Th, U, Np, Pu), synthesized at temperatures from 773–873 to 1373–1573 K, form most often crystalline modifications similar in the structure to $KTh_2(PO_4)_3$ (see Table 6).[24, 306] In uranium-, neptunium- and plutonium-based systems with the rubidium cation,

monoclinic $KTh_2(PO_4)_3$ either does not form at all (the NZP phase arises immediately) or an individual phase of a different structure is detected instead.[255] As the temperature increases to 1773–1873 K, one or two polymorphic transformations take place to give, most often, NZP-type structures. For $LiPu_2(PO_4)_3$ and $NaU_2(PO_4)_3$, no NZP modifications were found.

Unlike the rhombohedral $KZr_2(PO_4)_3$ (see Fig. 1), in the monoclinic $KTh_2(PO_4)_3$ and its analogues, the coordination polyhedron of the actinide atom is formed by nine oxygen atoms. In this structural type (Fig. 23), two PO_4^{3-} groups

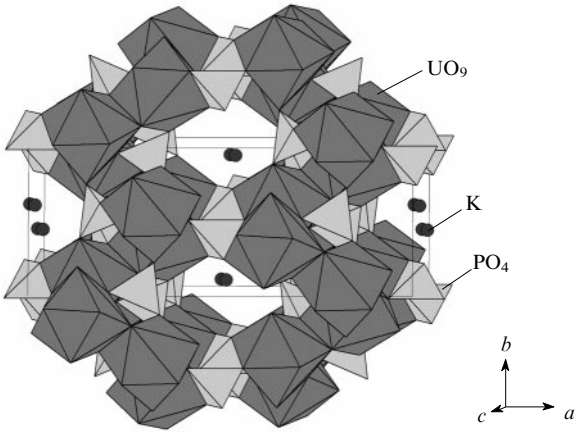


Figure 23. Fragment of the structure $KU_2(PO_4)_3$.[254]

are attached to the actinide atom in the bidentate fashion and five PO_4^{3-} groups are linked in a monodentate fashion giving an irregular nine-vertex polyhedron resembling a tricapped trigonal prism. Each of the $E^{IV}O_9$ polyhedra is connected to three similar polyhedra by sharing three edges. The alkali metal cations coordinated by eight oxygen atoms occupy the framework cavities of $\{[E_2^{IV}(PO_4)_3]^-\}_{3\infty}$. In the three-dimensional NZP structure, the actinide coordination polyhedra $E^{IV}O_6$ have no common elements and are connected by the bridging PO_4^{3-} groups and alkali metal cations.[252] According to the third Pauling rule, a structure is crystal-chemically less stable if its coordination polyhedra share edges. Apparently, as a certain temperature has been reached, a structural rearrangement accompanied by a change in the mode of combination of the polyhedra (without edge sharing), by a decrease in the coordination number and by an increase in the distances between the actinide atoms in the framework becomes thermodynamically favourable. As a consequence, the framework packing becomes looser (but more symmetrical), as indicated by a 29% increase in the volume per formula unit (V/Z). This rearrangement is accompanied by cleavage of the existing chemical bonds (or some of them) in the actinide coordination polyhedron and formation of new bonds. The new bonds in the octahedral environment are stronger: the average interatomic U–O distances in the UO_6 polyhedra of the rhombohedral $KU_2(PO_4)_3$ modification (2.27–2.32 Å)[252] are shorter than those in the UO_9 polyhedron of the monoclinic modification (2.28–2.61 Å).[253, 254] It is known that low coordination numbers are unusual for rather large actinide atoms in the oxidation states +3 and +4. The existence of actinide orthophosphates $M^IE_2^{IV}(PO_4)_3$ (E = U, Np, Pu) as NZP-type modifications makes them similar to derivatives of d metals in the oxidation state +4 as regards the crystal chemical features.

Some NZP phosphates contain PO_4^{3-} anions together with other tetrahedral anions. Best studied are silicophosphates $M^I_{1+x}E^{IV}_2(SiO_4)_x(PO_4)_{3-x}$, owing to the high cationic conductivity of the basic NASICON solid solutions, $Na_{1+x}Zr_2Si_xP_{3-x}O_{12}$ ($0 \leqslant x \leqslant 3$) (Refs 7, 16, 112, 273, 307 and 308). Depending on the composition of the silicophosphate, the cell symmetry varies from trigonal to monoclinic (Table 8). As the temperature increases to 403–503 K, the monoclinic solid solutions ($1.8 \leqslant x \leqslant 2.2$) undergo phase transitions accompanied by a change in the symmetry [$C2/c$ ($B2/b$) → $R\bar{3}c$].

The phases of variable composition $NaTi_2As_xP_{3-x}O_{12}$ ($0 \leqslant x \leqslant 1.2$) and $Na_{1+2x}Ti_{2-x}B_xP_{3-x}O_{12}$ ($0 \leqslant x \leqslant 0.9$) form NZP-type structures and rhombohedral cells.[323, 324] Upon the isovalent substitution $P^{5+} \rightarrow As^{5+}$, as x increases, the unit cell volume of the solid solution $NaTi_2As_xP_{3-x}O_{12}$ increases in conformity with the relationship between the P^{5+} and As^{5+} ionic radii; the ionic conductivity also

Table 8. Crystallographic characteristics and electric-conducting properties of the solid solutions $Na_{1+x+4y}Zr_{2-y-z}Si_xP_{3-x}O_{12-2z}$, $Na_3Zr_{1.88}Y_{0.12}Si_2PO_{11.94}$ and solid electrolytes based on $LiTi_2(PO_4)_3$.[a]

Composition	Space group	Unit cell parameters				$\sigma_{573\ K}$ /mS cm^{-1}	E_σ /kJ mol^{-1}	Ref.
		a/Å	b/Å	c/Å	β (or γ)/deg			
$Na_{1.4}Zr_2(SiO_4)_{0.4}(PO_4)_{2.6}$	$R\bar{3}c$	8.840		22.731		0.5	25.1	112, 309
$Na_{1.8}Zr_2(SiO_4)_{0.8}(PO_4)_{2.2}$	$R\bar{3}c$	8.898		22.774		3	29.8	112, 309
$Na_2Zr_2(SiO_4)(PO_4)_2$ (see [b])	$R\bar{3}c$	8.9309		22.9998		–	–	310
	$R\bar{3}c$ (573 K)	8.9348		22.8486		28	30.4	310
$Na_{2.2}Zr_2(SiO_4)_{1.2}(PO_4)_{1.8}$	$R\bar{3}c$	8.940		22.855		26	26.0	112
$Na_{3.33}Zr_{1.77}(SiO_4)_{1.4}(PO_4)_{1.6}$ (see [b])	$R\bar{3}c$	9.240		23.39		–	–	311
$Na_{2.6}Zr_2(SiO_4)_{1.6}(PO_4)_{1.4}$ (see [b])	$R\bar{3}c$ (593 K)	9.003		23.09		–	–	312
	$R\bar{3}c$	8.980		22.906		48	30.8	112
$Na_{2.8}Zr_2(SiO_4)_{1.8}(PO_4)_{1.2}$	$C2/c$	15.567	9.003	9.217	123.76	125	23.1	112
$Na_{3.31}Zr_{1.67}Si_{1.85}P_{1.15}O_{11.57}$ (see [b])	$C2/c$	15.67	9.066	9.220	123.84	–	–	313
$Na_{3.17}Zr_{1.93}Si_{1.9}P_{1.1}O_{12}$ (see [b])	$C2/c$	15.64	9.049	9.215	123.72	–	–	313
$Na_3Zr_{1.93}Si_{1.9}P_{1.1}O_{11.91}$ (see [b])	$C2/c$	15.64	9.048	9.221	123.87	–	–	313
$Na_3Zr_2(SiO_4)_2(PO_4)$ [b]	$C2/c$ (293 K)	15.6513	9.0550	9.2198	123.742	–	–	310

Table 8 (continued).

Composition	Space group	Unit cell parameters				$\sigma_{573\ K}$ /mS cm^{-1}	E_σ /kJ mol^{-1}	Ref.
		a /Å	b /Å	c /Å	β (or γ) /deg			
$Na_3Zr_2(SiO_4)_2(PO_4)$ [b]	$C2/c$	15.586	9.029	9.205	123.70	200	27.9	112, 309
	$R\bar{3}c$ (573 K)	9.0580		23.0705		190	28.9	310
	$R\bar{3}c$ (593 K)	9.053		23.06		215	18.8	312
$Na_{3.05}Zr_2(SiO_4)_{2.05}(PO_4)_{0.95}$ (see [b])	$R\bar{3}c$	9.068		22.98		—	—	314
$Na_{3.09}Zr_{2.01}(SiO_4)_{2.09}(PO_4)_{0.91}$ (see [b])	$R\bar{3}c$	9.074		23.05		—	—	315
$Na_{3.12}Zr_2(SiO_4)_{2.12}$ $(PO_4)_{0.88}$ (see [b])	$B2/b$	15.66	9.246	9.055	γ = 124.12	—	—	314, 315
$Na_{3.15}Zr_2(SiO_4)_{2.15}(PO_4)_{0.85}$ (see [b])	$R\bar{3}c$	9.079		22.96		—	—	314
$Na_{3.2}Zr_2(SiO_4)_{2.2}(PO_4)_{0.8}$	$C2/c$	15.618	9.051	9.210	123.93	167	23.1	112, 309
$Na_{3.25}Zr_2(SiO_4)_{2.25}(PO_4)_{0.75}$ (see [b])	$R\bar{3}c$	9.084		22.92		—	—	314
$Na_{3.35}Zr_2(SiO_4)_{2.35}(PO_4)_{0.65}$ (see [b])	$R\bar{3}c$	9.097		22.68		—	—	314
$Na_{3.4}Zr_2(SiO_4)_{2.4}(PO_4)_{0.6}$	$R\bar{3}c$	9.079		22.685		111	25.0	112, 309
$Na_{3.6}Zr_2(SiO_4)_{2.6}(PO_4)_{0.4}$	$R\bar{3}c$	—		—		36	23.1	309
$Na_{3.8}Zr_2(SiO_4)_{2.8}(PO_4)_{0.2}$	$R\bar{3}c$	9.148		22.239		18	23.1	112, 309
$Na_3Zr_{1.88}Y_{0.12}Si_2PO_{11.94}$	$C2/c$	—	—	—	—	240	29	316
$LiTi_2(PO_4)_3$	$R\bar{3}c$	8.512		20.858		0.1	34.7	269, 317
$Li_{1.4}Ti_{1.6}Al_{0.4}(PO_4)_3$	$R\bar{3}c$	8.503		20.847		28	24.1	318
$Li_{1.3}Ti_{1.7}Sc_{0.15}Y_{0.15}(PO_4)_3$	$R\bar{3}c$	8.555		20.939		20	27.9	319
$Li_{1.1}Ti_{1.9}Ga_{0.1}(PO_4)_3$	$R\bar{3}c$	8.51		20.88		0.2	60	320
$Li_{1.6}Ti_{1.4}Ga_{0.6}(PO_4)_3$	$R\bar{3}c$	25.64		62.83		8.4	49.1	321
$Li_{1.6}Ti_{1.7}Mg_{0.3}(PO_4)_3$	—	—	—	—	—	5.3	42.4	321
$Li_{0.9}Ti_{1.9}$ $Nb_{0.1}(PO_4)_3$	$R\bar{3}c$	8.527		20.90		0.02	60	322

[a] The subscripts z and y in the formula are respectively the deficiency in the number of ZrO_2 moles and the number of Zr^{4+} vacancies, each being compensated by four Na^+ cations (for the sake of electrical neutrality); [b] for these compounds, the crystal structures have been determined.

increases.[323] Upon the heterovalent substitution $P^{5+} \rightarrow B^{3+} + 2\,Na^+$, the unit cell volume of the solid solution $Na_{1+2x}Ti_{2-x}B_xP_{3-x}O_{12}$ increases; the increase in the occupancy of the vacant sites in the crystal lattice by mobile sodium ions is accompanied by an increase in the ionic conductivity of the solid solution compared with the sodium titanium phosphate.[324]

Data on arsenatophosphates $M^IZr_2As_{1.5}P_{1.5}O_{12}$ (M = Na, K)[325] and a continuous series of solid solutions $NaZr_2As_xP_{3-x}O_{12}$ have been reported.[326] They form rhombohedral cells (space group $R\bar{3}c$) and NZP-type structures.

The trigonal symmetry of the crystal structure of the solid solutions $M^I_{1-x}Zr_2(MoO_4)_x(PO_4)_{3-x}$ (M = Na, K, Rb, Cs; space group $R\bar{3}c$) occurs at $x \leqslant 0.6$.[327, 328] The boundary x value for the existence of the solid solution depends on the alkali metal cation size and the thermal stability of molybdatophosphates. The unit cell parameters (a, c, V) of the variable-composition phases $M^I_{1-x}Zr_2Mo_xP_{3-x}O_{12}$ change smoothly following the change in the composition (Fig. 24). An increase in the unit cell volume with an increase in x is attributable to replacement of the P^{5+} ion by larger Mo^{6+} ion. In this case, isomorphous exchange occurs

$$M^+ + P^{5+} \longrightarrow \square + Mo^{6+}$$

$\square$ is vacancy

It was proposed to use the crystalline NZP matrices for immobilization of molybdenum present in spent nuclear fuel.[329] Molybdatophosphates are promising as catalysts in methanol conversions.[330] The major products formed in this process under inert atmosphere include dimethyl ether (environmentally safe energy carrier) and water.

The prospects of using mixed phosphates depend on the properties important for technical applications, which are either new or improved with respect to those of monoanionic phosphates.

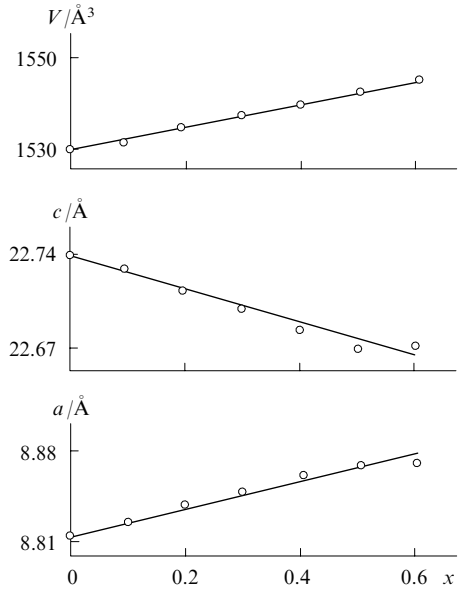


Figure 24. Crystallographic parameters a, c and V of the molybdatophosphates $Na_{1-x}Zr_2(MoO_4)_x(PO_4)_{3-x}$ *vs.* the composition (x).[329]

3. Properties

a. Ionic conduction

The high sodium-ion conductivity in the variable-composition phases $Na_{1+x}Zr_2Si_xP_{3-x}O_{12}$ was found by Hong *et al.*[112, 309] The compounds with $1.8 \leqslant x \leqslant 2.4$ possess superionic conductivity (> 0.1 S cm^{-1}) at moderate temperatures (523–573 K) (see Table 8). All of the oxygen atoms that surround the three-dimensional connected free space in the structure of NASICON solid solutions are simultaneously linked to quadruply and quintiply charged cations and have rather low electron-donating properties. Together with the only partial occupancy of the extra-framework cavities by sodium ions and the absence of steric hindrance to their movement along the migration channels, this ensures high mobility of the ions.[16, 268] For improving the electrophysical characteristics of $Na_{1+x}Zr_2Si_xP_{3-x}O_{12}$, various types of atomic substitution were accomplished: Zr^{4+} was replaced by other cations in the oxidation state $+4$ or by cations in the oxidation state $+3$ either with simultaneous replacement of Si^{4+} by P^{5+} or with a change in the sodium concentration.[7, 16, 272, 331–333] These substitutions, as well as the replacement of the phosphate anions by other anions (also with tetrahedrally directed chemical bonds), did not bring any noticeable enhancement of the transport characteristics as compared with the silicophosphate $Na_3Zr_2Si_2PO_{12}$; however, important advantages in some cases include lowering of the phase transition temperature or the disappearance of the phase transition [in this case, the kink in the $\sigma(T)$ curve disappears], simplification of the procedure of synthesiss and improvement of the characteristics of ceramic samples.

The conductivity level of the phosphates $M^{I}E_2^{IV}(PO_4)_3$ can be controlled by changing the size of the conducting channels *via* iso- and heterovalent replacement of the framework-forming cations; in the latter case, the occupancy of vacant sites in the crystal lattice by mobile ions changes.[7, 334–336] The partial replacement of the structure-forming E^{IV} cations in $M^{I}E_2^{IV}(PO_4)_3$ by metal cations in lower oxidation states results in an increase in the M^{I} ion concentration in the extraframework sites, which is accompanied by an increase in the ionic conductivity.[269, 270, 336] An increase in the concentration of lithium and sodium ions can also be achieved by decreasing the oxidation state of titanium in $LiTi_2(PO_4)_3$ and $NaTi_2(PO_4)_3$.[204–206, 337, 338] Similarly, the replacement of E^{IV} ions by higher-charged ions leads to the targeted formation of an enhanced concentration of cationic vacancies: for example, replacement of only 5% of zirconium in $LiZr_2(PO_4)_3$ by niobium induces complete transition of the compound into the high-temperature phase, the initial conductivity being increased by several orders of magnitude.[339] The replacement of lithium ions in $LiZr_2(PO_4)_3$ by hydrogen ions *via* ion exchange may give proton conductors with the NASICON structure, $(H_3O)Zr_2(PO_4)_3$ and $HZr_2(PO_4)_3$, the latter being one of the best proton-conducting solid electrolytes for the temperature range of 650–850 K.[271, 276, 277] The electrical conductivity of $Li_{0.5}Na_{0.5}Ti_2(PO_4)_3$ is comparable with the conductivity of NASICON solid electrolytes.[294] Note that in most cases, the isomorphous replacement in phosphates did not result in a noticeable improvement of the conductivity of the superionic phase. This is apparently due to the weak dependence of the concentration of mobile ions on the doping additives and the potential relief on the possible structure distortions.

The ionic conductivity of the NASICON materials has been mainly studied for ceramic samples. The conductivity values for the same systems obtained by different authors differ, which is caused by the complexity of preparation of dense and homogeneous ceramics, the use of different procedures of electrical conductivity measurements and the possible variation of the real composition of samples due to the use of different synthetic procedures. The data on the ionic conductivity of solid electrolytes with the NASICON structure obtained by different research groups were integrated in a recent review.[308] Unfortunately, this review almost does not reflect the works of Russian scientists devoted to lithium, sodium and hydrogen ion-conducting materials. These data are reported in a number of publications.[5, 6, 14, 334, 335, 340, 341]

After the thermodynamic instability of NASICON in the sodium melt had been established,[342] the search was started for possible applications of these materials in the devices where there is no need to use electrode materials with high activity with respect to sodium. It appears promising to use NASICON as thin-film materials (in particular, nanometre-thick) deposited on substrates for the design of miniature devices based on solid-state ionic conductors.[343, 344] Using solid electrolytes with ionic conductivity, a large number of highly sensitive sensors were designed. The possibilities of using silicophosphates in sensors for the detection and quantification of CO_2, NO_2, NH_3, H_2S and SO_2 are being discussed.[345–350] The NASICON material doped with rare earth elements and solid solutions $Na_{1-x}Cu_xZr_2(PO_4)_3$ are promising as effective luminophores.[351–354]

b. Catalytic activity

The materials in the crystal lattices of which reversible redox reactions take place can be used as catalysts. The ability of the $\{[L_2(PO_4)_3]^{p-}\}_{3\infty}$ framework to held cations of one element in different oxidation states [for example, Cu^+ (Refs 235 and 355) and Cu^{2+} (Ref. 356)] promotes reversible redox reactions, which allows using these phosphates [for example, $CuZr_2(PO_4)_3$] as catalysts for dehydrogenation of alcohols.[357] The reduction is accompanied by inclusion of protons into the crystal lattice, and oxidation is accompanied by proton exit from the lattice.[358, 359] In the case of $Na_{1-x}Cu_xZr_2(PO_4)_3$, $AgZr_2(PO_4)_3$, $AgHf_2(PO_4)_3$ and $NaZr_2(PO_4)_3$, which catalyze dehydration and dehydrogenation of methanol, isopropyl alcohol and butyl alcohol, their activity depends on the conditions of synthesis, porosity characteristics, specific surface area and catalyst loading.[9, 236, 242, 360–363] Sadykov *et al.*[171] ascertained that $NbTi_{0.75}V_{0.25}(PO_4)_3$ and $M_{0.5}Zr_2(PO_4)_3$ (M = Mn, Co, Cu) are active catalysts for alkane isomerization and selective oxidation.

c. Thermophysical properties

The knowledge of thermodynamic and thermophysical characteristics is needed to estimate the thermodynamic and chemical stability of phosphates, optimize their syntheses, compose thermal balances, construct phase diagrams, perform the physicochemical analysis of model systems and study the defect formation. The investigation of the thermophysical properties (heat capacity, thermal expansion and thermal conductivity) over a broad temperature range helps to determine the thermal stability of materials, the allowable range of temperature fluctuations and temper-

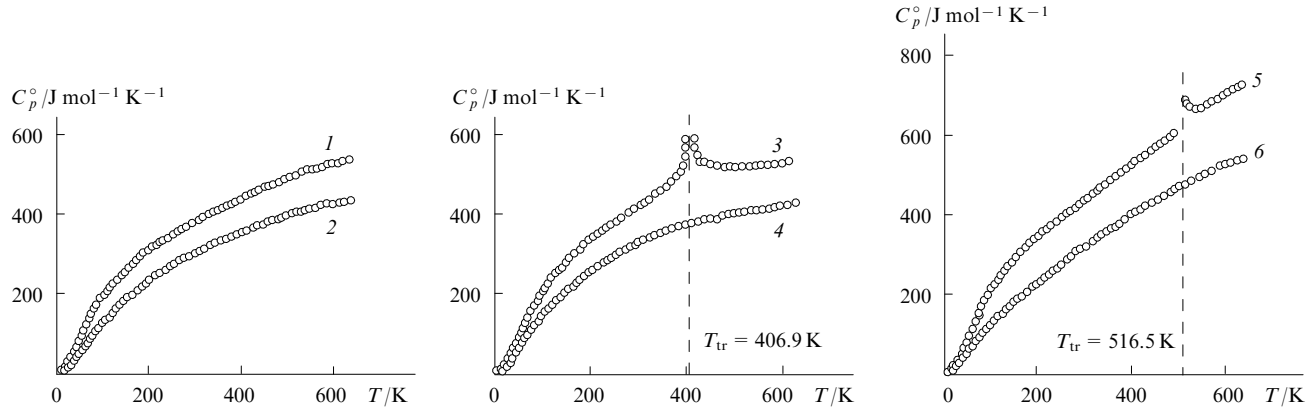


Figure 25. Temperature dependences of the heat capacity of $Na_5Ti(PO_4)_3$ (*1*), $NaTi_2(PO_4)_3$ (*2*), $Na_5Zr(PO_4)_3$ (*3*), $NaZr_2(PO_4)_3$ (*4*), $Na_5Hf(PO_4)_3$ (*5*), $NaHf_2(PO_4)_3$ (*6*). T_{tr} is the phase transition temperature.[286]

ature gradients in an article for its heat treatment during the manufacture or application.

For various representatives of NZP and related structures, the specific heat capacity is 0.5 – 1.2 J g^{-1} K^{-1} in the range of 273 – 650 K, and at $T > 500$ K it changes insignificantly.[19, 286, 364 – 366] An important feature is the lack of dependence of the heat capacity at high temperature on the material macrostructure, namely, the apparent density, porosity and pore size and shape distributions. On passing from the phosphates $NaE_2^{IV}(PO_4)_3$ to $Na_5E^{IV}(PO_4)_3$, the heat capacity increases (Fig. 25), *i.e.*, the general trend of increasing the heat capacity of compounds following an increase in the number of atoms in the unit cell holds in this case.[286] The decrease in the Debye temperature calculated from the $C_p^\circ(T)$ data in the series $NaE_2^{IV}(PO_4)_3 \rightarrow Na_5E^{IV}(PO_4)_3$ (E = Ti, Zr, Hf) (Table 9) provide the conclusion that the crystal lattices of $NaE_2^{IV}(PO_4)_3$ are more rigid than those of $Na_5E^{IV}(PO_4)_3$, where the structural framework contains, apart from the $E^{IV}O_6$ octahedra, also more deformable NaO_6 polyhedra. The lower rigidity of the structure results in unfreezing of lattice vibrations in $Na_5E^{IV}(PO_4)_3$ at lower temperature. The heat capacity curves of $Na_5Zr(PO_4)_3$ and $Na_5Hf(PO_4)_3$ exhibit phase transitions at temperatures of 406.9 and 516.5 K, respectively,[286, 370 – 372] associated with the change in the positional ordering of the Zr^{4+}, Hf^{4+} and Na^+ cations. $Na_5Ti(PO_4)_3$ possessing no polymorphism contains a non-split Ti^{4+} site and is characterized by lower mobility of Na^+ cations in relatively small framework cavities compared to the zirconium and hafnium phosphates of the same general formula.

Table 9. Characteristic Debye temperatures for $NaE_2^{IV}(PO_4)_3$ and $Na_5E^{IV}(PO_4)_3$ (E = Ti, Zr, Hf).

Compound	θ_D/K	δ (%)[a]	ΔT/K	Ref.
$NaTi_2(PO_4)_3$	169.1	1.1	7 – 12	367
$Na_5Ti(PO_4)_3$	104.1	2.0	7 – 11	368
$NaZr_2(PO_4)_3$	128.8	2.2	9 – 12	369
$Na_5Zr(PO_4)_3$	117.8	1.0	7 – 11	370, 371
$NaHf_2(PO_4)_3$	132.0	1.0	6 – 11	367
$Na_5Hf(PO_4)_3$	100.6	1.9	6 – 11	372

[a] δ is the root-mean-square error.

The data on the heat capacity, enthalpy, entropy and Gibbs energy of formation (Table 10) demonstrated that the solid-phase synthesis processes are thermodynamically allowed at 430 K for $NaZr_2(PO_4)_3$, at 410 K for $CsZr_2(PO_4)_3$ and at 570 K for $Na_5Zr(PO_4)_3$.[366] These phosphates are usually synthesized at higher temperatures [$\geqslant$ 1273 K for $CsZr_2(PO_4)_3$]. Using the precipitation procedure and optimization of the temperature conditions, $CsZr_2(PO_4)_3$ was obtained at 1023 K.[281]

Table 10. Standard thermodynamic functions of $NaE_2^{IV}(PO_4)_3$, $CsZr_2(PO_4)_3$ and $Na_5E^{IV}(PO_4)_3$ (E = Ti, Zr, Hf; T = 298.15 K, p = 0.1 MPa).

Compound	$C_{p,m}^\circ$ (see [a])	$-\Delta_f H$ (see [b])	$-\Delta_f S$ (see [a])	$-\Delta_f G$ (see [b])	Ref.
$NaTi_2(PO_4)_3$	293.2	–	1174	–	367
$Na_5Ti(PO_4)_3$	368.9	–	1217	–	366, 368
$NaZr_2(PO_4)_3$	305.9	5231	1156	4886	364, 369
$Na_5Zr(PO_4)_3$	388.9	5586	1216	5223	370, 371
$CsZr_2(PO_4)_3$	307.4	5301	1184	4948	364, 365
$NaHf_2(PO_4)_3$	292.3	–	1207	–	367
$Na_5Hf(PO_4)_3$	402.4	–	1202	–	372

[a] In J mol^{-1} K^{-1}; [b] in kJ mol^{-1}.

Detailed investigations of the thermodynamic properties of the variable-composition phases $Na_{1+x}Zr_2Si_xP_{3-x}O_{12}$ in the temperature range from 1.5 to 800 K by adiabatic and scanning calorimetry and e.m.f. measurements for electrochemical cells with NASICON showed that solid solutions are thermodynamically stable but on contact with sodium, degradation of the material is observed.[373, 374] For $Na_3Zr_2Si_2PO_{12}$, a first-order phase transition was found, which occurs over a broad temperature range (420 – 503 K).[375]

The heat capacity of a substance is related to the change in the average lattice vibrational energy and the amplitude of atom vibrations and depends on the thermal expansion coefficient (TEC). The thermal expansion directly affects the average kinetic energy of the vibrating particles in a body and the average distances between the crystal lattice points and is related to the asymmetry (anharmonicity) of the thermal vibrations of atoms; as a result, under variable temperature conditions, the interatomic distances

change.[376, 377] By investigating thermal expansion, it is possible to draw separate conclusions concerning the character of interaction between the atoms in the crystal, as the TEC is associated with the strength of chemical bonds in the structure: the weaker the bonds between the atoms, the greater the expansion. For rhombohedral lattices, the thermal expansion is determined by two linear expansion coefficients measured in the parallel (α_c) and perpendicular (α_a) directions to the principal threefold axis of the crystal and by the mean linear thermal expansion coefficient

$$\alpha_{av} = \frac{\alpha_V}{3} = \frac{2\alpha_a + \alpha_c}{3}.$$

The thermal expansion of the phosphates $M^{I}E_2^{IV}(PO_4)_3$ is the subject of numerous studies (Refs 4, 17, 167, 243, 245, 257, 262, 300, 378–385). Most of NZP compounds show thermal expansion anisotropy and large magnitudes of the linear thermal expansion coefficient (LTEC), but, nevertheless, low average TEC, for example, $NaE_2^{IV}(PO_4)_3$ and $RbZr_2(PO_4)_3$ (Table 11). When an NZP compound, for example, $NaZr_2(PO_4)_3$, is heated, the weakest Na–O bonds are elongated to a greater extent than the strong Zr–O and P–O bonds. On heating, the size of the trigonal antiprism around the Na site (M1 sites, see Fig. 1) increases and elongates the column of polyhedra along the *c* axis ($\alpha_c > 0$); as a result, the ZrO_6 octahedra and PO_4 tetrahedra that share corners rotate, causing angular distortions in the polyhedra. The tetrahedral O–P–O angle increases along the *c* axis, the distance between the columns of the framework structure shortens, and the structure is compressed along the *a* axis ($\alpha_a < 0$).[2, 379] As a result, the average TEC of compounds is very low. Similarly, the best known low-expansion materials — zircon, cordierite and quartz glass — have almost zero average expansion [$\alpha_{av} = (0.5–4.2)\times10^{-6}\ K^{-1}$ in the temperature range of 273–1273 K]. Different values of thermal expansion in different directions in a single-phase material induce mechanical stress at grain boundaries, which is sufficient to cause fracturing and breakdown of the continuity of the article. Owing to the ultra-low thermal expansion, in particular, nearly-zero LTEC and expansion anisotropy, some phosphates of the NZP family can withstand repeated sharp changes of thermal load (thermal shocks) and are most promising for the fabrication of thermomechanically stable materials. These properties are inherent in the phosphates $CsZr_2(PO_4)_3$ and $CsHf_2(PO_4)_3$ (see Table 11).

The behaviour of NZP structure in response to heat treatment depends on the nature, the ratio of sizes and the number of cations that occupy crystallographic sites, the number of vacant sites and the unit cell symmetry. Pet'kov and Orlova [4] proposed a system of empirical heat expansion rules for the lattice of NZP phosphates, which is suitable for extending the data to compounds that have not yet been studied and for targeted change in the thermal expansion characteristics. Thus, by combining the NZP compounds whose LTEC are similar in magnitude and have opposite signs and that form broad ranges of solid solutions, it is possible to predict ceramic compositions with controlled, in particular, ultra-low, thermal expansion. For example, we estimated the radius of the r_{M^+} cation corresponding to zero anisotropy ($\alpha_a = \alpha_c$) for a system of framework titanium and alkali metal phosphates.[291] The extrapolated LTEC lines along the *a* and *c* axes intersect at point $r_{M^+} \approx 1.48$ Å (Fig. 26). This value was used for predicting the phosphate $K_{0.5}Rb_{0.5}Ti_2(PO_4)_3$ with the radius of the 'formal' alkali metal cation ($K_{0.5}Rb_{0.5}$) of 1.45 Å; the LTEC of this phosphate are as follows: $\alpha_a = 0.7\times10^{-6}$, $\alpha_c = 3.0\times10^{-6}$, $\alpha_{av} = 1.4\times10^{-6}\ K^{-1}$ for 298–1173 K.

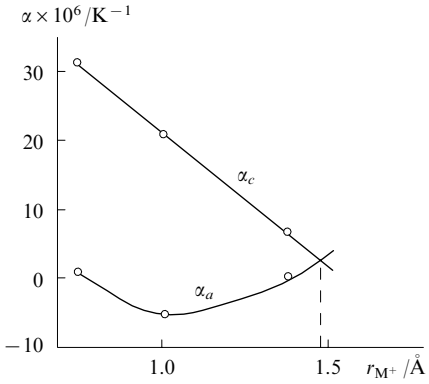


Figure 26. Thermal linear expansion coefficients (298–1073 K) of the phosphates $MTi_2(PO_4)_3$ along the *a* and *c* axes *vs*. the cation M^+ radius.[291]

Table 11. Thermal expansion coefficients ($\alpha\times10^6/K^{-1}$) of $M^{I}E_2^{IV}(PO_4)_3$ between room temperature and upper temperature of measurements (873–1273 K).

Compound	α_a	α_c	α_{av}	Anisotropy $/\lvert\alpha_a-\alpha_c\rvert$	Ref.
$LiTi_2(PO_4)_3$	0.49	30.8	10.6	30.3	167
$NaTi_2(PO_4)_3$	−5.3	20.8	3.4	26.1	167
$AgTi_2(PO_4)_3$	−2	12	5.3	14	385
$KTi_2(PO_4)_3$	−0.13	6.6	2.12	6.7	167
$NaZr_2(PO_4)_3$	−5.50	22.30	3.8	27.8	381
$KZr_2(PO_4)_3$	−5.30	5.41	−1.73	10.7	381
$RbZr_2(PO_4)_3$	−8	13	−1	21	382
$CsZr_2(PO_4)_3$	−0.56	0.45	−0.22	1.0	382
$NaHf_2(PO_4)_3$	−6.55	21.0	2.63	27.5	382
$CsHf_2(PO_4)_3$	−1.1	1	−0.4	2.1	382
$LiGe_2(PO_4)_3$	−0.75	22.5	7.0	23.2	243
$NaGe_2(PO_4)_3$	12	12.1	12.0	0.1	245
$KGe_2(PO_4)_3$	21.4	7.6	16.8	13.8	245

A comparison of the effect of heat treatment and crystal chemical substitution on the geometric characteristics of the crystal lattice demonstrates that as the temperature increases, the occupied octahedron, for example, $Na(M1)O_6$, expands but not to an extent sufficient for obtaining the equivalent-size polyhedron $M^{I}(M1)O_6$ with M^{I} = K, Rb or Cs with isomorphous replacement of sodium by a larger alkali metal cation. Thus, the crystal chemical effects of substitution and thermal expansion have common features but are not strictly equivalent, although both factors affect the same atomic bonds in the structure.

To predict the applications and improve the production process of ceramics, it is necessary to know its thermal conductivity. The thermal conductivity of the ceramics $NaE_2^{IV}(PO_4)_3$ and $Na_5E^{IV}(PO_4)_3$ in temperature range of 298–673 K smoothly increases with temperature (Fig. 27). In the series

$$NaTi_2(PO_4)_3 \rightarrow NaZr_2(PO_4)_3 \rightarrow NaHf_2(PO_4)_3$$

$$Na_5Ti(PO_4)_3 \rightarrow Na_5Zr(PO_4)_3 \rightarrow Na_5Hf(PO_4)_3,$$

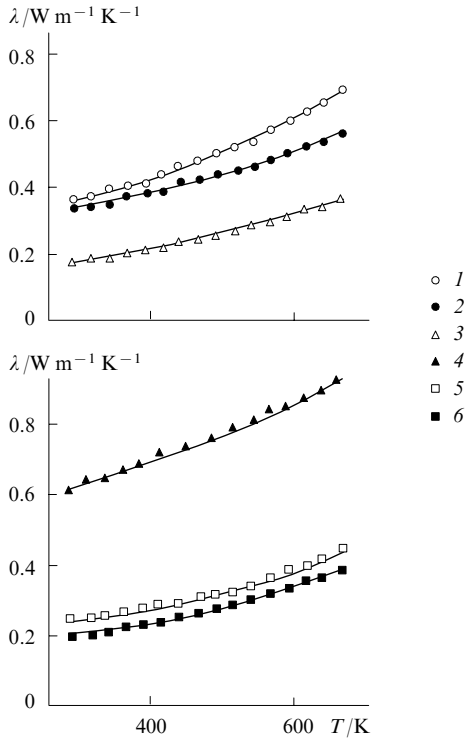


Figure 27. Temperature dependences of the thermal conductivity of $NaTi_2(PO_4)_3$ (*1*), $NaZr_2(PO_4)_3$ (*2*), $NaHf_2(PO_4)_3$ (*3*), $Na_5Ti(PO_4)_3$ (*4*), $Na_5Zr(PO_4)_3$ (*5*), $Na_5Hf(PO_4)_3$ (*6*).[291]
The relative density is 70%–80% of the theoretical value.

the thermal conductivity coefficient decreases when heavier atoms with smaller thermal vibration amplitude enter the structure.[19, 22] Loose air-containing ceramics with loss of contact between the grains would have lower thermal conductivity coefficients. An increase in the porosity enhances thermal-insulating properties, while a decrease in the porosity enhances the resistance against mechanical breakdown. At zero porosity, NZP ceramics have lower thermal conductivity (0.5–1.4 W m^{-1} K^{-1} in the range of 298–673 K) than zirconium dioxide (1.95–2.44 W m^{-1} K^{-1}, 373–1673 K), which is the major component of industrial refractory materials. Low thermal conductivity, high melting temperatures and low thermal expansion allow considering the NZP ceramics as promising highly resistant refractory materials and thermal insulators, which surpass the known materials in the ability to withstand thermal shocks.

High tolerance of the NZP-type structure to the change in the chemical composition, resistance against destructive environmental factors and good processability are prerequisites for the formation of single-phase ceramics capable of incorporating radionuclides and process elements present in highly active fractions of nuclear wastes.[3, 13, 302] As regards the level of hydrolytic stability (the achieved minimum leaching rates are $\sim 10^{-6}$ g cm^{-2} day^{-1}), the NZP phosphates are not inferior to the currently used matrix materials for radionuclide immobilization (glass, $\sim 10^{-4}$–10^{-6}; ceramics Synroc D, $\sim 10^{-5}$ g cm^{-2} day^{-1}) and their resistance to high temperatures and thermal shocks often surpasses the stability of these matrices.[304, 386]

IV. Conclusion

The information presented in this review demonstrates extension of the range of objects and crystal structures of various groups of complex phosphates containing M^I and E^{IV} cations. Their comparison reveals not only formal similarity (composition, simplest structural polyhedra) but also some structural features depending on dimensional factors (ionic radii of the cations), the nature of cations and anions, the presence of water molecules and hydrogen bonding.

Layered phosphates typically form compositions with the ratio $E^{IV}:PO_4^{3-} = 1:2$, for example, $M^I_2E^{IV}(PO_4)_2$, $M^I_2E^{IV}(PO_4)_2 \cdot n\,H_2O$, $M^IHE^{IV}(PO_4)_2 \cdot n\,H_2O$, $E^{IV}(HPO_4)_2 \cdot$ $\cdot n\,H_2O$. The presence of water molecules gives rise to phosphates differing both in the composition and the structure. Framework structures are typical of phosphates with $E^{IV}:PO_4^{3-}$ ratios of 1:1.5 and 1:3, for example, $M^IE^{IV}_2(PO_4)_3$ and $M^I_5E^{IV}(PO_4)_3$. Unlike layered phosphates, in the three-dimensional lattice of NZP and related structures, the $P-O-E^{IV}$ bonds are formed with the participation of all oxygen atoms of the anion and the framework itself changes little upon the variation of cations. Deep dehydration and thermal decomposition of both acid and neutral layered phosphates results in rearrangement of the solid phase and gives crystalline products with framework structure and higher thermal stability.

The structures of complex phosphates of all presented types are composed of $E^{IV}O_6$, $E^{IV}O_9$, PO_4 or HPO_4 polyhedra (the functions of the PO_4 tetrahedra can partly be performed by other tetrahedral TO_4 oxo anions). The polyhedra of E^{IV} d metal ions with the ionic radius $r \leqslant 0.8$ Å are more or less distorted octahedra the corners of which are occupied by oxygen atoms of the PO_4, HPO_4, TO_4 groups or water molecules. As the radius increases, the E^{IV} cations tend to increase their coordination polyhedra and, as a consequence, to change the structural type. This conclusion is true for actinide compounds: the polyhedra of E^{IV} f metal ions are either octahedra or nine-vertex polyhedra, which resemble tricapped trigonal prisms. The coordination numbers of M^I alkali metal ions in the structures of presented phosphates are 4, 6, 7, 8 and 12.

Currently complex and mixed phosphates are investigated at several levels: apart from the polycrystalline structure of materials with inherent defects such as domain boundaries, pores and cracks, studies also deal with the electronic and magnetic structures of compounds, the crystal structure defects characteristic of them, distribution of microimpurities, nanostructure and the influence of these characteristics on the physical properties. Intensive studies directed at the use of phosphates in chemistry and chemical engineering are in progress in Russia, the USA, UK, France, Japan, India and China. The information presented in this review attests to broad possibilities opened up by the use of phosphates as functional (ceramic electrolytes, gas sensors, fuel cells, luminophores, ion exchange resins, selective catalysts, radiation-resistant immobilizing matrices for toxic waste disposal) and structural articles (engine parts, lining elements, dimension-stable semiconductor substrates, catalyst supports).

Consider the trends of studies into this interesting family of materials expected in the near future. In the field of synthesis, the key tasks are to extend the ranges of energy treatment of compounds aimed at development of new methods for the manufacture of materials, development of

production processes of single crystalline samples and compounds that contain organic groups in addition to the inorganic components. Resorting to semiempirical methods of structural modelling that do not require considering the intraatomic interactions would make it possible to predict the structures of a broad range of crystals, optimize the properties of phosphates and determine their ultimate characteristics. New experimental data and simpler concepts of the mechanism of thermal expansion are needed for better understanding of the specific behaviour (nearly zero expansion) of the NZP materials.

The above-listed fields of application of the materials based on complex phosphates require the production of high-density ceramics. It is known that the key drawback of ceramics is the trend for brittle fracture. The fracture threshold at defects of the type of voids (between the material grains) can be exceeded well before the total load on the article reaches the threshold. The production of ceramics with nearly theoretical density minimizes the number of such defects, improves the properties of materials, decreases the rate of interaction with salt solutions and melts on their surface. Powders of NZP compounds with predominantly interatomic covalent bonds cannot be sintered to a density close to theoretical density without introducing special additives that form the structure of grain boundaries in the ceramic materials. The studies dealing with production of high-density NZP ceramics are few but quite topical. In a number of studies,[387–392] the density of sintered ceramics reached 89% – 99% of the theoretical value with the use of 1 mass % – 5 mass % of sintering additives: MgO, ZnO, $Co_3(PO_4)_2$, NaCl, Ti, Sn, Sb. The researchers cited[387, 392] made assumptions about the sintering mechanisms of NZP materials, the liquid-phase and reaction mechanisms. By using a new method for the production of ceramics, spark plasma sintering, it is possible to reach a nearly theoretical density without using the sintering additives.[318, 391, 393, 394] The progress in these studies concerned with the kinetics and mechanisms of sintering of NZP materials, identification of the routes for intensification of sintering, development of the methods for the preparation of high-density ceramics, would provide the possibility of preparing high-density and fracture-resistant ceramic materials with perfect structure, high characteristics and performance reliability.[395]

This review was prepared with the partial financial support of the Russian Foundation for Basic Research (Project Nos 08-03-00082a and 11-03-00032a).

References

1. Yu D Tretyakov *Russ. Chem. Rev.* **72** 651 (2003) [*Usp. Khim.* **72** 731 (2003)]
2. J Alamo *Solid State Ionics* **63 – 65** 547 (1993)
3. B E Scheetz, D K Agrawal, E Breval, R Roy *Waste Manage.* **14** 489 (1994)
4. V I Pet'kov, A I Orlova *Neorg. Mater.* **39** 1177 (2003) [a]
5. A B Yaroslavtsev, I A Stenina *Russ. J. Inorg. Chem.* (*Suppl. 1*) **51** S97 (2006)
6. V B Kalinin, S Yu Stefanovich, in *Kationnaya Podvizhnost' v Ortofosfatakh. Khimiya Tverdogo Tela (Itogi Nauki i Tekhniki)* [Cation Mobility in Orthophosphates. Solid State Chemistry (Advances in Science and Engineering Series)] Vol. 8 (Moscow: Izd. VINITI, 1992) p. 1
7. E Breval, H A McKinstry, D K Agrawal *Br. Ceram. Trans.* **93** 239 (1994)
8. B I Lazoryak *Russ. Chem. Rev.* **65** 287 (1996) [*Usp. Khim.* **65** 307 (1996)]
9. V I Pet'kov, M V Sukhanov, M M Ermilova, N V Orekhova, G F Tereshchenko *Zh. Prikl. Khim.* **83** 1591 (2010) [b]
10. M E Brownfield, E E Foord, S J Sutley, T Botinelly *Am. Mineral.* **78** 653 (1993)
11. L-O Hagman, P Kierkegaard *Acta Chem. Scand.* **22** 1822 (1968)
12. V I Pet'kov, G I Dorokhova, A I Orlova *Kristallografiya* **46** 76 (2001) [c]
13. A I Orlova *Radiokhimiya* **44** 385 (2002) [d]
14. I A Stenina, A R Shaykhlislamova, I Yu Pinus, A B Yaroslavtsev, in *Fast Proton-Ion Transport Compounds* (Eds U B Mioč, M Davidovič) (Trivandrum, Kerala, India: Research Signpost, 2010) p. 127
15. P Knauth *Solid State Ionics* **180** 911 (2009)
16. A K Ivanov-Shits, I V Murin *Ionika Tverdogo Tela* Vol. 1 (Ionics of Solids) (St Petersburg: St Petersburg State University, 2001)
17. E Breval, D K Agrawal *Br. Ceram. Trans.* **94** 27 (1995)
18. NZP Ceramics, a New Class of Materials *Am. Ceram. Soc. Bull.* **76** 71 (1997)
19. V I Pet'kov, E A Asabina *Steklo Keram.* (7) 23 (2004) [e]
20. A A Lukuttsov, M L Spiridonova, N A Kulagina, A I Orlova, V I Pet'kov, I A Kulikov *Zh. Prikl. Khim.* **77** 1249 (2004) [b]
21. D-M Liu *J. Mater. Sci. Lett.* **13** 129 (1994)
22. V I Pet'kov, V N Loshkarev, E A Asabina *Zh. Prikl. Khim.* **77** 184 (2004) [b]
23. V Brandel, N Dacheux *J. Solid State Chem.* **177** 4743 (2004)
24. V Brandel, N Dacheux *J. Solid State Chem.* **177** 4755 (2004)
25. I V Tananaev, I A Rozanov, K A Avduevskaya, E N Beresnev, V R Berdnikov *Fosfaty Chetyrekhvalentnykh Elementov* (Phosphates of Tetravalent Elements) (Moscow: Nauka, 1972)
26. A Clearfield, G H Nancollas, R H Blessing, in *Ion Exchange and Solvent Extraction* Vol. 5 (Eds J A Marinsky, Y Marcus) (New York: Marcel Dekker, 1973) Ch. 1
27. Yu V Efremov, A I Shafiev, N G Chernorukov, I A Korshunov, G N Yakovlev *Sintez, Svoistva i Primenenie Fosfata Tsirkoniya (Obzor) (Preprint)* [Synthesis, Properties and Applications of Zirconium Phosphate] (Review) (Preprint)] (Dimitrovgrad: Research Institute of Atomic Reactors, 1973)
28. G Alberti, U Costantino *J. Chromatogr. A* **102** 5 (1974)
29. A Clearfield *Annu. Rev. Mater. Res.* **14** 205 (1984)
30. R Llavona, M Suárez, J P Garcia, J Rodriguez *Inorg. Chem.* **28** 2863 (1989)
31. G Alberti, M Casciola, U Costantino, R Vivani *Adv. Mater.* **8** 291 (1996)
32. A B Yaroslavtsev *Russ. Chem. Rev.* **66** 579 (1997) [*Usp. Khim.* **66** 641 (1997)]
33. M Suárez, L M Barcina, R Llavona, J Rodríguez *J. Mol. Struct.* **470** 105 (1998)
34. A B Yaroslavtsev, V Yu Kotov *Izv. Akad. Nauk, Ser. Khim.* 515 (2002) [f]
35. L Sun, W J Boo, H-J Sue, A Clearfield *New J. Chem.* **31** 39 (2007)
36. G Alberti, R Vivani, F Marmottini, P Zappelli *J. Porous Mater.* **5** 205 (1998)
37. F Odobel, B Bujoli, D Massiot *Chem. Mater.* **13** 163 (2001)
38. A Clearfield, C V K Sharma, B Zhang *Chem. Mater.* **13** 3099 (2001)
39. A B Yaroslavtsev *Solid State Ionics* **176** 2935 (2005)
40. M Casciola, G Alberti, A Donnadio, M Pica, F Marmottini, A Bottino, P Piaggio *J. Mater. Chem.* **15** 4262 (2005)
41. R Vivani, G Alberti, F Costantino, M Nocchetti *Microporous Mesoporous Mater.* **107** 58 (2008)
42. M Casciola, D Capitani, A Comite, A Donnadio, V Frittella, M Pica, M Sganappa, A Varzi *Fuel Cells* **8** 217 (2008)

43. E Brunet, H M H Alhendawi, O Juanes, L Jiménes, J C Rodríguez-Ubis *J. Mater. Chem.* **19** 2494 (2009)
44. L Sun, J Y O'Reilly, D Kong, J Y Su, W J Boo, H-J Sue, A Clearfield *J. Colloid Interface Sci.* **333** 503 (2009)
45. A B Yaroslavtsev *Russ. Chem. Rev.* **78** 1013 (2009) [*Usp. Khim.* **78** 1094 (2009)]
46. A Clearfield, J A Stynes *J. Inorg. Nucl. Chem.* **26** 117 (1964)
47. V Veselý, V Pekárek *Talanta* **19** 219 (1972)
48. A Clearfield, in *Ion Exchange Materials* (Ed. A Clearfield) (Boca Raton, FL: CRC Press, 1982) Ch. 2
49. Y Hasegawa *Seramikkusu (Ceram. Jpn.)* **20** 1090 (1985); *Chem. Abstr.* **104** 217946 (1986)
50. H Benhamza, P Barboux, A Bouhaouss, F-A Josien, J Livage *J. Mater. Chem.* **1** 681 (1991)
51. Yu I Sukharev, Yu V Egorov *Neorganicheskie Ionity Tipa Fosfata Tsirkoniya* (Inorganic Ion Exchangers of the Zirconium Phosphate Type) (Moscow: Energoatomizdat, 1993)
52. C Trobajo, S A Khainakov, A Espina, J R García *Chem. Mater.* **12** 1787 (2000)
53. P L Stanghellini, E Boccaleri, E Diana, G Alberti, R Vivani *Inorg. Chem.* **43** 5698 (2004)
54. R Thakkar, H Patel, U Chudasama *Bull. Mater. Sci.* **30** 205 (2007)
55. Z Yan, C W Kirby, Y Huang *J. Phys. Chem. C* **112** 8575 (2008)
56. A F Ali, A A Hanna, A E Gad *Phosphorus Res. Bull.* **22** 32 (2008)
57. D Capitani, M Casciola, A Donnadio, R Vivani *Inorg. Chem.* **49** 9409 (2010)
58. *Inorganic Ion Exchangers* (Ed. C B Amphlett) (Amsterdam: Elsevier, 1964)
59. S Ahrland, G Carleson *J. Inorg. Nucl. Chem.* **33** 2229 (1971)
60. L Zsinka, L Szirtes, J Mink, A Kálmán *J. Inorg. Nucl. Chem.* **36** 1147 (1974)
61. F L Moore *Anal. Chem.* **43** 487 (1971)
62. L M Sharygin, V E Moiseev, A P Shtin, V N Pyshkin, V M Galkin, R V Kuz'mina, A A D'yakov *Radiokhimiya* **26** 156 (1984) [d]
63. A Nilchi, M G Maragheh, A Khanchi, M A Farajzadeh, A A Aghaei *J. Radioanal. Nucl. Chem.* **261** 393 (2004)
64. G Alberti, E Torracca *J. Inorg. Nucl. Chem.* **30** 317 (1968)
65. G Alberti, U Costantino, R Giulietti *J. Inorg. Nucl. Chem.* **42** 1062 (1980)
66. S Bruque, M A G Aranda, E R Losilla, P Olivera-Pastor, P Maireles-Torres *Inorg. Chem.* **34** 893 (1995)
67. A N Christensen, E Krogh-Andersen, I G Krogh-Andersen, G Alberi, M Nielsen, M S Lehmann *Acta Chem. Scand.* **44** 865 (1990)
68. L Peters, J S O Evans *J. Solid State Chem.* **180** 2363 (2007)
69. J M Troup, A Clearfield *Inorg. Chem.* **16** 3311 (1977)
70. M I Zhuk, N G Chernorukov, I A Korshunov, G F Sibrina *Zh. Neorg. Khim.* **29** 2253 (1984) [g]
71. M A Salvadó, P Pertierra, S García-Granda, J R García, J Rodríguez, M T Fernández-Díaz *Acta Crystallogr., Sect. B* **52** 896 (1996)
72. I Nakai, K Imai, T Kawashima, K Ohsumi, F Izumi, I Tomita *Anal. Sci.* **6** 689 (1990)
73. G Alberti, U Costantino, R Millini, G Perego, R Vivani *J. Solid State Chem.* **113** 289 (1994)
74. M A Salvadó, S García-Granda, J Rodríguez *Mater. Sci. Forum* **166–169** 619 (1994)
75. D M Poojary, B Shpeizer, A Clearfield *J. Chem. Soc. Dalton Trans.* 111 (1995)
76. M Suárez, L M Barcina, R Llavona, J Rodríguez, M A Salvadó, P Pertierra, S García-Granda *J. Chem. Soc. Dalton Trans.* 99 (1998)
77. V A Burnell, J E Readman, C C Tang, J E Parker, S P Thompson, J A Hriljac *J. Solid State Chem.* **183** 2196 (2010)
78. A Clearfield *Chem. Rev.* **88** 125 (1988)
79. B B Sahu, K Parida *J. Colloid Interface Sci.* **248** 221 (2002)
80. R Romano, A I Ruiz, O L Alves *J. Solid State Chem.* **177** 1520 (2004)
81. G Alberti, U Costantino, J P Gupta *J. Inorg. Nucl. Chem.* **36** 2109 (1974)
82. J Albertsson, A Oskarsson, R Tellgren, J O Tomas *J. Phys. Chem.* **81** 1574 (1977)
83. G Schuck, R Melzer, R Sonntag, R E Lechner, A Bohn, K Langer, M Casciola *Solid State Ionics* **77** 55 (1995)
84. G Alberti, U Costantino, M L L Giovagnotti *J. Inorg. Nucl. Chem.* **41** 643 (1979)
85. V P Titov, S V Yakubovskaya, R Ya Mel'nikova, Yu G Zonov, N A Akulich *Zh. Neorg. Khim.* **33** 563 (1988) [g]
86. S Yamanaka, M Tanaka *J. Inorg. Nucl. Chem.* **41** 45 (1979)
87. G Alberti, R Vivani, S M Mascarós *J. Mol. Struct.* **470** 81 (1998)
88. N J Clayden *J. Chem. Soc. Dalton Trans.* 1877 (1987)
89. A M Krogh Andersen, P Norby, J C Hanson, T Vogt *Inorg. Chem.* **37** 876 (1998)
90. L Kullberg, A Clearfield *J. Phys. Chem.* **85** 1585 (1981)
91. A B Yaroslavtsev *Khimiya Tverdogo Tela* (Solid State Chemistry) (Moscow: Nauchnyi Mir, 2009)
92. V Yu Kotov, I A Stenina, A B Yaroslavtsev *Zh. Neorg. Khim.* **43** 1786 (1998) [g]
93. I A Stenina, V Yu Kotov, A B Yaroslavtsev *Elektrokhimiya* **38** 968 (2002) [h]
94. M N Kislitsyn, V Yu Kotov, A B Yaroslavtsev *Zh. Neorg. Khim.* **45** 376 (2000) [g]
95. I A Stenina, A D Aliev, I V Glukhov, F M Spiridonov, A B Yaroslavtsev *Solid State Ionics* **162–163** 191 (2003)
96. A Clearfield, L B McCusker, P R Rudolf *Inorg. Chem.* **23** 4679 (1984)
97. P R Rudolf, A Clearfield *Inorg. Chem.* **24** 3714 (1985)
98. P R Rudolf, A Clearfield *Inorg. Chem.* **28** 1706 (1989)
99. D M Poojary, A Clearfield *Inorg. Chem.* **33** 3685 (1994)
100. A Clearfield, J Troup *J. Phys. Chem.* **74** 314 (1970)
101. I Tomita, K Magami, H Watanabe, K Suzuki, T Nakamura *Bull. Chem. Soc. Jpn.* **56** 3183 (1983)
102. A Clearfield, W L Duax, A S Medina, G D Smith, J R Thomas *J. Phys. Chem.* **73** 3424 (1969)
103. N G Chernorukov, M I Zhuk, E N Velikzhanina *Zh. Neorg. Khim.* **34** 1738 (1989) [g]
104. A Clearfield, W L Duax, J M Garces, A S Medina *J. Inorg. Nucl. Chem.* **34** 329 (1972)
105. I Tomita, M Banju, K Noguchi, T Nakamura *Bull. Chem. Soc. Jpn.* **57** 3281 (1984)
106. G Alberti, U Costantino, S Allulli, M A Massucci *J. Inorg. Nucl. Chem.* **37** 1779 (1975)
107. N G Chernorukov, T V Prokof'eva *Izv. Vyssh. Ucheb. Zaved., Khim. Khim. Tekhnol.* **21** 1252 (1978)
108. Y Hasegawa, I Tomita *Ionics. Ion. Sci. Technol.* (120) 121 (1985)
109. P Rudolf, A Clearfield *Acta Crystallogr. Sect. B* **41** 418 (1985)
110. D M Poojary, B Zhang, Y Dong, G Peng, A Clearfield *J. Phys. Chem.* **98** 13616 (1994)
111. I G Trubach, Candidate Thesis in Chemical Sciences, Nizhnii Novgorod State University, Nizhnii Novgorod, 2003
112. H Y-P Hong *Mater. Res. Bull.* **11** 173 (1976)
113. V I Pet'kov, A I Orlova, O V Egor'kova *Zh. Strukt. Khim.* **37** 1104 (1996) [i]
114. M Dörffel, J Liebertz *Z. Kristallogr.* **193** 155 (1990)
115. P Tarte, C Merckaert-Ansay *Bull. Soc. Roy. Sci. Liege* **49** 358 (1980)
116. A V Barabanova, A O Turakulova, V V Lunin, P Afanasiev *J. Mater. Chem.* **7** 791 (1997)
117. F Mounier, L Winand *Bull. Soc. Chim. Fr.* 1829 (1968)
118. A I Orlova, I G Trubach, V I Pet'kov, Yu P Klapshin, V S Kurazhkovskaya *Radiokhimiya* **43** 195 (2001) [d]
119. A Clearfield, J M Troup *J. Phys. Chem.* **77** 243 (1973)
120. A B Yaroslavtsev, Z N Prozorovskaya, V F Chuvaev *Zh. Neorg. Khim.* **35** 1379 (1990) [g]

121. N V Karyakin, N G Chernorukov, A K Koryttseva, G N Chernorukov *Zh. Neorg. Khim.* **43** 1511 (1998) [g]
122. N V Karyakin, N G Chernorukov, A K Koryttseva, G N Chernorukov *Zh. Neorg. Khim.* **43** 1667 (1998) [g]
123. N V Karyakin, N G Chernorukov, A K Koryttseva, G N Chernorukov *Zh. Neorg. Khim.* **43** 1885 (1998) [g]
124. N G Chernorukov, I A Korshunov, T V Prokof'eva in *Ionity i Innyi Obmen* (Ion-exchange Resins and Ion Exchange) (Eds G V Samsonov, P G Romankov) (Leningrad: Nauka, 1975) p. 75
125. A Clearfield, S P Pack, J M Troup *J. Inorg. Nucl. Chem.* **39** 1437 (1977)
126. N G Chernorukov *Zh. Prikl. Khim.* **51** 431 (1978) [b]
127. N G Chernorukov, G F Sibrina *Zh. Prikl. Khim.* **53** 939 (1980) [b]
128. A Clearfield, P Jirustithipong, R N Cotman, S P Pack *Mater. Res. Bull.* **15** 1603 (1980)
129. A Clearfield *Eur. J. Solid State Inorg. Chem.* **28** 37 (1991)
130. Y Sadaoka, M Matsuguchi, Y Sakai, S Mitsui, M Toitu, K Hatanaka *J. Mater. Sci.* **24** 432 (1989)
131. M N Kislitsyn, V A Ketsko, A B Yaroslavtsev *Zh. Neorg. Khim.* **49** 367 (2004) [g]
132. V A Ketsko, M N Kislitsyn, V Yu Kotov, A B Yaroslavtsev *Zh. Neorg. Khim.* **44** 1984 (1999) [g]
133. Yu A Karavanova, I A Stenina, A B Yaroslavtsev *Zh. Neorg. Khim.* **54** 1059 (2009) [g]
134. M N Kislitsyn, A E Baranchikov, V K Ivanov, Yu D Tretyakov, A B Yaroslavtsev *Neorg. Mater.* **38** 858 (2002) [a]
135. A Clearfield, A S Medina *J. Inorg. Nucl. Chem.* **32** 2775 (1970)
136. M L Chavez, P Quitana, A R West *Br. Ceram. Trans. J.* **85** 167 (1986)
137. J Wang, I D Raistrick, R A Huggins *J. Electrochem. Soc.* **136** 2529 (1989)
138. M Barj, H Perthuis, P Colomban *Solid State Ionics* **9 – 10** 845 (1983)
139. M Barj, H Perthuis, P Colomban *Solid State Ionics* **11** 157 (1983)
140. L N Komissarova, M G Zhizhin, A A Filaretov *Russ. Chem. Rev.* **71** 619 (2002) [*Usp. Khim.* **71** 707 (2002)]
141. S J Milne, A R West *Solid State Ionics* **9 – 10** 865 (1983)
142. N S Slobodyanik, P G Nagornyi, Z I Kornienko, E S Lugovskaya *Zh. Neorg. Khim.* **33** 443 (1988) [g]
143. A Clearfield *Ind. Eng. Chem. Res.* **34** 2865 (1995)
144. S Yamanaka *J. Inorg. Nucl. Chem.* **42** 717 (1980)
145. M Casciola, D Fabiani *Solid State Ionics* **11** 31 (1983)
146. G Alberti, M Casciola, U Costantino, M Leonardi *Solid State Ionics* **14** 289 (1984)
147. M Casciola, D Bianchi *Solid State Ionics* **17** 287 (1985)
148. M de L Chavez, P Quintana, A R West *Mater. Res. Bull.* **21** 1411 (1986)
149. Y Sadaoka, Y Sakai *J. Mater. Sci. Lett.* **5** 731 (1986)
150. G Alberti, M Casciola, U Costantino, A Peraio, T Rega *J. Mater. Chem.* **5** 1809 (1995)
151. A B Yaroslavtsev, A L Mirak'yan, V F Chuvaev, L N Sokolova *Zh. Neorg. Khim.* **42** 900 (1997) [g]
152. Y-I Park, J-D Kim, M Nagai *J. Mater Sci. Lett.* **19** 1735 (2000)
153. G Alberti, M Casciola, D Capitani, A Donnadio, R Narducci, M Pica, M Sganappa *Electrochim. Acta* **52** 8125 (2007)
154. M Casciola, G Bagnasco, A Donnadio, L Micoli, M Pica, M Sganappa, M Turco *Fuel Cells* **9** 394 (2009)
155. D M Mognonov, M S Dashitsyrenova, I Yu Pinus, Zh P Mazurevskaya, Yu E Doroshenko, A B Yaroslavtsev *Vysokomol. Soedin., Ser. A* **52** 956 (2010) [j]
156. A B Yaroslavtsev *Ros. Khim. Zh.* **53** 131 (2009) [k]
157. M Casciola, U Costantino, A Calevi *Solid State Ionics* **61** 245 (1993)
158. P Giannoccaro, M Aresta, S Doronzo, C Ferragina *Appl. Organomet. Chem.* **14** 581 (2000)
159. G Alberti, G M Lombardo, G C Pappalardo, R Vivani *Chem. Mater.* **14** 295 (2002)
160. U Costantino, R Vivani, V Zima, L Beneš, K Melánová *Langmuir* **18** 1211 (2002)
161. L Liu, Z-F Chen, H-B Wei, Y Li, Y-C Fu, H Xu, J-P Li, A M Z Slawin, J-X Dong *Inorg. Chem.* **49** 8270 (2010)
162. C Ferragina, R Di Rocco, P Giannoccaro, L Petrilli *Mater. Res. Bull.* **42** 1422 (2007)
163. X Yang, X Chen, L Yang, W Yang *Bioelectrochemistry* **74** 90 (2008)
164. A Hayashi, H Nakayama, M Tsuhako *Solid State Sci.* **11** 1007 (2009)
165. E Brunet, H M H Alhendawi, C Cerro, M J de la Mata, O Juanes, J C Rodríguez-Ubis *Chem. Eng. J.* **158** 333 (2010)
166. G Alberti, S Murcia-Mascarós, R Vivani *J. Am. Chem. Soc.* **120** 9291 (1998)
167. D A Woodcock, P Lightfoot *J. Mater. Chem.* **9** 2907 (1999)
168. S Krimi, I Mansouri, A El Jazouli, J P Chaminade, P Gravereau, G Le Flem *J. Alloys Compd.* **188** 120 (1992)
169. V I Pet'kov, A I Orlova, D A Kapranov *Zh. Neorg. Khim.* **43** 1534 (1998) [g]
170. P Yu Butyagin *Russ. Chem. Rev.* **63** 965 (1994) [*Usp. Khim.* **63** 1031 (1994)]
171. V A Sadykov, S N Pavlova, G V Zabolotnaya, M V Chaikina, R I Maksimovskaya, S V Tsybulya, E B Burgina, V I Zaikovskii, G S Litvak, Yu V Frolova, D I Kochubei, V V Kriventsov, E A Paukshtis, V N Kolomiichuk, V V Lunin, N N Kuznetsova, D Agraval, R Roi *Kinet. Katal.* **42** 432 (2001) [l]
172. I A Stenina, Yu A Velikodnyi, V A Ketsko, A B Yaroslavtsev *Neorg. Mater.* **40** 1106 (2004) [a]
173. D K Agrawal, J H Adair *J. Am. Ceram. Soc.* **73** 2153 (1990)
174. A K Kuriakose, T A Wheat, A Ahmad, J Dirocco *J. Am. Ceram. Soc.* **67** 179 (1984)
175. G E Lenain, H A McKinstry, D K Agrawal *J. Am. Ceram. Soc.* **68** C224 (1985)
176. S Zhang, B Quan, Z Zhao, B Zhao, Y He, W Chen *Mater. Lett.* **58** 226 (2004)
177. B E Yoldas, I K Lloyd *Mater. Res. Bull.* **18** 1171 (1983)
178. P Porkodi, V Yegnaraman, P Kamaraj, V Kalyanavalli, D Jeyakumar *Chem. Mater.* **20** 6410 (2008)
179. M L Di Vona, E Traversa, S Licoccia *J. Sol-Gel Sci. Technol.* **19** 463 (2000)
180. US P. 3330697 (1967)
181. C R Mariappan, C Galven, M P Crosnier-Lopez, F Le Berre, O Bohnke *J. Solid State Chem.* **179** 450 (2006)
182. W H Rhodes *J. Am. Ceram. Soc.* **64** 19 (1981)
183. A V Galakhov, I V Vyazov, V Ya Shevchenko, A A Ezhov *Izv. Akad. Nauk SSSR, Neorg. Mater.* **26** 828 (1990) [a]
184. K Byrappa, D Y Pushcharovsky *Prog. Cryst. Growth Charact. Mater.* **24** 269 (1992)
185. S Komarneni *Int. J. High Technol. Ceram.* **4** 31 (1988)
186. Y Yue, W Pang *Mater. Res. Bull.* **25** 841 (1990)
187. A Clearfield, M A Subramanian, W Wang, P Jerus *Solid State Ionics* **9 – 10** 895 (1983)
188. S Yamanaka, K Yoshioka, M Hattori *Solid State Ionics* **40 – 41** 43 (1990)
189. Y Yue, W Pang *J. Mater. Sci. Lett.* **9** 1392 (1990)
190. A E Baranchikov, V K Ivanov, Yu D Tretyakov *Russ. Chem. Rev.* **76** 133 (2007) [*Usp. Khim.* **76** 147 (2007)]
191. I Yu Pinus, A E Baranchikov, A G Veresov, A B Yaroslavtsev *Zh. Neorg. Khim.* **53** 1253 (2008) [g]
192. A I Kryukova *Zh. Neorg. Khim.* **36** 1962 (1991) [g]
193. P Afanasiev, C Geantet *Coord. Chem. Rev.* **178 – 180** 1725 (1998)
194. M Nagai, T Nishino, T Kanazawa *Solid State Ionics* **18 – 19** 964 (1986)
195. N S Slobodyanik, P G Nagornyi, V V Skopenko, E S Lugovskaya *Zh. Neorg. Khim.* **32** 1724 (1987) [g]
196. N S Slobodyanik, P G Nagornyi, G D Byalkovskii *Ukr. Khim. Zh.* **51** 770 (1985) [m]

197. M Šljukić, B Matković, B Prodić, S Ščavnicar *Croat. Chim. Acta* **39** 145 (1967)
198. A K Ivanov-Schitz, A B Bykov *Solid State Ionics* **100** 153 (1997)
199. A K Ivanov-Shits, A B Bykov, I A Verin *Kristallografiya* **41** 1060 (1996) [c]
200. D Petit, P Colomban, G Collin, J P Boilot *Mater. Res. Bull.* **21** 365 (1986)
201. B Matković, B Prodić, M Šljukić *Bull. Soc. Chim. Fr.* 1777 (1968)
202. J P Boilot, G Collin, R Comes *J. Solid State Chem.* **50** 91 (1983)
203. S Krimi, I Mansouri, A El Jazouli, J P Chaminade, P Gravereau, G Le Flem *J. Solid State Chem.* **105** 561 (1993)
204. U V Varadaraju, K A Thomas, B Sivasankar, G V Subba Rao *Izv. Sib. Otd. Akad. Nauk, Ser. Khim. Nauk.* (6/19) 10 (1987)
205. A Nadiri, C Delmas *C. R. Acad. Sci., Ser. II* **304** 415 (1987)
206. C Delmas, F Cherkaoui, A Nadiri, P Hagenmuller *Mater. Res. Bull.* **22** 631 (1987)
207. N A Dhas, K C Patil *J. Mater. Chem.* **5** 1463 (1995)
208. B Vaidhyanathan, K J Rao *J. Solid State Chem.* **132** 349 (1997)
209. B Vaidhyanathan, D K Agrawal, in *The 101st Annual Meeting and Exposition 'Setting the Pace for the Next Century' (Abstracts)* (Westerville, OH: American Ceramic Society, 1999) p. 224
210. H Güler, F Kurtuluş *Mater. Chem. Phys.* **99** 394 (2006)
211. A H Naik, S B Deb, A B Chalke, M K Saxena, K L Ramakumar, V Venugopal, S R Dharwadkar *J. Chem. Sci.* **122** 71 (2010)
212. Yu D Tretyakov *Russ. Chem. Rev.* **73** 831 (2004) [*Usp. Khim.* **73** 899 (2004)]
213. S C Abrahams, J L Bernstein *J. Chem. Phys.* **45** 2745 (1966)
214. A Wagh *Chemically Bonded Phosphate Ceramics* (Amsterdam: Elsevier, 2004)
215. I A Verin, E A Genkina, B A Maksimov, L A Muradyan, M I Sirota *Kristallografiya* **30** 677 (1985) [c]
216. Yu A Ivanov, E L Belokoneva, Yu K Egorov-Tismenko, M A Simonov, N V Belov *Dokl. Akad. Nauk SSSR* **252** 1122 (1980) [n]
217. J L Rodrigo, P Carrasco, J Alamo *Mater. Res. Bull.* **24** 611 (1989)
218. E S Lunezheva, B A Maksimov, O K Mel'nikov *Kristallografiya* **34** 1119 (1989) [c]
219. R Masse, A Durif, J C Guitel, I Tordjman *Bull. Soc. Fr. Mineral. Cristallogr.* **95** 47 (1972)
220. R Duhlev *Acta Crystallogr. Sect. C.* **50** 1525 (1994)
221. T S Sysoeva, E A Asabina, V I Pet'kov, V S Kurazhkovskaya *Zh. Neorg. Khim.* **54** 894 (2009) [g]
222. A Ono *Bull. Chem. Soc. Jpn.* **58** 381 (1985)
223. A Mbandza, E Bordes, P Courtine, A El Jazouli, J L Soubeyroux, G Le Flem, P Hagenmuller *React. Solids* **5** 315 (1988)
224. *Natl. Bur. Stand. (U.S.) Monogr. 25* **21** 114 (1984)
225. R Masse *Bull. Soc. Fr. Mineral. Cristallogr.* **93** 500 (1970)
226. M Catti, S Stramare *Solid State Ionics* **136–137** 489 (2000)
227. M Catti, S Stramare, R Ibberson *Solid State Ionics* **123** 173 (1999)
228. M Catti, N Morgante, R M Ibberson *J. Solid State Chem.* **152** 340 (2000)
229. M Šljukić, B Matković, B Prodić, , D Anderson *Z. Kristallogr.* **130** 148 (1969)
230. E R Gobechiya, Yu K Kabalov, V I Pet'kov, M V Sukhanov *Kristallografiya* **49** 829 (2004) [c]
231. A Clearfield, B D Roberts, M A Subramanian *Mater. Res. Bull.* **19** 219 (1984)
232. A Ono, Y Yajima *Bull. Chem. Soc. Jpn.* **59** 2761 (1986)
233. P R Rudolf, M A Subramanian, A Clearfield, J D Jorgensen *Solid State Ionics* **17** 337 (1985)
234. A Ono *J. Mater. Sci. Lett.* **4** 936 (1985)
235. I Busserau, M S Belkhiria, P Gravereau, A Boireau, J L Soubeyroux, R Olazcuaga, G Le Flem *Acta Crystallogr. Sect. C* **48** 1741 (1992)
236. S Arsalane, M Ziyad, G Coudurier, J C Védrine *J. Catal.* **159** 162 (1996)
237. A P Wilkinson *Inorg. Chem.* **36** 1602 (1997)
238. E Morin, T Le Mercier, M Quarton, E R Losilla, M A G Aranda, S Bruque *Powder Diffr.* **14** 53 (1999)
239. B E Taylor, A D English, T Berzins *Mater. Res. Bull.* **12** 171 (1977)
240. H F McMurdie, M C Morris, E H Evans, B Paretzkin, W Wong-Ng, Y Zhang, C R Hubbard *Powder Diffr.* **2** 41 (1987)
241. J-M Winand, A Rulmont, P Tarte *J. Solid State Chem.* **107** 356 (1993)
242. Y Brik, M Kacimi, F Bozon-Verduraz, M Ziyad *Microporous Mesoporous Mater.* **43** 103 (2001)
243. M Alami, R Brochu, J L Soubeyroux, P Gravereau, G Le Flem, P Hagenmuller *J. Solid State Chem.* **90** 185 (1991)
244. D Zhao, Z Xie, J-M Hu, H Zhang, W-l Zhang, S-L Yang, W-D Cheng *J. Mol. Struct.* **922** 127 (2009)
245. R Brochu, M Louër, M Alami, M Alqaraoui, D Louer *Mater. Res. Bull.* **32** 113 (1997)
246. M P Carrasco, M C Guillem, J Alamo *Mater. Res. Bull.* **28** 793 (1993)
247. J Alamo, J L Rodrigo *Mater. Res. Bull.* **27** 1091 (1992)
248. A Serghini, R Brochu, R Olazcuaga, P Gravereau *Mater. Lett.* **22** 149 (1995)
249. B Matković, B Kojić-Prodić, M Šljukić, M Topić, R D Willett, F Pullen *Inorg. Chim. Acta* **4** 571 (1970)
250. B Matković, B Prodić, M Šljukić,, S W Peterson *Croat. Chim. Acta* **40** 147 (1968)
251. M A Salvadó, P Pertierra, A I Bortun, C Trobajo, J R García *Inorg. Chem.* **47** 7207 (2008)
252. E R Gobechiya, Yu K Kabalov, S V Tomilin, A N Lukinykh, A A Lizin, A I Orlova *Kristallografiya* **50** 418 (2005) [c]
253. A Guesdon, J Provost, B Raveau *J. Mater. Chem.* **9** 2583 (1999)
254. H T Hawkins, D R Spearing, D K Veirs, J A Danis, D M Smith, C D Tait, W H Runde, M N Spilde, B E Scheetz *Chem. Mater.* **11** 2851 (1999)
255. Yu F Volkov, S V Tomilin, A I Orlova, A A Lizin, V I Spiryakov, A N Lukinykh *Zh. Neorg. Khim.* **50** 1776 (2005) [g]
256. H Kohler, H Schulz *Mater. Res. Bull.* **21** 23 (1986)
257. S G Samoilov, A I Kryukova, G N Kazantsev, G Yu Artem'eva *Neorg. Mater.* **28** 2197 **(**1992) [a]
258. N N Eremin, V S Urusov, in *Problemy Kristallologii* (The Problems of Crystallography) No. 5 (Moscow: GEOS, 1999) p. 228
259. J D Gale *J. Chem. Soc. Faraday Trans.* **93** 629 (1997)
260. N N Eremin, M V Sukhanov, V I Pet'kov, V S Urusov *Dokl. Akad. Nauk* **396** 496 (2004) [n]
261. F Sudreau, D Petit, J P Boilot *J. Solid State Chem.* **83** 78 (1989)
262. I Yu Pinus, A R Shaikhlislamova, I A Stenina, N A Zhuravlev, A B Yaroslavtsev *Neorg. Mater.* **45** 1466 (2009) [a]
263. E R Losilla, M A G Aranda, M Martínez-Lara, S Bruque *Chem. Mater.* **9** 1678 (1997)
264. A Martinez-Juarez, J M Rojo, J E Iglesias, J Sanz *Chem. Mater.* **7** 1857 (1995)
265. E Morin, J Angenault, J C Couturier, M Quarton, H He, J Klinowski *Eur. J. Solid State Inorg. Chem.* **34** 947 (1997)
266. M Catti, A Comotti, S Di Blas *Chem. Mater.* **15** 1628 (2003)
267. K Arbi, M Ayadi-Trabelsi, J Sanz *J. Mater. Chem.* **12** 2985 (2002)
268. V I Pet'kov, A I Orlova, G Sh Shekhtman *Elektrokhimiya* **32** 621 (1996) [h]
269. H Aono, E Sugimoto Y Sadaoka, N Imanaka, G-y Adachi *J. Electrochem. Soc.* **137** 1023 (1990)

270. A S Best, M Forsyth, D R MacFarlane *Solid State Ionics* **136 – 137** 339 (2000)
271. I A Stenina, I Yu Pinus, A I Rebrov, A B Yaroslavtsev *Solid State Ionics* **175** 445 (2004)
272. A Essoumhi, C Favotto, M Mansori, K Ouzaouit, P Satre *Solid State Sci.* **9** 240 (2007)
273. E I Burmakin *Tverdye Elektrolity s Provodimost'yu po Kationam Shchelochnykh Metallov* (Solid Electrolytes with Alkali Metal Cation Conductivity) (Moscow: Nauka, 1992)
274. K Arbi, J M Rojo, J Sanz *J. Eur. Ceram. Soc.* **27** 4215 (2007)
275. J-Y Luo, L-J Chen, Y-J Zhao, P He, Y-Y Xia *J. Power Sources* **194** 1075 (2009)
276. M A Subramanian, B D Roberts, A Clearfield *Mater. Res. Bull.* **19** 1471 (1984)
277. M Ohta, A Ono, F P Okamura, K Hirota *J. Mater. Sci. Lett.* **6** 583 (1987)
278. M Catti, R Ibberson *J. Phys. Chem., Sect. B* **106** 11916 (2002)
279. L E Bove, M Catti, A Paciaroni, F Sacchetti *J. Phys. Chem. B* **108** 8910 (2004)
280. I A Stenina, M N Kislitsyn, I Y Pinus, A B Yaroslavtsev *Mendeleev Commun.* 191 (2004)
281. E A Asabina, V I Pet'kov, V N Loshkarev, A A Rodinov, D B Kitaev *Radiokhimiya* **48** 205 (2006) [d]
282. R Chourasia, A Bohre, R D Ambastha, O P Shrivastava, P K Wattal *J. Mater. Sci.* **45** 533 (2010)
283. M V Sukhanov, E R Gobechiya, Yu K Kabalov, V I Pet'kov *Kristallografiya* **53** 1031 (2008) [c]
284. E Asabina, V Pet'kov, E Gobechiya, U Kabalov *Solid State Sci.* **10** 377 (2008)
285. J P Boilot, G Collin, R Comès *Solid State Commun.* **45** 231 (1983)
286. V I Pet'kov, E A Asabina, A V Markin, N N Smirnova *J. Therm. Anal. Cal.* **91** 155 (2008)
287. A I Orlova, V I Pet'kov, V S Kurazhkovskaya, D V Kemenov, I G Trubach, V T Demarin *Radiokhimiya* **41** 304 (1999) [d]
288. S J Milne, J A Gard, A R West *Mater. Res. Bull.* **20** 557 (1985)
289. V I Pet'kov, A I Orlova, I G Trubach, Y A Asabina, V T Demarin *Czech. J. Phys.* **53** (Suppl. A) A639 (2003)
290. V I Pet'kov, V N Loshkarev, A I Orlova, V S Kurazhkovskaya, V T Demarin *Zh. Neorg. Khim.* **47** 1162 (2002) [g]
291. E A Asabina, Candidate Thesis in Chemical Sciences, Nizhnii Novgorod State University, Nizhnii Novgorod, 2006
292. A R Kotel'nikov, I V Ulin, A M Koval'skii, A N Nekrasov, Z A Kotel'nikova, A I Orlova, V I Pet'kov *Radiokhimiya* **42** 325 (2000) [d]
293. E A Asabina, V I Pet'kov, A R Kotel'nikov, A M Koval'skii *Zh. Neorg. Khim.* **51** 1066 (2006) [g]
294. E A Asabina, V I Pet'kov, M V Boguslavskii, A P Malakho, B I Lazoryak *Zh. Neorg. Khim.* **51** 1252 (2006) [g]
295. E A Asabina, V I Pet'kov, D A Rusakov, B I Lazoryak, V S Kurazhkovskaya *J. Solid State Chem.* **183** 1980 (2010)
296. V S Kurazhkovskaya, A I Orlova, V I Pet'kov, D V Kemenov, L N Kaplunnik *Zh. Strukt. Khim.* **41** 74 (2000) [i]
297. M A Subramanian, R Subramanian, A Clearfield *Solid State Ionics* **18 – 19** 562 (1986)
298. M Casciola, U Costantino, I G Krogh Andersen, E Krogh Andersen *Solid State Ionics* **37** 281 (1990)
299. J-M Winand, A Rulmont, P Tarte *J. Solid State Chem.* **93** 341 (1991)
300. I Yamai, T Ota *J. Am. Ceram. Soc.* **75** 2276 (1992)
301. U Ahmadu, A O Musa, S A Jonah, N Rabiu *J. Therm. Anal. Cal.* **101** 175 (2010)
302. A R Zaripov, O M Slyunchev, S I Rovnyi, V I Pet'kov *Khim. Tekhnol.* **8** 82 (2007) [o]
303. A V Bychkov, S K Vavilov, P T Porodnov, O V Skiba, in *Zamknutyi Toplivnyi Tsikl: Piroelektrokhimiya, Tekhnologiya, Vibrouplotneniya, Tvely (Sbornik Trudov GNTs RF NIIAR)* [Closed Fuel Loop: Pyroelectrochemistry, Engineering, Vibrocompactions, Fuel Elements (Proceedings of GNTs RF NIIAR) (Dimitrovgrad: GNTs NIIAR, 1994) No. 1, p. 13
304. A A Lizin, S V Tomilin, A N Lukinykh, S V Parnosova, in *Novye Tekhnologii dlya Energetiki, Promyshlennosti i Stroitel'stva* (New Technologies for Power Engineering, Industry and Construction) (Dimitrovgrad: GNTs NIIAR, 2003) No. 6, p. 298
305. A I Kryukova, I A Kulikov, G Yu Artem'eva, O V Pechenevskaya, V A Alferov *Radiokhimiya* **34** 82 (1992) [d]
306. V B Kalinin, A M Golubev, V A Tafeenko, S Yu Stefanovich *Kristallografiya* **37** 1220 (1992) [c]
307. *High Conductivity Solid Ionic Conductors: Recent Trends and Applications* (Ed. T Takahashi) (Singapore: World Scientific, 1989)
308. N Anantharamulu, K K Rao, G Rambabu, B V Kumar, V Radha, M Vithal *J. Mater. Sci.* **46** 2821 (2011)
309. J B Goodenough, H Y-P Hong, J A Kafalas *Mater. Res. Bull.* **11** 203 (1976)
310. W H Baur, J R Dygas, D H Whitmore, J Faber *Solid State Ionics* **18 – 19** 935 (1986)
311. H Kohler, H Schulz *Mater. Res. Bull.* **20** 1461 (1985)
312. J-J Didisheim, E Prince, B J Wuensch *Solid State Ionics* **18 – 19** 944 (1986)
313. P R Rudolf, A Clearfield, J D Jorgensen *Solid State Ionics* **21** 213 (1986)
314. J P Boilot, G Collin, P Colomban *J. Solid State Chem.* **73** 160 (1988)
315. J P Boilot, G Collin, P Colomban *Mater. Res. Bull.* **22** 669 (1987)
316. R O Fuentes, F M Figueiredo, M R Soares, F M B Marques *J. Eur. Ceram. Soc.* **25** 455 (2005)
317. M A París, A Martínez-Juárez, J M Rojo, J Sanz *J. Phys.: Condens. Matter* **8** 5355 (1996)
318. X Xu, Z Wen, X Yang, L Chen *Mater. Res. Bull.* **43** 2334 (2008)
319. A F Orliukas, T Šalkus, A Dindune, Z Kanepe, J Ronis, A Určinskas, E Kazakevičius, A Kežionis, V Kazlauskienė, J Miškinis *Solid State Ionics* **179** 159 (2008)
320. I Yu Pinus, I V Arkhangel'skii, N A Zhuravlev, A B Yaroslavtsev *Zh. Neorg. Khim.* **54** 1235 (2009) [g]
321. Z-x Lin, H-j Yu, S-c Li, S-b Tian *Solid State Ionics* **18 – 19** 549 (1986)
322. I Yu Pinus, I A Stenina, A I Rebrov, N A Zhuravlev, A B Yaroslavtsev *Zh. Neorg. Khim.* **54** 1240 (2009) [g]
323. R Shimanouchi-Futagami, M Nishimori, H Nishizawa *J. Mater. Sci. Lett.* **20** 1881 (2001)
324. R Shimanouchi-Futagami, M Nishimori, H Nishizawa *J. Mater. Sci. Lett.* **19** 405 (2000)
325. D Mazza, M Lucco-Borlera, S Ronchetti *Powder Diffr.* **13** 227 (1998)
326. M V Sukhanov, V I Pet'kov, D V Firsov, V S Kurazhkovskaya, E Yu Borovikova *Zh. Neorg. Khim.* **56** 1423 (2011) [g]
327. M V Sukhanov, V I Pet'kov, V S Kurazhkovskaya, N N Eremin, V S Urusov *Zh. Neorg. Khim.* **51** 773 (2006) [g]
328. R Chourasia, O P Srivastava, P K Wattal *J. Alloys Compd.* **473** 579 (2009)
329. V I Pet'kov, M V Sukhanov, V S Kurazhkovskaya *Radiokhimiya* **45** 560 (2003) [d]
330. M V Sukhanov, I A Shchelokov, M M Ermilova, N V Orekhova, V I Pet'kov, G F Tereshchenko *Zh. Prikl. Khim.* **81** 19 (2008) [b]
331. R J Cava, E M Vogel, D W Johnson Jr *J. Am. Ceram. Soc.* **65** C157 (1982)
332. K Shimazu, Y Yamamoto, Y Saito, O Nakamura *Solid State Ionics* **79** 106 (1995)
333. E M Vogel, R J Cava, E Rietman *Solid State Ionics* **14** 1 (1984)
334. S E Sigarev *Kristallografiya* **37** 1055 (1992) [c]
335. S E Sigarev *Kristallografiya* **38** 203 (1993) [c]
336. G-y Adachi, N Imanaka, H Aono *Adv. Mater.* **8** 127 (1996)
337. S Wang, S-J Hwu *J. Solid State Chem.* **90** 377 (1991)

338. A Aatiq, M Ménétrier, L Croguennec, E Suard, C Delmas *J. Mater. Chem.* **12** 2971 (2002)
339. I A Stenina, M N Kislitsyn, I Yu Pinus, I V Arkhangel'skii, N A Zhuravlev, A B Yaroslavtsev *Zh. Neorg. Khim.* **50** 985 (2005) [g]
340. I A Stenina, M G Zhizhin, B I Lazoryak, A B Yaroslavtsev *Mater. Res. Bull.* **44** 1608 (2009)
341. I A Stenina, M N Kislitsyn, N A Ghuravlev, A B Yaroslavtsev *Mater. Res. Bull.* **43** 377 (2008)
342. K D Kreuer, U Warhus *Mater. Res. Bull.* **21** 357 (1986)
343. D Horwat, J F Pierson, A Billard *Surf. Coat. Technol.* **201** 7013 (2007)
344. D Horwat, J F Pierson, A Billard *Surf. Coat. Technol.* **201** 7060 (2007)
345. Y Sadaoka *Sens. Actuators, B* **121** 194 (2007)
346. M Zhou, A Ahmad *Sens. Actuators, B* **122** 419 (2007)
347. K Obata, S Matsushima *Sens. Actuators, B* **130** 269 (2008)
348. X Liang, T Zhong, H Guan, F Liu, G Lu, B Quan *Sens. Actuators, B* **136** 479 (2009)
349. X Liang, Y He, F Lie, B Wang, T Zhong, B Quan, G Lu *Sens. Actuators, B* **125** 544 (2007)
350. T Zhong, B Quan, X Liang, F Liu, B Wang *Mater. Sci. Eng. B* **151** 127 (2008)
351. G Le Polles, C Parent, R Olazcuaga, G Le Flem, P Hagenmuller *C. R. Acad. Sci., Ser. II* **306** 765 (1988)
352. Y He, B Quan, Y Wang, C Cheng, B Wang *Mater. Lett.* **61** 4519 (2007)
353. A M dos Santos, F M B Marques, L D Carlos, J Rocha *J. Mater. Chem* **16** 3139 (2006)
354. I Koguma, K Oishi, S Takase, Y Shimizu *ECS Trans.* **16** (31) 81 (2008)
355. P C Yao, D J Fray *Solid State Ionics* **8** 35 (1983)
356. V I Pet'kov, V S Kurazhkovskaya, A I Orlova, M L Spiridonova *Kristallografiya* **47** 802 (2002) [c]
357. A Serghini, R Brochu, M Ziyad, M Loukah, J C Védrine *J. Chem. Soc. Faraday Trans.* **87** 2487 (1991)
358. G Le Pollès, A El Jazouli, R Olazcuaga, J M Dance, G Le Flem, P Hagenmuller *Mater. Res. Bull.* **22** 1171 (1987)
359. I Taoufik, M Haddad, R Brochu, R Berger *J. Mater. Sci.* **34** 2943 (1999)
360. I Shchelokov, E Asabina, M Sukhanov, M Ermilova, N Orekhova, V Pet'kov, G Tereshchenko *Solid State Sci.* **10** 513 (2008)
361. A La Ginestra, C Ferragina, P Patrono *Mater. Res. Bull.* **14** 1099 (1979)
362. M V Sukhanov, M M Ermilova, N V Orekhova, V I Pet'kov, G F Tereshchenko *Zh. Prikl. Khim.* **79** 622 (2006) [b]
363. A I Pylinina, I I Mikhalenko, M M Ermilova, N V Orekhova, V I Pet'kov *Zh. Fiz. Khim.* **84** 465 (2010) [p]
364. V I Pet'kov, K V Kir'yanov, A I Orlova, D B Kitaev *J. Therm. Anal. Cal.* **65** 381 (2001)
365. E A Asabina, V I Pet'kov, N N Smirnova, A V Markin *Zh. Neorg. Khim.* **50** 1607 (2005) [g]
366. V I Pet'kov, E A Asabina, A V Markin, N N Smirnova, D B Kitaev *J. Therm. Anal. Cal.* **80** 695 (2005)
367. V I Pet'kov, E A Asabina, A V Markin, N N Smirnova *J. Chem. Eng. Data* **55** 856 (2010)
368. E A Asabina, V I Pet'kov, A V Markin, N N Smirnova, A M Koval'skii *Zh. Fiz. Khim.* **79** 2174 (2005) [p]
369. V I Pet'kov, K V Kir'yanov, A I Orlova, D B Kitaev *Neorg. Mater.* **36** 478 (2000) [a]
370. V I Pet'kov, K V Kir'yanov, E A Asabina *Zh. Fiz. Khim.* **77** 797 (2003) [p]
371. V I Pet'kov, E A Asabina, A V Markin, K V Kir'yanov *Thermochim. Acta* **403** 185 (2003)
372. E A Asabina, V I Pet'kov, A V Markin, N N Smirnova *Zh. Fiz. Khim.* **83** 1222 (2009) [p]
373. J Maier, U Warhus, E Gmelin *Solid State Ionics* **18 – 19** 969 (1986)
374. U Warhus, J Maier, A Rabenau *J. Solid State Chem.* **72** 113 (1988)
375. U von Alpen, M F Bell, W Wichelhaus *Mater. Res. Bull.* **14** 1317 (1979)
376. S I Novikova *Teplovoe Rasshirenie Tverdykh Tel* (Thermal Expansion of Solids) (Moscow: Nauka, 1974)
377. S K Filatov *Vysokotemperaturnaya Kristallokhimiya. Teoriya, Metody i Rezul'taty Issledovanii* (High-temperature Crystal Chemistry. Theory, Methods and Results of Investigations) (Leningrad: Nedra, 1990)
378. T Oota, I Yamai *J. Am. Ceram. Soc.* **69** 1 (1986)
379. G E Lenain, H A McKinstry, J Alamo, D K Agrawal *J. Mater. Sci.* **22** 17 (1987)
380. C-Y Huang, D K Agrawal, H A McKinstry *J. Mater. Sci.* **30** 3509 (1995)
381. V I Pet'kov, A I Orlova, G N Kasantsev, S G Samoilov, M L Spiridonova *J. Therm. Anal. Cal.* **66** 623 (2001)
382. A I Orlova, G N Kazantsev, S G Samoilov *High Temp. – High Press.* **31** 105 (1999)
383. A I Orlova, D V Kemenov, V I Pet'kov, M V Zharinova, G N Kazantsev, S G Samoilov, V S Kurazhkovskaya *High Temp. – High Press.* **34** 315 (2002)
384. P Oikonomou, C Dedeloudis, C J Stournaras, C Ftikos *J. Eur. Ceram. Soc.* **27** 1253 (2007)
385. I Yu Pinus, T O Bok, A B Yaroslavtsev *Neorg. Mater.* **46** 473 (2010) [a]
386. I W Donald, B L Metcalfe, R N J Taylor *J. Mater. Sci.* **32** 5851 (1997)
387. E Breval, G Harshe, D K Agrawal, in *Advances in Ceramic-Matrix Composites (Ceramic Transactions)* (Ed. N P Bansal) (Westerville, OH: American Ceramic Society, 1993) Vol. 38, p. 837
388. C J Leo, G V Subba Rao, B V R Chowdary *Solid State Ionics* **159** 357 (2003)
389. N Chacraborty, W Fisher, A D Gupta, D Basu *Surf. Coat. Tecnol.* **201** 1152 (2006)
390. J Wolfenstine, D Foster, J Read, J L Allen *J. Power Sources* **182** 626 (2008)
391. M Barré, F Le Berre, M-P Crosnier-Lopez, C Galven, O Bohnké, J-L Fourquet *Ionics* **15** 681 (2009)
392. M V Sukhanov, V I Pet'kov, D V Firsov *Neorg. Mater.* **47** 753 **(**2011) [a]
393. J-S Lee, C-M Chang, Y I Lee, J-H Lee, S-H Hong *J. Am. Ceram. Soc.* **87** 305 (2004)
394. C-M Chang, Y I Lee, S-H Hong, H-M Park *J. Am. Ceram. Soc.* **88** 1803 (2005)
395. RF P. 2440957; *Byull. Izobret.* (3) (2012)

[a] — *Inorg Mater. (Engl. Transl.)*
[b] — *Russ. J. Appl. Chem. (Engl. Transl.)*
[c] — *Crystallograph. Rep. (Engl. Transl.)*
[d] — *Radiochemistry (Engl. Transl.)*
[e] — *Glass Ceram. (Engl. Transl.)*
[f] — *Russ. Chem. Bull., Int. Ed. (Engl. Transl.)*
[g] — *Russ. J. Inorg. Chem. (Engl. Transl.)*
[h] — *Russ. J. Electrochem. (Engl. Transl.)*
[i] — *J. Struct. Chem. (Engl. Transl.)*
[j] — *Polym. Sci. (Engl. Transl.)*
[k] — *Mendeleev Chem. J. (Engl. Transl.)*
[l] — *Kinet. Catal. (Engl. Transl.)*
[m] — *Ukr. Chem. J. (Engl. Transl.)*
[n] — *Dokl. Chem. Phys. (Engl. Transl.)*
[o] — *Theor. Found. Chem. Eng. (Engl. Transl.)*
[p] — *Russ. J. Phys. Chem., Ser. A (Engl. Transl.)*